Title
HIV Infection and the Retroviral Restriction Factor APOBEC3G Influence Multilineage Hematopoiesis

Author
Nixon, Christopher

Publication Date
2012

Peer reviewed|Thesis/dissertation

UNIVERSITY OF CALIFORNIA

Los Angeles

HIV Infection and the Retroviral Restriction Factor APOBEC3G Influence Multilineage Hematopoiesis

A dissertation submitted in partial satisfaction of the

requirements for the degree Doctor of Philosophy

in Microbiology, Immunology, and Molecular Genetics

by

Christopher Courtney Nixon

2012

ABSTRACT OF THE DISSERTATION

HIV Infection and the Retroviral Restriction Factor APOBEC3G Influence Multilineage Hematopoiesis

by

Christopher Courtney Nixon

Doctor of Philosophy in Microbiology, Immunology, and Molecular Genetics

University of California, Los Angeles, 2012

Professor Jerome Zack, Chair

Multilineage hematopoiesis suffers in the presence of HIV infection. While the hallmark of HIV infection is the massive loss of CD4+ T-cells, a number of studies have shown that the development of all blood phenotypes is disturbed through the course of infection. However, antiretroviral drugs, opportunistic infections, and the drugs used to treat them all impair hematopoiesis and confound the study of the mechanism of hematopoietic impairment in HIV-infected patient samples. These factors underscore the need to develop controlled in vitro and in vivo models to study the impact of HIV infection in the bone marrow. Here we present data that demonstrates intermediate hematopoietic progenitors are susceptible to infection both in vitro and in vivo and direct infection in part impairs hematopoietic lineage development. Further, these results were supported using the BLT humanized mouse model thus demonstrating its utility as a model to study HIV associated bone marrow pathogenesis. Innate HIV restriction

factors are popular targets for manipulating infection from hematopoietic stem cells. Of the known HIV restriction factors, APOBEC3G(A3G) is unique in that it is expressed in early hematopoiesis and whose expression fluctuates significantly throughout the process of hematopoiesis. When A3G is knocked down by siRNA in hematopoietic progenitors, hematopoietic lineage commitment is clearly skewed. Erythroid and megakaryocyte lineages are impaired while granulocyte and macrophage lineages are enriched. This phenotype is maintained in a humanized mouse model. When human hematopoietic progenitors are isolated from the bone marrow of BLT mice that are reconstituted with stable A3G knockdown vectors, they show a similar skewing of hematopoietic lineage commitment. Microarray analysis of A3G knockdown in the common myeloid progenitor confirms that a number of hematopoiesis-specific genes are dysregulated when A3G expression is diminished. Further analysis suggests A3G may be exerting its effects through the cellular mRNA editing machinery.

The dissertation of Christopher Courtney Nixon is approved.

Christel Uittenbogaart

Benhur Lee

Samson Chow

Jerome Zack, Committee Chair

University of California, Los Angeles

2012

This dissertation is dedicated to my parents Jan and Bill Nixon. Without them, none of this work would have been possible. To them I would like to say, "Thank you. You have always been there for me. Throughout my time as a student I have only known your boundless support and encouragement. For that I cannot thank you enough."

I also wish to extend the dedication to my beloved uncle, Leonard Frost. He fought his battle with HIV and AIDS as hard as anyone. It was he who set me forth upon this journey. I only hope my work will prevent for others what he and so many others have had to, and continue to, face.

Table of Contents

List of Figures

VITA

1995-1999	B.A., University of California, Berkeley
1999-2003	Advanced Cardiac Life Support Education Director
	American Heart Association
	Berkeley, CA
2003-2005	M.S. Candidate
	Joseph Romeo Lab
	Department of Molecular Virology
	San Francisco State University
2005-2006	Graduate Student Researcher
	ACCESS Program
	University of California, Los Angeles
2006-2009	Graduate Student Researcher
	Jerome Zack Lab
	Department of Microbiology, Immunology & Molecular Genetics
	University of California, Los Angeles
2006-2007	Teaching Assistant
	Department of Microbiology, Immunology & Molecular Genetics
2009-2012	Doctoral Candidate
	Jerome Zack Lab
	Department of Microbiology, Immunology & Molecular Genetics

University of California, Los Angeles

PUBLICATIONS AND PRESENTATIONS

Christopher C. Nixon and Joseph M. Romeo. 2004. Analysis of the Interaction between Clinical Variants of the Human Immunodeficiency Virus Type 1 Transactivator Tat and the Host Cell Transcriptional Activators, Cyclin T1 and CDK9. California State University Sixteenth Annual Biotechnology Symposium, San Jose, California.

Christopher C. Nixon and Joseph M. Romeo. 2004. Tagging the HIV-1 Tat Protein to Examine Binding Affinity within the Transactivation Complex. California State University Sixteenth Annual Biotechnology Symposium, San Jose, California.

Christopher C. Nixon and Joseph M. Romeo. 2005. An Alphavirus Based Transcellular Transactivation Assay for HIV-1 Tat. California State University Seventeenth Annual Biotechnology Symposium, Los Angeles, California.

Dimitrios N. Vatakis, Christopher C. Nixon, Gregory Bristol, Jerome A. Zack. 2008. Understanding the Block in HIV Replication in Quiescent CD4+ T Cells. Symposium on HIV/AIDS, Palm Springs, California.

Differentially stimulated CD4+ T cells display altered human immunodeficiency virus infection kinetics: implications for the efficacy of antiviral agents. Vatakis D, Nixon C, Bristol G, Zack JA. J Virol. 2009 Apr;83(7):3374-8.

Christopher C. Nixon, Dimitrios N. Vatakis, Gregory Bristol, Jerome A. Zack. 2010. APOBEC3G Influences Human Hematopoiesis. UCLA Department of Medicine Research Day

Christopher C. Nixon, Dimitrios N. Vatakis, Jerome A. Zack. 2010. APOBEC3G Influences Human Hematopoiesis. Broad Stem Cell Tri-Institute Retreat, Asilomar, California.

Quiescent T cells and HIV: an unresolved relationship. Vatakis DN, Nixon CC, Zack JA. Immunol Res. 2010 Dec;48(1-3):110-21.

Christopher C. Nixon, Dimitrios N. Vatakis, Gregory Bristol, Jerome A. Zack. 2011. APOBEC3G Influences Human Hematopoiesis. Symposium on HIV/AIDS, Palm Springs, California.

Antitumor activity from antigen-specific CD8 T cells generated in vivo from genetically engineered human hematopoietic stem cells. Vatakis DN, Koya RC, Nixon CC, Wei L, Kim SG,

Avancena P, Bristol G, Baltimore D, Kohn DB, Ribas A, Radu CG, Galic Z, Zack JA. Proc Natl Acad Sci. 2011 Dec 20;108(51):E14

Christopher C. Nixon, Dimitrios N. Vatakis, Scott N. Reichelderfer, Dhaval Dixit, Sohn G. Kim, Jerome A. Zack, 2012. HIV Infection in Early Myeloid Progenitors Impairs Multilineage Hematopoiesis . Symposium on HIV/AIDS, Palm Springs, California.

Christopher C. Nixon, Dimitrios N. Vatakis, Jerome A. Zack. 2012. APOBEC3G Influences Human Hematopoiesis. Broad Stem Cell Tri-Institute Retreat, Asilomar, California.

Chapter 1

Background

1.1 Prologue

Human hematopoiesis is a complex process that is subject to control on many levels. While a great deal is known about such regulation, still much remains a mystery. Both intracellular and extracellular processes govern blood cell development and hemostasis. Intracellular factors include intrinsic signals that are determined by the developmental state of the cell partially controlled by expression of particular transcription factors and microRNAs. Extracellular factors include cytokines present in the bone marrow microenvironment as well as the general health status of an individual. Many cancers and systemic infections are known to disrupt normal hematopoiesis as wells as the means used to treat them.

1.2 Human Hematopoiesis

Human hematopoiesis proceeds through a series of ordered developmental stages from a small, regenerating population of long-term hematopoietic stem cells (LT-HSC) that gives rise to all terminally differentiated blood cell phenotypes (Figure1.1). As development proceeds, HSC become progressively restricted in lineage commitment. The LT-HSC develops to a short-term hematopoietic stem cell (ST-HSC) and then the multipotent-progenitor (MPP). At this stage a cell can still give rise to each of the mature blood phenotypes. The cell next develops to either the common myeloid progenitor (CMP) or the common lymphoid progenitor (CLP). The CMP gives rise to all cells of the

myeloid lineage in addition to erythroid and megakaryocytic lineages while the CLP gives rise to all T and B lymphocytes (1,2,3). The developmental stage of a cell is determined by a unique pattern of expression of cell surface proteins. Early hematopoietic progenitors are the LT-HSC and the ST-HSC and intermediate progenitors are the CMP, CLP, GMP, and MEP. Early and intermediate progenitors can be distinguished by CD34 and CD38 expression. Early hematopoietic progenitors are CD34+CD38- while intermediate hematopoietic progenitors are CD34+CD38+. Hematopoietic progenitor cell (HPC) refers to all CD34+ progenitors.

While the majority of adult hematopoiesis takes place in the bone marrow, T-lymphocyte development is unique in that it takes place in the thymus. T-cell precursors migrate from the bone marrow to the thymus in a chemokine mediated process. Once in the thymus, T-cell development is characterized by the expression of the surface proteins CD4 and/or CD8. Thymocytes are initially double negative for both and thus classified as at the double-negative (DN) stage of thymopoiesis. There is then transient expression of one or the other followed by expression of both CD4 and CD8 on the surface of the developing T-cell. The cell then becomes committed to expression of a single T-cell marker, either CD4 or CD8, thereby becoming a single-positive thymocyte(4,5,6).

1.3 The Bone Marrow Microenvironment

Stromal elements of the bone marrow are critical to hematopoiesis and hemostasis. The stroma includes mesenchymal stem cells , reticular cells, osteoblasts, osteoclasts, fibroblasts, endothelial cells, macrophages, and adipocytes. Stromal cells secrete

cytokines that regulate hematopoiesis and express surface proteins that are necessary developmental signals for successful commitment to certain lineages(7,8,9).

Cytokines are pleiotropic small protein messengers that interact with specific surface receptors on target cells. Cytokines are best known for their role in regulation of immune responses though they are critical to the regulation of various functions and processes, including hematopoiesis. The earliest stages of blood cell development are in part controlled by stem cell factor (SCF), FLT-3 ligand, and thrombopoietin (TPO). The first point of development at which a hematopoietic progenitor cell initiates commitment is the bifurcation between the common myeloid progenitor (CMP) and the common lymphoid progenitor(CLP). Interleukin-7 (IL-7) specifically promotes development to lymphoid lineages while interleukins-1, 3, and 6 (IL-1, IL-3, IL-6) promote myeloid development. The multipotent myeloid progenitor develops under the influence of the granulocyte-monocyte colony stimulating factor (GMCSF) and IL-3. Erytthroid and megakaryocyte lineages are promoted in the presence of erythropoietin (EPO) and TPO, respectively. Monocyte colony stimulating factor (MCSF) promotes monocyte commitment and granulocyte colony stimulating factor (GCSF) supports development of all granulocytes (10,11,12).

Bone marrow stromal cells express a number of surface proteins that guide hematopoiesis. The most notable of these is the family of notch ligands. Notch receptor ligands direct a number of lines of development when bound to surface notch expressed by developing cells. There are two subtypes of Notch ligand- the Delta-like and Jagged

subtypes. In mammals, there are four single-pass transmembrane Notch receptors (Notch1-4) and five transmembrane ligands (Delta-like-1, 3, and 4 as well as Jagged-1 and 2). Notch signaling is best known for directing B-cell vs T-cell lineage commitment in the hematopoietic system (13,14).

1.4 MicroRNA Regulation of Hematopoiesis

MicroRNAs have emerged as important regulators of lineage commitment and maintenance in developing and differentiated blood cells. MicroRNAs (miRNA) are 21-25 nucleotide long RNA molecules that exercise post-transcriptional control over the human genome. They are found in either non-coding RNAs or in the introns of protein coding genes. Multiple miRNAs are expressed in a tissue-specific and/or developmental stage-specific fashion. Following transcription of the precursor pri-miRNAs, they are processed by the RNase-III enzymes Drosha and Dicer. The processed pri-miRNA, now termed the pre-miRNA, is exported to the cytoplasm where it is cleaved by Dicer to form a mature miRNA. This miRNA is assembled into the miRNA containing ribonucleoprotein particle (miRNP) which is the effector complex. While the miRNP is not itself distinct but rather an array of diverse proteins and RNAs, the one protein that is consistently detected in every miRNP is Argonaute (AGO). The minimal requirement for a miRNP is AGO complexed with the single-strand miRNA. The miRNA targets the complex to mRNA by complimentary base-pairing, usually in the 3' untranslated region (UTR) of the target. For example, miRNA 142 and miRNA 223 are known to be

upregulated in myeloid lineages while miR221 and miR222 expression is known to impair erythropoiesis (15,16,17,18).

The proteins that are responsible for mRNA degradation are found in cytoplasmic processing bodies (P-bodies). Indeed, p-bodies are the sites of miRNA activity. Degradation of mRNA occurs by decapping by the enzyme Dcp1/2 and then 5'-3' exonuclease digestion by Xrn1. P-bodies are dynamic structures and their maintenance requires the presence of mRNA and it is thought that an equilibrium exists between P body formation and active translation(19).

1.5 Transcription Factors in Hematopoiesis

Transcription of genes important in early hematopoiesis is largely driven by the transcription factors SCL, PU.1, GATA-1, GATA-2 and GATA-3. Development from the HSC to the CMP requires expression of PU.1 and GATA-1 while development to the CLP requires PU.1, GATA-3, and IKAROS (20, 21, 22).

1.6 Systemic Infection Impairs Hematopoiesis

It is not uncommon for systemic infections to alter human bone marrow morphology. Viral, bacterial, fungal, and protozoal infections can all manifest their symptoms in bone marrow pathology(23, 24). It is common for systemic infections that involve the bone marrow to arise in immunosuppressed patients, especially those with HIV (25).

The severity of HIV-1 associated bone marrow pathology mirrors disease progression. Further, bone marrow cellularity is influenced by the presence of opportunistic infections,

neoplasms, and drug regimen (26,27). Common HIV associated bone marrow abnormalities include hypercellularity, pyknotic megakaryocytes, polyclonal plasmacytosis, lymphohistriocytic aggregates, and gelatinous transformation (28,29,30). Hemophagocytosis is also common as is erythroid dysplasia (31).

1.7 Human Immunodeficiency Virus

The Human Immunodeficiency Virus (HIV) is the etiological agent responsible for the Acquired Immune Deficiency Syndrome. At the time of this publication, 34 million people worldwide are thought to be infected with HIV. In 2010 alone, 1.8 million people are estimated to have died as a result of HIV infection. In all, more than 30 million deaths can be attributed to AIDS since the first description of HIV in the United States in 1981(32).

1.8 HIV Viral Genome and Gene Products

Many strains of HIV have been isolated and the viral genome is approximately 9.2 kb long. The HXB2 strain is considered the reference sequence for this virus (Fig1.2). The HIV viral genome consists of 9 genes that give rise to 15 proteins. The GAG gene encodes the viral capsid proteins while the POL gene encodes all viral enzymes: protease, reverse transcriptase, and integrase. The ENV gene encodes the viral envelope glycoproteins, one of the processed products of which being GP120 which possess the binding sites for human cellular CD4 and the corresponding chemokine receptors necessary as coreceptors for viral entry. In addition to these canonical viral genes, HIV consists of a number of accessory genes. TAT, the transactivator of viral transcription, and REV are regulatory elements indispensable to viral gene expression. TAT binds to

the TAR RNA element and initiates transcription from the viral LTR. REV acts by binding the REV response element (RRE) and promotes nuclear export of unspliced and singly-spliced viral mRNA. VIF, the viral infectivity factor, promotes infectivity but is dispensible to the production of viral particles. VPR encodes viral protein R, is important in nuclear import and induces cell cycle arrest. The VPU gene encodes viral protein-U, degrades CD4 in the endoplasmic reticulum and promotes virus budding from the plasma membrane. NEF encodes a multifunctional protein that is crucial to productive infection. Nef downregulates the expression of CD4 and MHC molecules in infected cells. A number of genomic structural elements are relevant to the HIV viral life cycle. The long terminal repeat (LTR) sequence that flanks each side of the proviral genome is critical for initiation of transcription and polyadenylation. The TAR (target sequence for viral transactivation) RNA element forms secondary structures necessary for Tat binding and then activation of transcription. The Rev response element (RRE) binds Rev with high affinity and is required for Rev function(33,34,35,36,37,38,39).

1.9 HIV Lifecycle

The HIV lifecycle can be completed in as little as 1.5 days (Fig1.3). Coreceptor binding results in a conformational change in GP120, allows GP41 to unfold, and insert its hydrobphobic terminus in the cell membrane. Nucleocapsid enters the cell as the preintegration complex. Following uncoating, two viral genomic RNA strands are released along with three viral enzymes: integrase, protease, and reverse transcriptase. Viral binding and uncoating induces reverse transcriptase to convert the viral genomic RNA strands to cDNA. Pol acts on a DNA-RNA double helix. This enzyme has

RNaseH activity and degrades the RNA strand prior to generating the complimentary cDNA strand to form the double stranded viral DNA. The nuclear pre-integration complex (PIC) consists of double-stranded viral DNA, Vpr, capsid, and Integrase. Vpr mediates nuclear import. The PIC is imported along microtubules through a nuclear pore of an intact nuclear membrane. Once inside the nucleus, Integrase mediates insertion of the viral genome, the proviral DNA, into host chromosomes.

Virus is produced in activated cells. Proviral DNA is transcribed to RNA by host cell machinery and the viral mRNA is exported to the cytoplasm. The viral RNA, the replication enzymes, and the core proteins come together in the cytoplasm to form the capsid. The immature viral particle buds from the cell with an envelope of host and viral proteins(40,41,42,43,44,45,46).

1.10 HIV Pharmacotherapy

Azidothymidine (AZT) was the first drug approved for the treatment of HIV infection in 1987. A major breakthrough came about in 1996 with the advent of combination therapy which remains in practice today. Multiple classes of drugs are currently available that target various parts of the viral life cycle. The current standard pharmacotherapy for the treatment of HIV infection is referred to as highly active antiretroviral therapy (HAART). HAART usually consists of two non-nucleotide reverse transcriptase inhibitors and a protease inhibitor(47,48,49). New regimes include integrase inhibitors.

1.11 Hematopoietic Stem Cell Therapy to Treat HIV Infection

In recent years the idea to engineer an HIV resistant immune system by altering hematopoietic progenitors with gene therapy approaches has gained tremendous

popularity. There are various approaches being developed including engineering stem cells to lack HIV coreceptors using zinc-finger nucleases or short-hairpin RNA (shRNA) directed against the genes or transcripts encoding these receptors. Also being explored is overexpression of innate HIV restriction factors in hematopoietic progenitors and then developing them into terminal phenotypes that are thereby resistant to infection. Also, engineered expression of anti-HIV T-cell receptors is actively being pursued as a means to generate CD8+ effector T-cells with specific antiviral activity (50,51,52,53,54).

1.12 HIV Infection Impairs Human Hematopoiesis

HIV primarily targets CD4+ T cells and to a lesser extent, macrophages. While it is apparent that HIV infection severely disrupts T-cell populations, it is also clear that HIV infection has much broader detrimental effects on normal hematopoiesis. Hematosuppression is common with systemic viral infection (55). Thrombocytopenia, neutropenia, and anemia have all been regularly documented in HIV infected individuals(56,57,58,59). As treatment continues to improve and individuals are living still longer with HIV, it is important to address these hematopoietic defects in order to maintain the heath of people living with infection. Moreover, as gene therapy becomes a more attractive approach to treating HIV infection, it is critical to address the health of the hematopoietic compartment and its potential for robust development.

Clinicians noted early in the course of the HIV/AIDS epidemic that patients commonly present with impaired hematopoiesis. The first report of HIV associated thrombocytopenia was published in 1987(60). Still, it remains unclear whether defects can be attributed to direct infection and death of hematopoietic stem cells or if there is an

indirect mechanism responsible for HIV associated bone marrow impairment. The bone marrow is subject to normal circulation and is thereby exposed to virus in infected individuals. A number of different cell types in the bone marrow are susceptible to infection including stromal cells(61,62), megakaryocytes(63), and eosinophils (64). In fact direct infection of megakaryocytes has been proposed as the primary mechanism of thrombocytopenia (65,66).

Early work showing that CD34+ hematopoietic progenitor cells (HPC) isolated from patients are impaired in their hematopoietic potential is difficult to interpret because of multiple possible confounding factors associated with patient samples. Drugs used to treat HIV infection can by hemotoxic, as can opportunistic infections and the drugs used to treat them. HIV-associated neoplasms of the bone marrow and blood further complicate analysis in patients (67,68,69).

Other than direct infection, a multitude of different mechanisms have been proposed to explain HIV-associated hematopoietic impairment. Some found no impairment of progenitor cells themselves but attributed the defect to an unknown soluble plasma factor (70). These studies are difficult to interpret due to the potential contribution of contaminating cells. It is important to note that CD34 was routinely used in these studies as the exclusive surface marker upon which to isolate hematopoietic stem cells. However, CD34 is expressed on multiple populations of hematopoietic and non-hematopoietic cells alike. Most CD34 hematopoietic cells are also CD38+, indicating they are committed progenitors and not true stem cells capable of infinite self-renewal.

It has been suggested that the HIV envelope protein GP120 mediates hematopoietic defects (72,73,74). Further, using the SCID-hu mouse model, disrupted megakaryopoiesis was demonstrated from CD34+ HSC that were exposed to virus but not infected (75,76). The viral nef protein has also been suggested as the responsible agent for HIV associated hematopoietic defects (77,78). However, these studies did not examine specific progenitors, nor consider the bone marrow microenvironment. Stomal elements are critical to the bone marrow microenvironment. Disruption of stroma in the presence of infection likely explains some HIV-associated impaired hematopoiesis. Multiple stromal cell types, including macrophages and fibroblasts, are reported to be susceptible to infection (79,80).

While a great deal was done early in the course of the HIV pandemic to examine the hematopoietic defects that result from HIV infection, the data are difficult to interpret due to limits of technology. Early studies relied solely upon CD34 expression to designate the hematopoietic stem cell (81,82,83). It is now known that CD34 is expressed on a number of different progenitors and other cell types, only a small fraction of which are the LT-HSC. Within the CD34+ population of cells, subpopulations vary tremendously in their developmental plasticity and in their capacity for self-renewal. Infection of each population would have very different implications in terms of pathology. Thus it is important to examine infection in distinct, specific cell populations.

1.13 Confounding Factors in Patients Makes New Models Necessary

Multiple factors confound studying HIV associated bone marrow suppression in infected patient samples. Drugs used to treat HIV infection, opportunisitic infections and the

drugs used to treat them, and HIV associated bone marrow neoplasms all impact normal hematopoiesis (84,85,86). Therefore, it is imperative to develop an in vivo model of HIV associated bone marrow pathology.

The past twenty years have witnessed tremendous advances in the technology of flow cytometry that allow much more precise characterization and isolation of specific hematopoietic progenitor populations. Moreover, our understanding of HSC culture techniques has greatly improved, allowing us to maintain stem cells as such for much longer periods of time in culture. Together these developments warrant revisiting the question of how HIV infection disrupts normal hematopoiesis.

1.14 HIV Entry Receptors

At the heart of the inquiry is the question of whether or not the hematopoietic stem cell is permissive to infection by HIV. Early reports were conflicted but relied upon crude methods to isolate HSC(87,88). Recent studies are also conflicted as to whether or not HIV+ patient bone marrow HSC become infected (89,90,91) but investigations were primarily focused on whether or not HSC serve as a potential reservoir for latent virus

The susceptibility of a cell to infection by HIV is determined by the expression of surface molecules CD4 and either of the7-transmembrane-domain chemokine receptors CXCR4 or CCR5 that bind the HIV envelope and mediate entry of the viral core into the cell. The natural ligand for CXCR4 is SDF-1 and for CCR5 are RANTES (regulated on activation normal T cell expressed and secreted), MIP1α, and MIP1β. Coreceptor especificity is dictated by the second and third variable loops of the HIV-1 envelope glycoprotein GP120. Coreceptor binding results in a conformational change in GP120,

allowing GP41 to unfold and insert its hydrophobic terminus into the cell membrane(92,93,94). Nucleocapsid enters the cell and following uncoating the two viral genomic RNA strands are released along with three viral enzymes: integrase, protease, and reverse transcriptase.

Transmitted viral isolates are almost always R5 tropic. It is only after the progression of disease that the virus shows X4 preference and the coreceptor switch does not always happen. Reports of HIV entry receptor expression on early hematopoietic stem cell populations are rare and incomplete(95,96). Early studies concluded there is low-level expression of the necessary surface proteins on early progenitors to allow viral entry, however hematopoietic stem cells are not infected at an appreciable level (97).

1.15 The BLT Mouse Models HIV Infection

The fact that only humans and chimpanzees are susceptible to HIV infection has always made study of the systemic effects of infection particularly challenging. The SCID-hu mouse model has been very useful in the study of latency and T-cell development in the context of infection but has shortcomings as the peripheral reconstitution in this model is sparse at best. The recent development of the bone marrow-liver-thymus (BLT) mouse model has paved the way for new research in human immunology and hematopoiesis. In this model, immunodeficient mice receive implants of human fetal thymus and liver that create a conjoined hematopoietic organ underneath the kidney capsule. Subsequently, the murine bone marrow is seeded with human hematopoietic stem cells. Together, these result in robust reconstitution of human leukocytes in various different compartments

(98,99). Further, a number of studies have shown that this model supports HIV infection incurred by various different routes (100,101102,103).

1.16 HIV Restriction Factors

In the past decade, a number of host restriction factors against HIV have been identified. Two members of the apoliporotein-B mRNA editing catalytic polypeptide like (APOBEC) family have been identified as restriction factors. APOBEC3G and APOBEC3F are cellular cytidine deaminases that can be incorporated into the virion and act at the point of reverse transcription to block RT and hypermutate the viral genome. Tripartite motif-containing protein 5 alpha (Trim5α) can bind the viral capsid and promotes premature uncoating . Tetherin (BST2) acts to tether mature viral particles to the cell. SAM domain and HD domain-containing protein 1 (SAMHD1) blocks viral replication in myeloid cells by depleting cellular pools of dNTPs, thereby inhibiting the formation of viral cDNA(104,105, 106, 107, 108, 109). Despite the interest in HIV infection in the bone marrow, these restriction factors have not been explored in human hematopoiesis. Further, these factors are popular gene therapy targets for anti-HIV therapeutics. Expression and function of these proteins in developing blood cells may be important. As HIV related restriction factors are becoming popular targets for gene therapy approaches to treating HIV infection, the potential role of these factors in the context of hematopoiesis was explored.

1.17 APOBEC3G in Hematopoiesis

Differentiation Map (dMap)is a database of gene expression through the process of human hematopoiesis (110). dMap provides gene expression microarray data for every

known stage of hematopoiesis from the ultimate hematopoietic stem cell to each terminally differentiated lineage and allows the tracking of the expression of a single gene through a course of lineage development (http://www.broadinstitute.org/dmap/home). Interestingly, APOBEC3G is the only known HIV restriction factor that shows levels of expression to be strictly delineated by lineage and developmental stage.

1.18 APOBEC3G Function

The APOBEC3 gene family is exclusive to primates (111,112). Expansion at this locus has given us seven cytidine deaminases expressed at different levels and in different tissues. Mice possess only a single APOBEC3, and its knockout does not produce an overt phenotype (113), though impaired response to MMLV has been demonstrated (114, 115). It is among a family of cytidine deaminases possessing either one or two deaminase domains (116) that includes Activation Induced Deaminase (AID), the enzyme responsible for somatic hypermutation and class-switch recombination in B cells. Of note, APOBEC3G (A3G) is expressed in lymphoid tissues and various hematopoietic subsets.

A3G has received much notoriety as an HIV restriction factor and has been studied almost exclusively as such. A3G activity was first noted to induce severe restriction of vif deficient virus in certain cell lines (117). A3G does not restrict infection in *de novo* infected cells. Rather, A3G is packaged in viral particles prior to budding and acts in target cells. A3G then acts to destabilize the viral genome by hypermutating viral DNA at the point of reverse transcription (118,119,120,121) or by physically interfering with

the reverse transcriptase enzyme. A3G causes C to U conversion in the viral minus stranded DNA during reverse transcription leading to lethal hypermutation of the viral genome. The fact that A3G retains antiviral activity when its deaminase activity is disrupted indicates function beyond its enzymatic capabilities (122,123).

The viral vif (virion infectivity factor) protein counteracts A3G by making use of the cullin5-E3 ligase complex to polyubiquitinate A3G, thereby targeting it for proteosomal degradation (124,125,126,127,128). Beyond its ability to restrict retroviral infection, A3G has also been ascribed the ability to inhibit the mobility of retroviral elements and thus maintain the integrity of the human genome (129,130,131,132). A3G does not seem to have this function in embryonic stem cells. One group examined the effects of knocking down A3G in various embryonic stem cell lines. It was determined that only A3B has the ability to restrict LINE-1 mobility in this context, but not A3G (133).

1.19 Regulation of A3G Expression and Activity

As a potent deaminase, it is not surprising that A3G expression and activity fall under tight regulation. The primary means by which this occurs is compartmentalization. A3G posseses a cytoplasmic retention domain and has not been localized to the nucleus(134). Further, recent evidence suggests the deaminase activity of A3G is post-transcriptionally regulated by phosphorylation(135,136). At the level of transcription, A3G is regulated by the nuclear factor of activated T-cells (NFAT) and the interferon regulatory factor (IRF) (138). Interferon-α has been shown to upregulate A3G expression as well (139,140). It has also been shown that activation of toll-like receptor 3 (TLR3) induces upregulation of A3G expression (141).

There is evidence that the APOBEC family of proteins is involved with tissue development. Levels of A3G expression have been reported by a number of groups to vary in terminally differentiated blood cell types (142). Further, two groups have reported increases in A3G in the terminal differentiation step of both macrophages and dendritic cells(143, 144, 145). AID is required for terminal differentiation in B-cells (146). Also, APOBEC2a and APOBEC2b are required for tissue regeneration in glial cells of the nervous system following injury (147).

1.20 Cellular Functions of APOBEC3G

There is compelling evidence that suggests a far more diverse role for A3G in other cellular functions than retroviral and retrotransposon restriction. To date, A3G has only been found in the cytoplasm and possesses a cytoplasmic retention signal (148). However, two groups have independently localized A3G to mRNA processing bodies (149,150,151,152). These bodies, also known as p-bodies, are transient cytoplasmic foci of ribonucleoproteins involved in mRNA sequestration and degradation. Not only was A3G localized subcellularly to p-bodies by immunohistochemistry, when A3G was immunoprecipitated and analyzed by mass spectrometry, it was found that A3G was directly associated with a number of proteins involved in mRNA processing. Of note, Argonaute2, Mov10 and GW182 PB were found in association with A3G.

Another group has implicated A3G in modifying microRNA activity (153). In this study, A3G was expressed at low levels in 293T and HeLa cells. In so doing it was found that A3G counteracts the translational inhibition that is imposed by several miRNAs including mir-10b, mir-25, and let-7a.

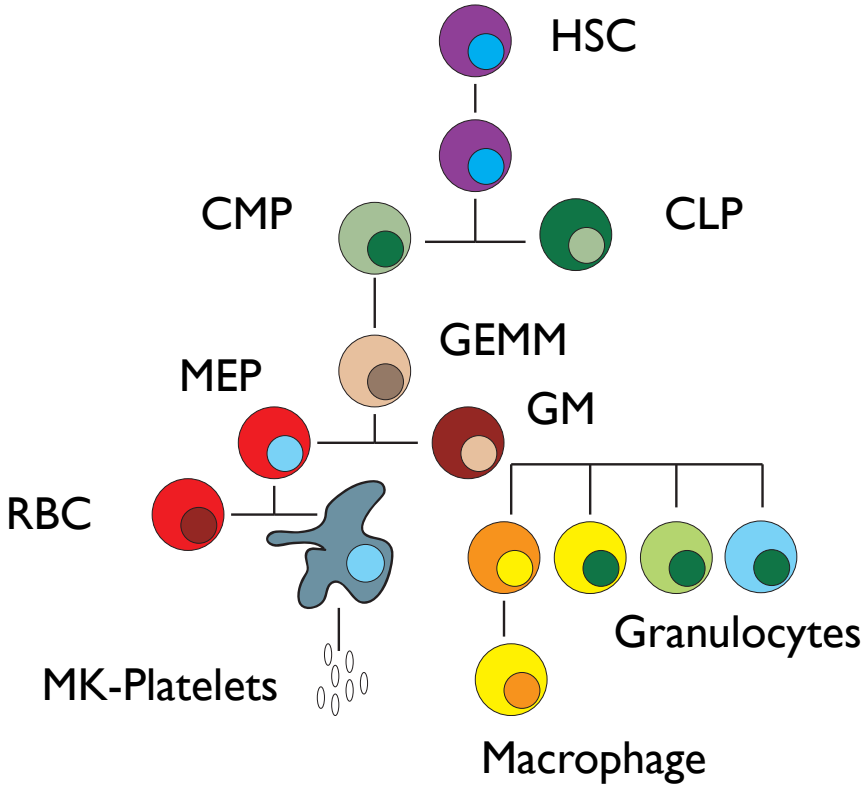

Figure 1.1 Multineage Hematopoiesis

Human hematopoiesis proceeds through a number of distinct stages as cells become increasingly restricted in their lineage commitment and lose their plasticity and capacity for self-renewal. The long-term hematopoietic stem cell (LT-HSC) gives rise to all lineages of blood cells. This is a small pool of long-lived, repopulating cells. The short-term hematopoietic stem cell (ST-HSC) is shorter lived and posseses less capacity for regeneration. The LT- HSC gives rise to either the common myeloid progenitor(CMP) or the common lymphoid progenitor (CLP).

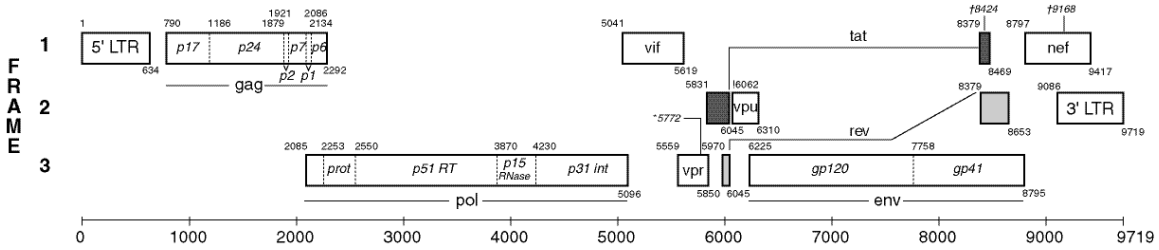

Figure 1.2 HIV-1 Genome

The GAG gene encodes the viral capsid proteins while the POL gene encodes all viral enzymes: protease, reverse transcriptase, and integrase. The ENV gene encodes the viral envelope glycoproteins. TAT, the transactivator of viral transcription, and REV are regulatory elements indispensable to viral gene expression. TAT binds to the TAR RNA element and initiates transcription from the viral LTR. REV acts by binding the REV response element (RRE) and promotes nuclear export of viral mRNA. VIF promotes infectivity but is dispensible to the production of viral particles. VPR encodes viral protein R, is important in nuclear import and induces cell cycle arrest. The VPU gene encodes viral protein-U, degrades CD4 in the endoplasmic reticulum and promotes virus budding from the plasma membrane. NEF encodes a multifunctional protein that is crucial to productive infection.

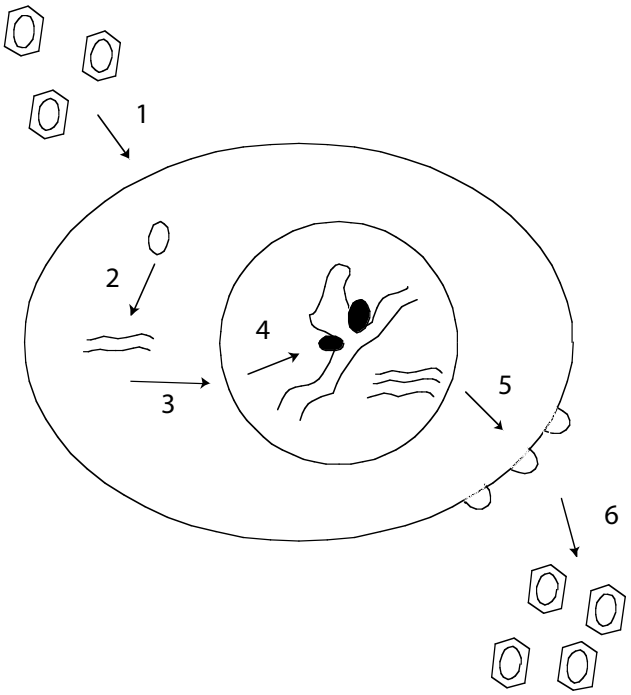

Figure 1.3 HIV Lifecycle

1. Coreceptor binding results in a conformational change in GP120, allows GP41 to unfold, and insert hydrophobic terminus in the cell membrane. Viral binding and uncoating induces 2. Reverse transcriptase to convert the viral genomic RNA strands to a single cDNA. 3. The nuclear pre-integration complex (PIC) is imported along microtubules through a nuclear pore. 4. Integrase mediates insertion of the viral genome into host chromosomes. Proviral DNA is transcribed to unspliced and singly spliced RNA by host cell machinery requiring the action of REV. 5. The viral RNA, the replication enzymes, and the core proteins come together in the cytoplasm to form the capsid. 6. The immature viral particle buds from the cell with an envelope of host and viral proteins.

Chapter 2

Results Part I: HIV Infection Impairs Hematopoiesis

2.1 Direct Infection of CD34+ HPC Impairs Multilineage Hematopoiesis

To determine if direct infection of HPC resulted in any untoward effects, a replication deficient vector based on the NL4-3 strain of HIV was used that was readily available. This $NL4_{HSA\text{-}eGFP}$ vector is deficient in the viral gene vpr due to an insertion of the coding sequence for the murine heat stable antigen (HSA) as well as in the viral envelope gene (env) due to an insertion of the coding sequence for enhanced green fluorescent protein (eGFP), The viral vector was generated by cotransfecting HEK 293FT cells with a plasmid containing the gene that encodes the envelope of the vesicular stomatitis virus (VSV-G) (Fig2.1A). Virus was titred by infection of HeLa cells and assayed by flow cytometry for GFP expression.

Fetal liver derived CD34+ HSC from three different donors were transduced with $NL4_{HSA\text{-}GFP}$ on Retronectin® coated plates. Retronectin® is a commercially available recombinant fibronectin protein that has been shown to increase efficiency of transduction (146). Forty-eight hours post-infection, cells were harvested and sorted by fluorescence activated cell sorting (FACS) to high purity for GFP expression before being plated in complete methylcellulose (Fig2.1B).

It is evident that GFP+ cells that were plated in methylcellulose show severely impaired development in all myeloid and erythroid lineages. The size of colonies in the cultures

derived from GFP+ progenitors were significantly smaller than in those derived from GFP- progenitors (Fig2.2A). Further, the total colony number was much lower in GFP+ derived cultures. While the average total number of colonies per plate from uninfected cells from three separate donors is 78+/-6, it is 24+/-14 for infected cells and this difference is statistically significant in a paired students t test(p=0.0396)(Fig2.2B). Notably, erythroid development is particularly impacted consistent with the erythroid deficit seen in HIV+ patients: no colonies from infected cells while the mean number from uninfected progenitors was 19+/-3 (p=0.02 paired t-test). Granulocyte colonies and mixed granulocyte/macrophage colonies were not statistically different between conditions. Interestingly, macrophage colonies showed significant differences: the mean number of colonies derived from GFP+ cells was 6+/-3 while it was 213+/-3 (p=0.008) in colonies derived from GFP- progenitors(Fig2.3A). Megakaryocytes require a different, collagen based media for growth so are not seen in the same cultures with myeloid or megakaryo-erythroid cells. When examined for megakaryopoietic potential, that of the GFP positive cells was severely impaired when compared to GFP- cells: the mean number of colonies derived from GFP+ cells 5+/-1 while it is 48+/-3 from GFP- progenitors, p=0.0032 (Fig2.3B). This indicates that direct infection is toxic to hematopoiesis.

2.2 HIV89.6 Can Infect CD34+ Hematopoietic Progenitors *in vitro*

To determine if human hematopoietic progenitors can become infected by HIV-1, CD34+ cells were isolated from fetal liver and cultured overnight. The following day, cells were incubated with $HIV_{89.6}$ at an multiplicity of infection (MOI) of 1. $HIV_{89.6}$ is a dual tropic

virus. That is, it can use either of the two coreceptors to enter a cell. Control cultures consisted of cells preincubated with AZT(10 μM) and Indinovir (100μM) for 2 hours prior to infection and maintained throughout infection and culturing in addition to cells that were not infected. Azidothymidine (AZT) is a nucleoside analog reverse-transcriptase inhibitor (NRTI) and Indinavir is a protease inhibitor (PI). Cells and virus were incubated together for one hour in a 37˚C 5%CO2 incubator on a rocking platform. The cell suspension was then pelleted and washed three times with 1ml sterile PBS. Each cell pellet was resuspended in 3ml media and cultured in 6-well plates at 37˚C for 24 or 48 hours. Cells were then harvested by pelleting and stored at -80˚C. To determine if cells were infected, they were assayed by quantitative real-time polymerase chain reaction (qRTPCR) for full –length viral DNA. Indeed, the bulk population of CD34+ HPCs is permissive to infection. When harvested at 24 hours post infection, 0.025+/- 0.004 copies of proviral DNA were detected per cell while neither uninfected nor AZT treated cells harbored HIV DNA (Fig2.4). At 48 hours post infection, the rate of infection rises to 0.047 +/- 0.005 copies of proviral DNA per cell.

2.3 Intermediate HPCs Express HIV Entry Receptors

We next asked whether early myeloid progenitors express the necessary receptors to allow viral entry. The CD34+ progenitor cell population is diverse and includes the hematopoietic stem cell(HSC), the common myeloid progenitor(CMP), the granulocyte-monocyte progenitor(GMP), and the megakaryocyte-erythroid progenitor(MEP). CD34+ hematopoietic progenitors were analyzed by flow cytometry for the presence of CD4, CXCR4, and CCR5 on each different intermediate population. Here we focused on the

CD34+CD38+ population which includes all early myeloid, megakaryocyte, and erythroid progenitors. While at a low frequency, some populations of multipotent progenitors were detected that coexpress CD4 and CXCR4 or CCR5 (Fig2.5). Representative flow cytometry shows 10% of the GMP population coexpress CD4 and CCR5 while 13% coexpress CD4 and CXCR4. In the CMP population, 3% coexpress CD4 and CCR5 and 7% coexpress CD4 and CXCR4 while the MEP appears to express a significant amount of CXCR4 , it is not coexpressed with CD4. This is interesting as these lineages are most clearly impacted by infection aside from the T-cell compartment. Therefore, a small but significant portion of some populations of early myeloid progenitors express the necessary cell surface receptors to allow viral entry.

2.4 Intermediate Hematopoietic Progenitors Show Varying Permissivity to HIV Infection

To determine if specific populations of early hematopoietic progenitors are susceptible to infection, fetal liver derived CD34+ HSC from three separate donors were FACS sorted to high purity based on CD38, CD45RA, and CD110 (TPOr) expression to purify the CMP, the GMP, and the MEP progenitors (Fig2.6)(91,92). All intermediate progenitors are CD34+CD38+ while early hematopoietic progenitors are CD34+CD38-. Within the double positive intermediate progenitor population, only the GMP is positive for CD45RA expression and only the MEP is positive for CD110. Cells were infected with $HIV_{89.6}$ immediately post-sort at an MOI of 1 and harvested 48 hours later. As controls, a portion of each sorted population was pretreated for two hours with AZT (10 μM) and Indinovir (100μM) prior to infection.

While statistically significant, qRTPCR shows low rates of infection in the HSC and CMP populations, 0.72+/-0.26 and 0.65+/-0.22 copies of proviral DNA per 100 cells, respectively . The GMP shows an average 5.24+/-0.87 copies of proviral DNA per 100 cells while the MEP shows an average 12.72+/-0.67 copies of proviral DNA per 100 cells (Fig2.7). These data indicate different intermediate hematopoietic progenitors show increasing susceptibility to infection with developmental stage.

2.5 BLT Mouse Bone Marrow Progenitors Are Susceptible to HIV Infection

While the *in vitro* data showing infection of intermediate hematopoietic progenitors is compelling, it was next important to determine if this takes place *in vivo*. Following confirmation of reconstitution of the hematopoietic compartment with human CD45+ leukocytes, NSG-BLT mice were infected retro-orbitally with 150ng p24 $HIV_{89.6}$ (Fig2.8). One month post infection, virus could be detected in the peripheral blood of infected mice. At two months post infection, 5 infected and three uninfected mice were sacrificed and human CD34+ cells were isolated from the bone marrow and enriched by magnetic activated cell sorting (MACS) to high purity. qRT-PCR was performed on a portion of these cells to determine the presence of proviral DNA. Low levels of infection could be detected in the CD34+ cells from all HIV infected mice (Fig2.9). Mouse #2 showed the highest rate of infection at 8.56+/-0.155 copies of proviral DNA per 1,000 cells while mouse #4 showed the lowest at 0.508+/-0.030 copies per 1,000 cells. All infected mice had copies of proviral DNA in sufficient quantity that they were all determined statistically different from zero at a p value of less than 0.001 (Fig2.9).

2.6 CD34+ Cells Derived From Infected Mice Show Impaired Hematopoiesis, Specifically Erythropoiesis

CD34+ hematopoietic progenitor cells were isolated from bone marrow of infected and uninfected BLT mice and plated in complete methylcellulose supplemented with AZT and Indinavir at a concentration of 1,000 cells/plate, 3 plates per mouse. Two weeks later, plates from mice infected with HIV showed drastically fewer colonies than those from uninfected mice. HSC isolated from uninfected mice consistently produce, on average, 60+/-3 colonies per plate while CD34+ HSC derived from infected mice produce, on average, 12+/-2 colonies per plate p=0.0002 (Fig2.10). Further, the percentage of erythroid colonies was significantly lower in cultures derived from infected mice. HPC derived from uninfected mice produce, on average, almost 30% erythroid colonies while HPC from infected mice do not even yield 15% erythroid colonies (Fig2.10). These data support our *in vitro* data that show infection is toxic to hematopoiesis, specifically erythropoiesis.

2.7 Proviral DNA Is Present in Colonies Derived From CD34+ HSC of HIV+ BLT Bone Marrow

Individual colonies from the above described methylcellulose cultures were assayed by PCR to detect the presence of full-length viral DNA. Approximately half of the colonies assayed were positive for viral DNA. Of the twenty colonies tested, nine of them were positive for full length viral DNA. This represents five different mice that were infected with $HIV_{89.6}$ in vivo and tested positive for virus in peripheral blood samples. Interestingly, each colony type- granulocyte, macrophage, erythroid, and

granulocyte/monocyte- tested positive for virus at approximately the same rate (Fig2.11). This demonstrates that intermediate progenitors can become infected and their progeny can harbor viral DNA. However, the rate of survival is low as the total number of colonies is severely diminished relative to colonies derived from uninfected mice.

A

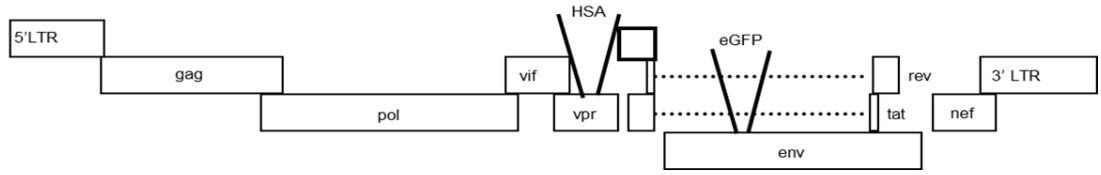

B

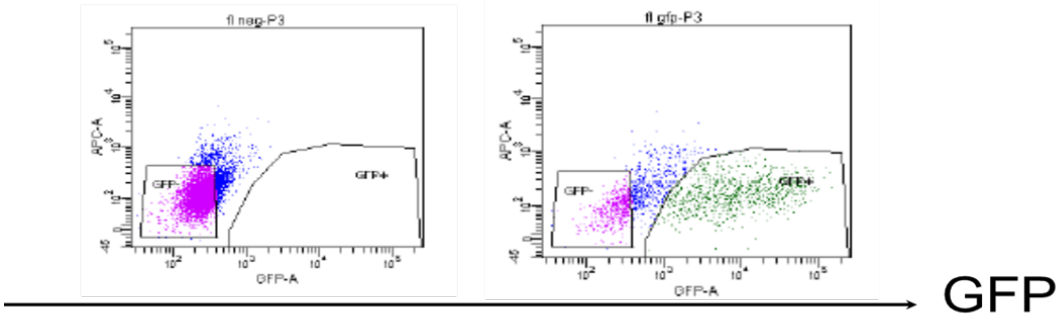

Figure 2.1 $NL4_{HSA\text{-}eGFP}$ Vector and Sort Strategy

A. The $NL4_{HSA\text{-}eGFP}$ vector is based on the NL4-3 strain of HIV-1. The vector is deficient in env and vpr due to the insertion of marker genes and is pseudotyped to produce viral vector particles.

B. FACS sorting strategy for differentiating GFP positive and negative CD34+ hematopoietic progenitor cells 48 hours after Retronectin® mediated transduction.

A B

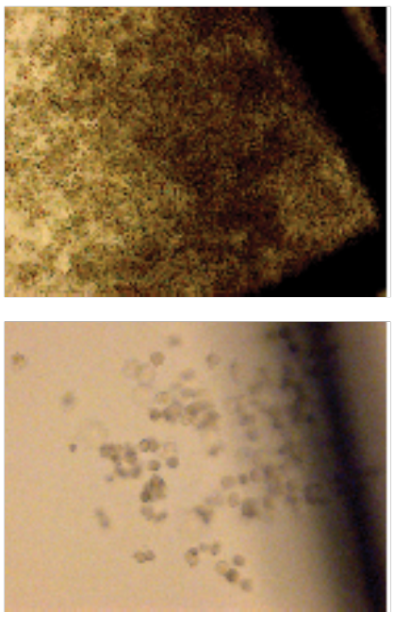

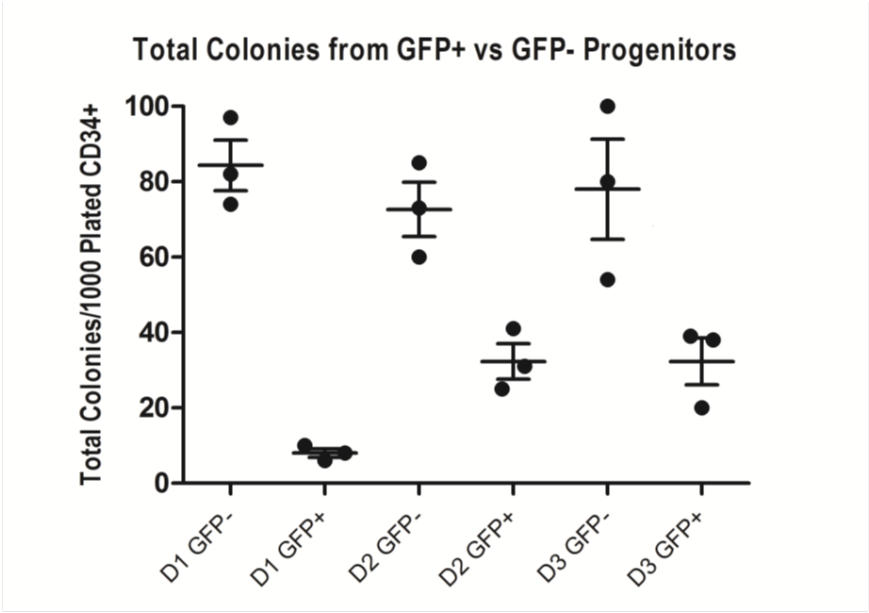

Figure 2.2 Direct Infection Impairs Hematopoiesis

A. Colonies grown in methylcellulose derived from $NL4_{HSA\text{-}eGFP}$ transduced cells (bottom) are in general much smaller than those derived from nontransduced cells (top).

B. Fetal liver derived CD34+ hematopoietic progenitors transduced with NL4-HSA-eGFP gave rise to far fewer colonies than do nontransduced cells. The average number for GFP- cultures was 78+/-6 while it was 24+/-14 for GFP+ cultures (*p=0.039). Each mark represents an individual methylcellulose plate.

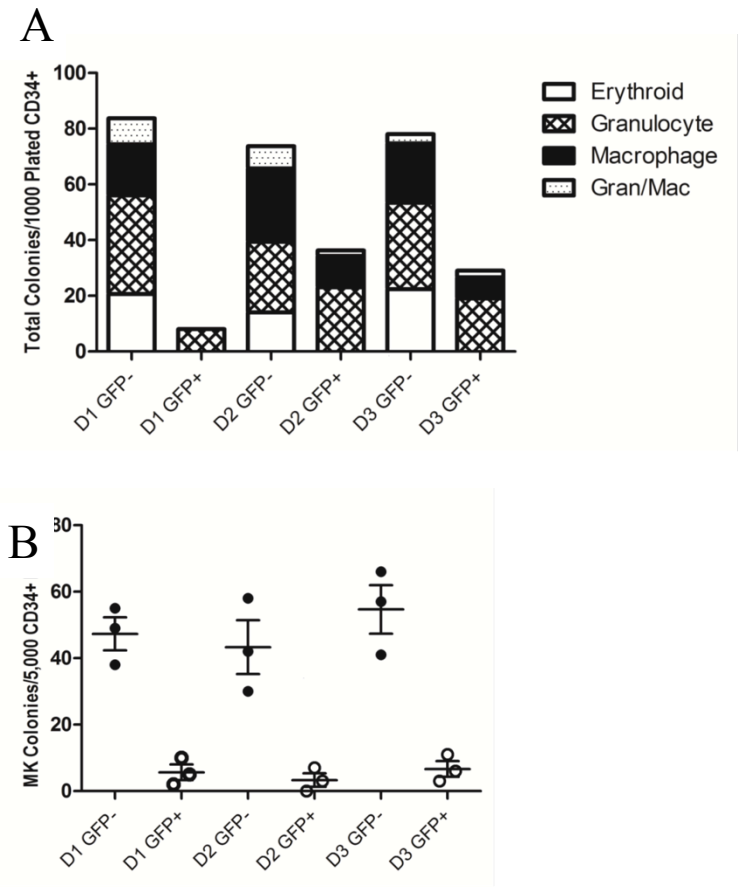

Figure 2.3 Hematopoietic Lineage Commitment is Skewed in HIV Infection

A. There is a skewing of lineages in NL4-$_{HSA\text{-}eGFP}$ transduced cultures compared to nontransduced. Erythroid colonies are particularly impacted. The average of the means of GFP- erythroid colonies was 19+/-3 while GFP+ cultures gave rise to no erythroid colonies.

B. Megakaryocyte colonies are likewise diminished when A3G is depleted from progenitors. The average of the mean of GFP- cultures was 48+/-3 while it was 5+/-1 in GFP+ cultures, p=0.0032.

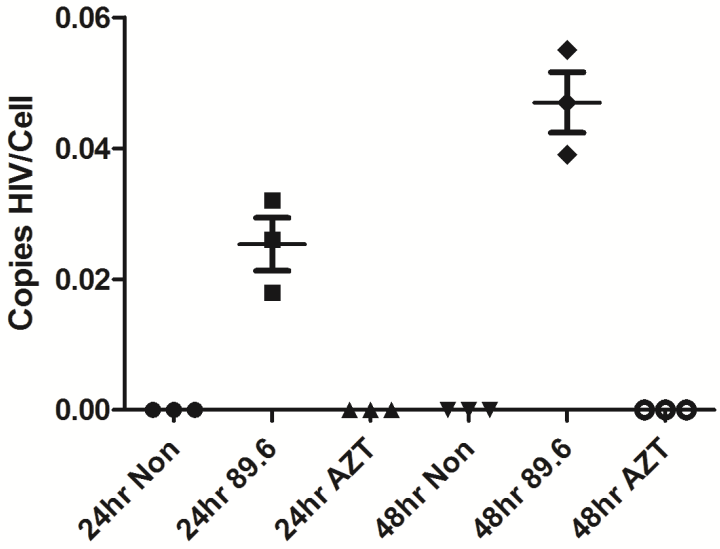

Figure 2.4 $HIV_{89.6}$ Infection of CD34 HPC *in vitro*

Fetal liver derived CD34+ hematopoietic progenitor cells from three donors were infected with $HIV_{89.6}$ and then assayed by qRT-RTPCR 24 or 48 hours post infection for the presence of full-length proviral DNA. While at a low rate, viral DNA was detected in all infected cultures while it was not in cells treated with AZT. The mean rate of infection detected at 24 hours was 0.025+/-0.004 copies of proviral DNA per cell while it was 0.047+/-0.005 at 48 hours post infection. These are both statistically significant from AZT controls (*$p<0.001$). Each mark represents the average of the mean of three plates from a separate donor.

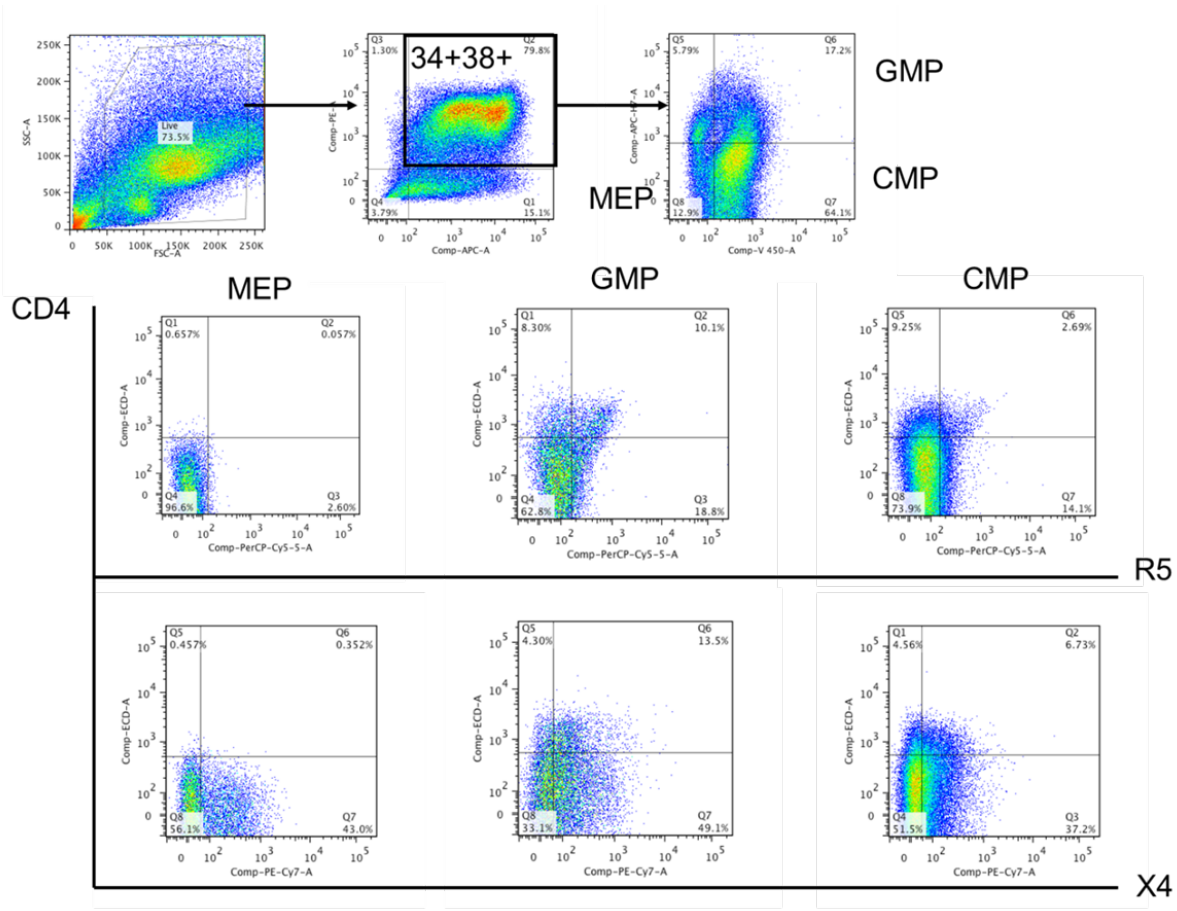

Figure 2.5 HIV Coreceptor Expression on Intermediate Hematopoietic Progenitors

Fetal liver derived CD34+ hematopoietic progenitors were enriched my MACS and then analyzed by flow cytometry for the presence of HIV coreceptors. To isolate the intermediate hematopoietic progenitor population, cells were initially gated on coexpression of CD34 and CD38 (see box upper center figure). Within this population, intermediate progenitors were discriminated based on their expression of CD45RA and CD123. Except for the MEP, coreceptors are expressed on all intermediate progenitors.

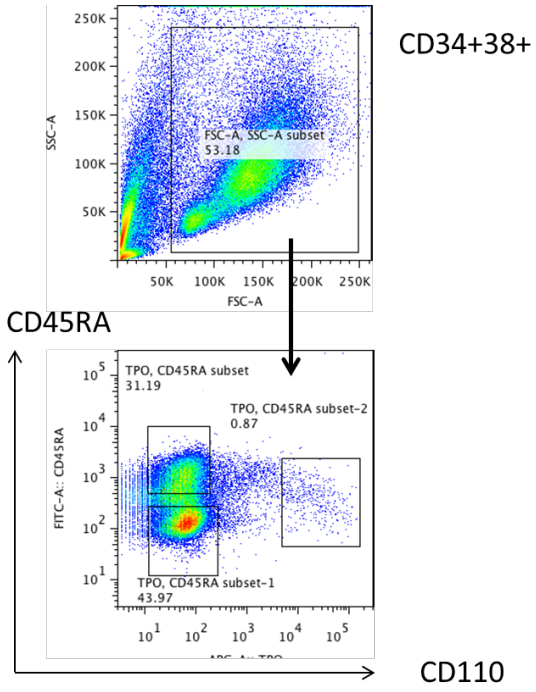

Figure 2.6 FACS sort strategy to isolate intermediate progenitors

To isolate populations of early and intermediate hematopoietic progenitors, cells were initially enriched for CD34 expression and then discriminated based on CD38 expression. The heterogeneous CD34+CD38- population is here defined as the HSC population. The CD34+CD38+ population is here defined as intermediate hematopoietic progenitors. Within this population, intermediate progenitors are discriminated based on CD45RA and CD110 expression. CD45RA-CD110- cells are defined as the common myeloid progenitor, CD45RA+CD110- cells are defined as the granulocyte monocyte progenitor, and CD45RA-CD110+ cells are defined as the megakaryocyte erythroid progenitor.

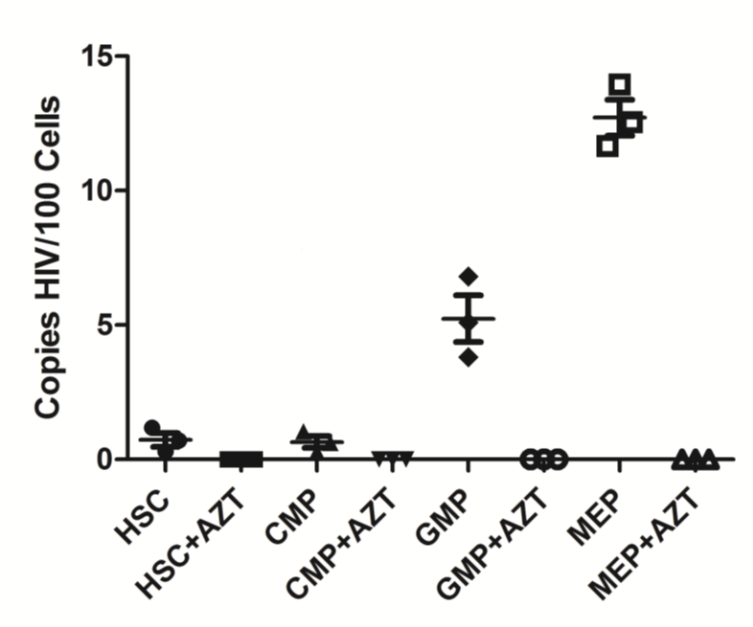

Figure 2.7 HIV Infection of Intermediate Hematopoietic Progenitors

FACS sorted fetal liver CD34+ HPC from three separate donors were infected with $HIV_{89.6}$ at an MOI of one. AZT pretreated cells were used as controls. Forty-eight hours post infection, cells were harvested and assayed by qRT-PCR for the presence of full-length viral DNA. The mean rate of infection in the HSC was 0.72+/-0.26, the CMP was 0.65+/-0.22, the GMP was 5.24+/-0.87, and the MEP was 12.72+/-0.67 per 100 cells. All were statistically different from AZT controls which were consistently negative (*$p<0.05$, **$p<0.01$). Each mark represents the average of the means of triplicate PCR assays for each donor.

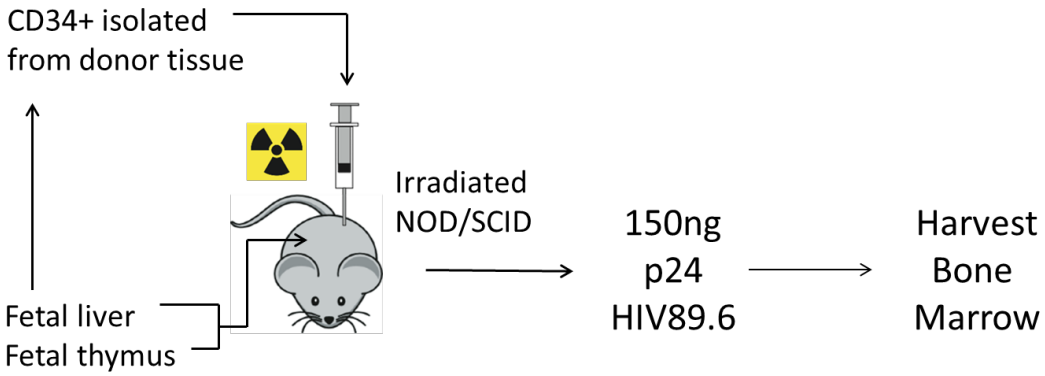

Figure 2.8 BLT Mouse Model of HIV Infection

Humanized BLT mice were prepared as previously described (98). The process is shown schematically here. Following confirmation of reconstitution of human hematopoietic cells, mice were infected with $HIV_{89.6}$. Two months following infection, productive infection was confirmed, mice were sacrificed, and bone marrow was harvested for hematopoiesis studies.

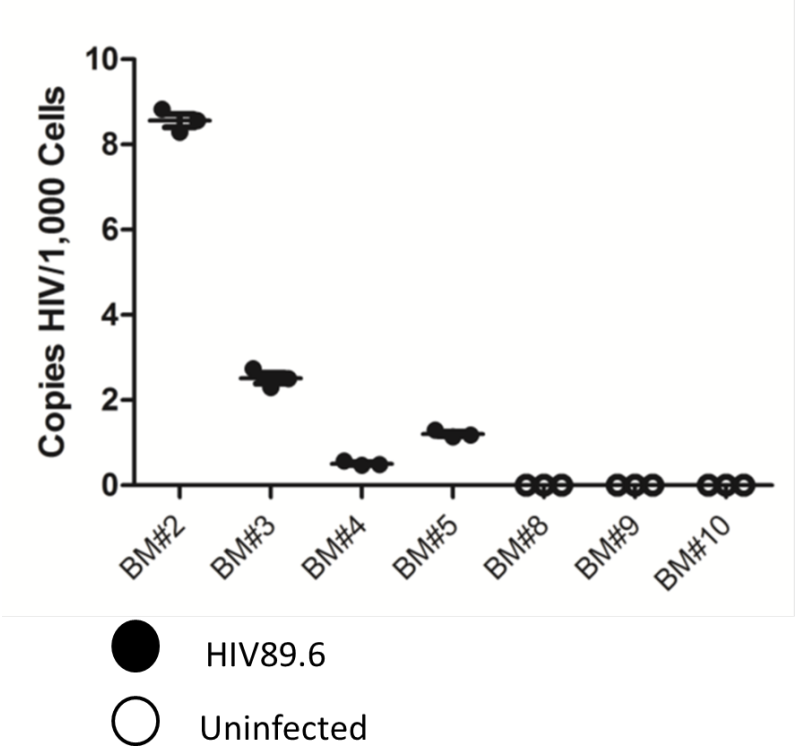

Figure 2.9 Proviral DNA in The Bone Marrow HPCs of Infected Mice

Human CD34+ hematopoietic progenitor cells were isolated from the bone marrow of infected or uninfected BLT mice. Cells were assayed by qRTPCR for full-length viral DNA. Viral DNA was detectible in the HPC of all infected mice while it could not be detected in uninfected mice. All were significantly different from the uninfected mice (*$p<0.001$). Each mark represents an individual PCR.

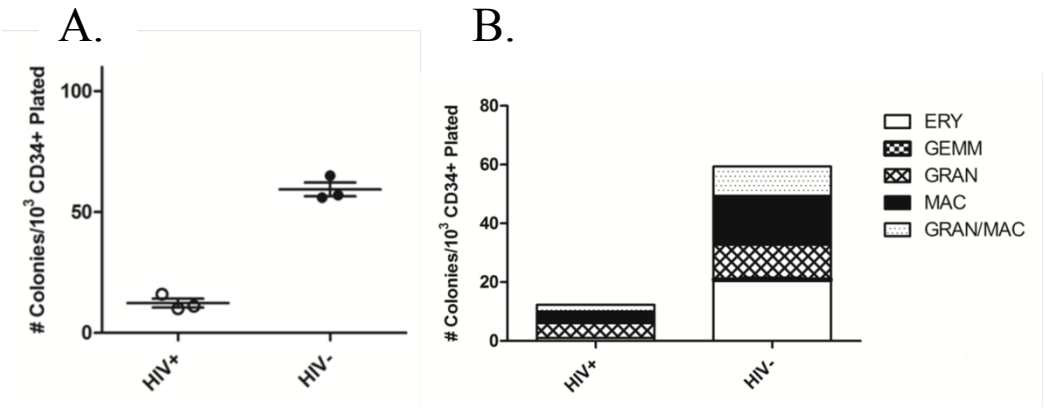

Figure 2.10 Bone Marrow Derived Colonies from $HIV_{89.6}$ Infected BLT Mice

A. The number of colonies that develop from 1,000 plated bone marrow derived human CD34+ HPC from infected mice is much smaller than from uninfected mice. The mean number of colonies that arise from cells from infected mice was only 12+/-2while it was 60+/-3 in uninfected mice (*p=0.0002).

B. Lineage commitment is also skewed in BLT mice infected with HIV. Notably there is a severe defect in erythroid colonies.

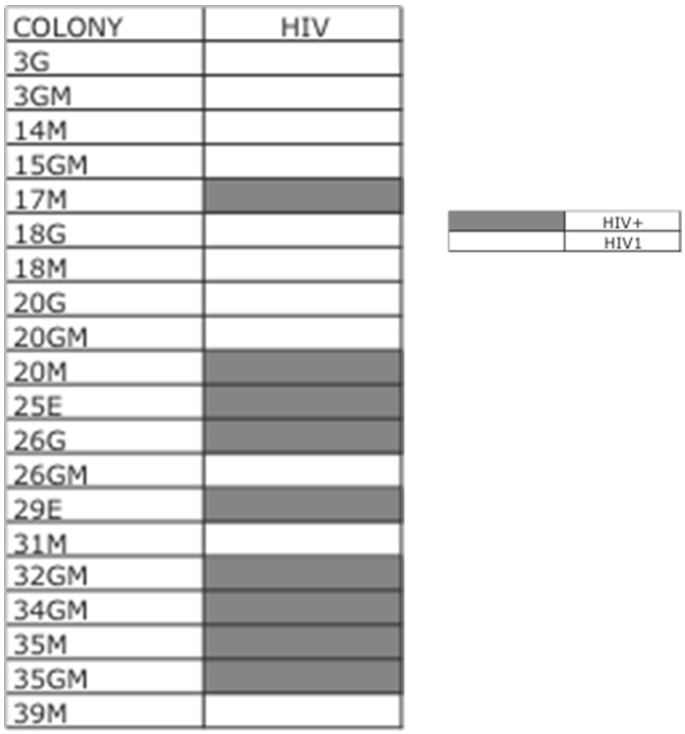

Figure 2.11 Colonies from infected mice harbor provirus

Single colonies were picked from methylcellulose plates derived from BLT mouse bone marrow CD34+ hematopoietic progenitors. Each bar represents a colony. The number of each represents a plate and is thus arbitrary. The letter following indicates the type of colony. G, granulocyte, M, macrophage, GM, mixed granulocyte-macrophage, E, Erythroid. Shaded bars indicate PCR positive for HIV proviral DNA.

Chapter 3

Results Part II: APOBEC3G Influences Multilineage Hematopoiesis

3.1 Knockdown of APOBEC3G

To determine the potential role A3G could play in hematopoiesis, anti-A3G siRNA was stably expressed in hematopoietic progenitors and these were examined for any impact on the development of terminal blood phenotypes. The FG-12 vector is a lentiviral siRNA expression vector that was derived from the HIV genome. The CMV promoter drives expression of the entire vector. The HIV LTR also enhances expression from two downstream expression cassettes. The upstream cassette is comprised of a PolIII promoter followed by a short hairpin RNA sequence. The downstream cassette is driven by the PolII ubiquitin-c promoter. This cassette was engineered to express marker and drug resistance genes. Marker genes were inserted immediately following the UbiC promoter followed by an internal ribosome entry site (IRES) to allow bicistronic expression of drug resistance genes. Either of two marker genes was used: enhanced green fluorescent protein (eGFP) or a truncated version of the low-affinity nerve growth factor receptor (ΔLNGFR). Previous studies have established the efficacy of using ΔLNGFR as a surface marker for selection and marking (147,148). Puromycin was used as the drug resistance gene.

Short hairpin RNA sequences were designed to knock-down A3G expression using the Ambion online siRNA design tools. When expressing siRNA from a lentiviral vector, it

must be designed as a precursor hairpin that will be processed in the target cell to the mature siRNA by host cellular machinery. Initial assays were performed with control siRNA that targets firefly luciferase and BLAST does not predict will cross-react with another cellular sequence. Five different sequences were designed that target different, distinct regions of the A3G transcript. They are designated by the number of the first nucleotide to which the siRNA binds in the A3G transcript (Fig3.1).

Due to the limited number of restriction sites in the FG12 vector, a two-step cloning process was required. First, the shRNA sequences were cloned into a pCDNA vector that contains either the H1 or U6 promoter. The promoter and the shRNA sequence were removed together and then inserted into the FG212 vector(Fig3.2). Anti-A3G shRNA were thereby cloned into the lentiviral shRNA expression vector FG12/ΔLNGFR-IRES-Puro or FG12/GFP-IRES-Puro (Fig3.3), referred to as FLIP and FGIP. Initially, all five knockdown sequences were tested under the control of the U6 promoter against a control knockdown sequence for firefly luciferase (siluc). CEM cells were transduced with each of the FLIP vectors expressing each shRNA. Forty-eight hours later, cells were sorted to high purity based on ΔLNGFR expression and analyzed by qRT-RTPCR for levels of A3G mRNA. Each of the five knockdown sequences effectively knocked down the expression of A3G while the control siluc sequence did not (Fig3.4). An A3G overexpression vector was also designed. A3G was inserted in place of the drug selection marker following the IRES. Interestingly, when CD34+ hematopoietic progenitors were transduced with this vector, colony growth was absolutely hindered suggesting A3G is toxic to these cells.

3.2 Colony Forming Assays-FGIPsi418 and FGIPsiluc

Once it was determined that the A3G knockdown siRNAs were effective, a single sequence was initially selected to assay for toxicity in hematopoietic stem and progenitor cells. FGIPsi418 was tested against FGIPsiluc and FGA3G. Fetal liver derived CD34+ HPC from three separate donors were transduced with each vector. Fourty-eight hours post-transduction, transduced cells and non-transduced controls were plated in complete methylcellulose and assayed two weeks later. A significant number of colonies were GFP+ when examined with a fluorescent microscope (Fig3.5). Further, colonies from all cultures were morphologically similar and all appeared normal and healthy.

When colonies were counted and scored for phenotype, there was a striking difference in the number of erythroid colonies in cultures derived from cells transduced with the A3G knockdown construct when compared to controls. Erythroid colony formation was significantly reduced in A3G cultures (Fig3.6). When considering the percentage of total colonies that are erythroid in nature, these colonies account for 44% of nontransduced and 47% of FGIPsiluc transduced cultures while accounting for only 23% in FGIPsi418 transduced colonies.

Next, all five sequences were assayed in HPC in part to determine if the previous observation of skewed lineage commitment could be attributed to off-target effects. For all subsequent in vitro studies, the FLIP panel of vectors was used to facilitate sorting of transduced cells. Fetal liver derived CD34+ cells were transduced with each of the knockdown sequences and the siluc control sequence. Forty-eight hours later, cells were sorted by MACS for ΔLNGFR expression and plated in complete methylcellulose. When

scored 14 days later, it was apparent that each of the five sequences produced a similar phenotype (Fig3.7A). While the total number of colonies remained relatively stable across samples, A3G depletion clearly skews hematopoietic lineage commitment away from erythropoiesis and toward myelopoiesis (Fig3.7B).

3.3 A3G Knockdown with the H1 Promoter

To address potential toxicity concerns with the U6 promoter, the shRNA panel was tested under the control of the H1 promoter. In addition, corresponding scramble control sequences were also designed as controls for each shRNA. CEM cells were again transduced with each knockdown and control sequence and MACS sorted for ΔLNGFR expression 48 hours later. RNA was isolated from a fraction of each sample and assayed by qRT-RTPCR for A3G expression. Again, all knockdown sequences were effective in diminishing A3G expression while it was maintained with scramble control sequences (Fig3.8). Fetal liver derived CD34+ HPC were again transduced with each knockdown and control sequence and MACS sorted for ΔLNGFR expression 48 hours later. When these sorted cells are cultured in complete methylcellulose for two weeks, the phenotype is similar to previous results (Fig3.9).

3.4 Confirmation of Knockdown in CD34+ Hematopoietic Progenitors

Further analysis, including western blots, animal experiments, and microarray analysis require a relatively large amount of starting material so two sequences, 418 and 718, and their scramble controls were selected for all subsequent studies as they were both effective in knocking down A3G, non-toxic, and target different parts of the A3G transcript. These sequences were then tested for the first time for their ability to

knockdown A3G expression in CD34+ hematopoietic stem cells, at both the mRNA level and the protein level. CD34+ HSC were transduced with these vectors and sorted by MACS to high purity for ΔLNGR expression before harvesting for RNA and protein analysis. As indicated by qRT-RTPCR, HPC transduced with knockdown constructs show a significant reduction in A3G expression from both shRNA constructs at the mRNA level while the scramble sequence controls did not interfere with A3G expression (Fig3.10A). To confirm depletion of A3G at the protein level, western blots were performed. These knockdown sequences were also effective in depleting A3G protein within 48 hours of transduction while the control scramble sequences do not impact A3G expression (Fig3.10B). It is of note that few antibodies targeting A3G were available when these studies were initiated thus, anti-sera against A3G was raised in rabbits against a synthetic N-terminal A3G peptide. Anti-sera was titred on lysates of E coli engineered to express A3G (Fig3.11)

3.5 A3G Knockdown in Hematopoietic Subsets- Detailed Colony Forming Assays

For a more detailed analysis of the impact of A3G on lineage commitment, HSC were transduced with each of the shRNA and control vectors, sorted to purity via MACS 48 hours later. Cells were either seeded in complete methylcellulose or harvested for RNA extraction. When scored 14 days later, it is evident that erythro-megakaryopoiesis is impaired in knockdown cultures. While total colony number remains consistent among knock-down and control groups, red colony formation is reduced by approximately 50% compared to controls (Fig3.12B). The total number of colonies averaged 123+/-6 per 1,000 cells plated from si418 transduced progenitors while it is 124.3+/-3 per 1,000 cells

plated from the corresponding control cells (NS, p=0.85). Colonies derived from si718 transduced progenitors gave rise to an average of 110+/-4 per 1,000 cells plated compared to those transduced with the scramble control sequence which give rise to an average of 121+/-4 per 1,000 cells plated (NS, p=0.18)(Fig3.12A).

The percentage of erythroid colonies that arise from si418 transduced progenitors was only 17+/-3 while 43+/-2% of colonies that develop from the corresponding scramble718 transduced progenitors (p=0.0012). Likewise, the percentage of erythroid colonies that arise from si718 transduced progenitors was 18+/-4% while it is 42+/-2 from scramble718 transduced cells (P=0.007). GEMM accounted for less than 5% of colonies on any given plate and did not vary between knockdown and controls(3.12B).

HSC transduced with the knockdown constructs likewise show impaired potential for megakaryocyte differentiation. There is an approximately 50% reduction in the number of megakaryocyte colonies in A3G knockdowns compared to controls when cells are plated in collagen based methylcellulose that suppports megakaryocyte growth. Progenitors transduced with the si418 construct gave rise to 54+/-4 megakaryocyte colonies per 5,000 cells plated while progenitors transduced with the correesponding scramble sequence gives rise to 91+/-5 per 5,000 cells plated (p<0.0001). Similary, progenitors that were transduced with the si718 construct gave rise to 46+/-4 megakaryocyte colonies per 5,000 cells plated while progenitors that were transduced with the corresponding control sequence gave rise to 96+/-6 colonies per 5,000 cells plated (p<0.0001). Non-transduced progenitors gave rise to 111+/-7 per 5,000 cells plated and this was not significantly different from progenitors transduced with the

scram418 construct (p=0.0757) nor the scram718 control construct (p=0.2095). Colony morphology does not appear to vary between conditions (Fig3.13B).

3.6 Knockdown of A3G in BLT Mice

To determine if A3G knockdown has any *in vivo* effect, humanized BLT-NSG mice were reconstituted with CD34+ cells transduced with FGIP-si418 or FGIP-scram418. Fetal liver and thymic tissue from a single donor were processed for implantation into 8 mice. A portion of the liver was processed further to isolate CD34+ HSC. Once isolated, cells were transduced with vectors on retronectin coated plates overnight. On the following day, all cells were harvested from the transduction and were injected/implanted with remaining liver and thymus. Half of the cells were mixed with matrigel and inserted into the implant and half were injected by tail vein. Three months following engraftment, bone marrow was harvested and cells isolated by FACS for CD34+GFP+ expression. At the time of harvest, there were three mice in the control group and five mice in the A3G knockdown group. At three months, mice were sacrificed and bone marrow was processed for each mouse. In all mice, bone marrow showed significant engraftment of transduced cells as indicated by flow cytometry. Of live cells in the marrow, ~30% were CD45/GFP double positive in each mouse (Fig3.14A).

Flow cytometry was performed on cells isolated from the bone marrow to determine the presence of erythroid and megakaryocyte progenitors. Interestingly, expression of the EPOr was strikingly reduced in the marrow of mice reconstituted with HPCs transduced with A3G knockdown constructs. TPOr is also significantly reduced in these cells, though not to as great an extent as EPOr. While the EPOr-TPOr coexpressing MEP is a

rare population, it is likewise diminished in mice reconstituted with A3G knockdown HPCs (Fig3.15).

Bone marrow CD34+ cells were isolated by MACS, then these CD34+ cells were FACS sorted to high purity for GFP expression(Fig2.26B). Sorted cells were plated in methylcellulose and scored after fourteen days. CD34+GFP+ cells isolated from the bone marrow of these mice and plated in methylcellulose showed diminished capacity for erythropoiesis (Fig3.16B). The mean of the percent red colonies produced from A3G knockdown cells was 6.5+/-0.4 compared to 20+/-0.8 in controls, $p<0.0001$. Again the total colony number remained approximately the same, 72+/-2 in A3G knockdowns and 66+/-2 in controls (Fig3.16A). This would suggest a switch between the erythro-megakaryocyte and granulo-monocyte lineages (Fig3.17). There were no apparent difference between groups in the distribution of granulocyte, monocyte, and mixed colonies.

3.7 Microarray Analysis of A3G Depleted CD34+ Hematopoietic Progenitors

RNA was isolated from the same population of vector transduced and sorted cells used to seed the methylcellulose in the above experiments. This RNA was used for microarray analysis to determine differential gene expression between A3G knockdown and control construct transduced cells. RNA was hybridized to Affymetrix (Santa Clara, CA) Human Gene 1.0 ST GeneChips™ and read at the University of California, San Diego Clinical Microarray Core. Data was subsequently analyzed with dChip software (http://biosun1.harvard.edu/complab/dchip/). While dysregulated genes were strikingly consistent with colony assay data, no gene showed more than two-fold difference

between knockdown and controls. No consistent or significant gene ontology assignments were made when analyzed by DAVID. Analysis of transcription factors associated with these genes, however, did prove interesting. TELiS (transcription element listening system) is an online data base of known transcription factor binding sites associated with specific genes. When the list of the 232 most disregulated genes was analyzed by TELiS (www.telis.ucla.edu) a strikingly strong association was made with the transcription factor GATA-1. The majority of the genes were shown to have a GATA-1 binding site with a p value >0.001. Interestingly GATA-1 itself was one of the downregulated genes in the absence of A3G (Fig3.18).

3.8 Lack ofConfirmation of GATA11 Downregulation

In order to confirm the downregulation of GATA1 expression, primers were designed to detect GATA-1 transcripts by qRT-PCR. The original samples submitted for microarray analysis and after repeated attempts, GATA-1 downregulation could not be confirmed in the original samples. Additional samples were tested in the same fashion but at different timepoints post-transduction: 24, 48, and 72 without success. Samples from cord blood were also tested to the same end. However, detection of a 1.8 fold downregulation is exceedingly difficult. As a small disruption of mRNA production could lead to an amplified effect in protein production, GATA-1 protein levels were examined in HPC transduced with A3G knockdown constructs compared to controls. While GATA-1 was readily detected in the bulk CD34+ population obtained from fetal liver, its expression did not diminish with the depletion of A3G.

3.9 microRNA RT-PCR

As A3G has been implicated in miRNA regulation, levels of miRNA that are known to influence human hematopoiesis were examined. Using a validated syber-green based assays for microRNA expression of miR-150, miR 15a, miR-126, and miR-28. Again, multiple samples from multiple donors showed no consistent disregulation in any of the miRNA known to influence human hematopoiesis.

3.10 APOBEC3G in Intermediate Hematopoietic Progenitors and Thymocytes

To address the mere >2 fold dysregulation of genes when A3G is knocked down in hematopoietic progenitors, the dMap hematopoietic gene expression database was examined. As revealed by the Differentiation Map database (21), A3G expression fluctuates tremendously through the process of developmental hematopoiesis (http://www.broadinstitute.org/dmap/home). The variability lies between cell types and stages of development. Interestingly, there are striking differences in levels of A3G in early and intermediate hematopoietic progenitors. It is unclear why a retroelement restrictive element would fluctuate in a lineage specific fashion.

According to dMap, levels of A3G are very low in the hematopoietic stem cell, but rise sharply in the common myeloid progenitor. There are likewise high levels of A3G in the megakaryocyte-erythroid progenitor, sharply contrasting the very low levels in the granulocyte-monocyte progenitor (Fig3.19A). These data were confirmed by qRT-RTPCR in sorted populations of intermediate hematopoietic progenitors. Differential A3G activity was first noted in the CEM and CEMss T cell lines . A3G is expressed at high levels in CEM cells and low levels in CEMSs cells. For this reason, these cells are used as the standards for A3G expression. The bulk population of CD34+CD38+

intermediate progenitors was initially isolated from fetal liver by MACS. The CMP, the GMP, and the MEP are then purified from this population by FACS. RNA extracted from these populations was then analyzed by qRT-PCR for levels of A3G transcript relative to 18s ribosomal RNA. A3G expression in the CMP and MEP was very similar to that in CEM cells while it was much lower in the HSC and GMP populations (Fig3.19B).

The only populations of developing cells not cataloged by dMap are developing T-cells. The database was compiled with samples from umbilical cord blood to obtain stem cell populations and peripheral blood to obtain terminally differentiated cells. Thymocytes reside in the thymus and were not analyzed. To determine the nature of A3G expression in developing T-cells, fetal thymus was obtained from three different donors and populations of developing thymocytes were isolated. Thymocytes were MACS sorted based on CD8 and CD4 expression into double negative, double positive, and single positive populations. In addition, CD34+ HPC were obtained from the livers of the same donors. Sorting was confirmed by flow cytometry (Fig3.20). Each population was then analyzed by qRT-PCR for A3G transcripts relative to 18s ribosomal RNA. When compared to the CEM T-cell line, CD34 HPC express high levels of A3G, levels that decline through T-cell development. Levels are still relatively high in double-negative thymocytes, dropping in double-positive thymocytes, and still lower in single positive 4 (SP4) thymocytes with a rebound in single positive 8 (SP8) thymocytes (Fig3.21).

3.11 A3G Knockdown in Sorted Hematopoietic Progenitors

Perhaps it is within these early and intermediate populations themselves that A3G is acting to influence development. To explore this possibility, each population of early and intermediate progenitors was sorted by FACS to determine how A3G knockdown influences each. Each population was distinguished by its expression of CD34, CD38, CD110 (TPOr), and CD45RA. These populations were FACS sorted from three separate fetal livers to high purity based on these markers. Each population was then transduced with either FLIPsi418 or FLIPscram418 at an MOI of 5 on Retronectin® coated plates. Twenty-four and forty-eight hours post-transduction, cells were harvested, washed, and sorted by MACS to high purity (98%) for dLNGFR expression and either plated in complete methylcellulose or lysed for RNA isolation. Two weeks later, colonies were counted and phenotyped. Again, the total number of colonies was similar between knockdowns and controls (Fig3.22). Total colonies derived from siRNA and control vector transduced HSC sorted for ΔLNGFR expression and plated 24 hours post-transduction averaged 53+/-6 and 56+/-11 respectively. This difference was not statistically significant. While the total colony number was consistent among all conditions, lineage commitment was skewed away from erythroid development. The HSC transduced with A3G siRNA and plated 24 hours post transduction gave rise to far fewer erythroid colonies than did its control sequence transduced counterpart. Only 9+/-2.5% colonies derived from siRNA transduced HSC were erythroid in nature while 27+/-4% of colonies were erythroid in cultures derived from control scramble418 transduced HSC ($p=0.0028$). Similar differences were seen in colonies derived from the CMP sorted and plated 24 hours post-transduction. Again, the total colony number was similar.

However, 18+/-1% of colonies derived from siRNA transduced cells were erythroid in nature while 40+/-2% of colonies from control cells were erythroid in nature (Fig3.23). This phenotype was consistent in cells sorted and plated at 48 hours post-transduction. Total colony number was again virtually the same between conditions. The relative proportion of erythroid and myeloid colonies was again skewed toward myeloid development when A3G expression was knocked down. Cultures derived from progenitors transduced with siRNA against A3G gave rise to 10+/-2% erythroid colonies while those transduced with the scramble sequence gave rise to 28+/-3% erythroid colonies ($p=0.0045$). The transduced CMPs plated at this timepoint yielded similar results. CMP depleted of A3G gave rise to 21+/-2% erythroid colonies while control transduced CMP gave rise to 43+/-2% erythroid colonies ($p=0.0015$)(Fig3.23).

3.12 Microarray analysis of sorted progenitors

RNA from three donors was extracted from sorted CMP forty-eight hours following transduction with FLIPsi418 or FLIPscram418 and then MACS sorted for high purity based on ΔLNGFR expression. RNA was submitted to the UCLA Clinical Microarray Core where it was hybridized to Affymetrix U133 plus 2 arrays. Data was analyzed by dCHIP and the DAVID gene ontology tools.

A number of genes relevant to human hematopoiesis were found to be dysregulated in expression in the context of A3G depletion. Again, a number of the hemoglobin genes, alpha, beta, and delta, were downregulated as was the canonical erythroid marker glycophorin-A. More interesting are the dysregulated genes specifically related to RNA editing. Of note, Dicer, the protein that is responsible for processing siRNA and miRNA

precursors was upregulated as were multiple members of the mediator complex that is responsible for mediating general transcription. Also, Decapping Enzyme Homolog-2 (DCP2), another critical member of the siRNA-miRNA pathway was found to be upregulated in A3G-knockdown hematopoietic progenitors. When gene ontology analysis was performed on the genes found to be most dysregulated, the functional and annotation ontology points to RNA editing and alternative splicing pathways. Indeed, 49% of genes were classified as being involved with alternative splicing, $p<0.001$. To validate these results, some of the dysregulated genes were selected for further analysis by qRT-RTPCR. The genes that were selected were Epor, Glycophorin-a, Transferrin2r, Il-6r, and Il-12r. The dysregulation that was detected by microarray analysis was confirmed for each of these (Fig3.24).

418	Top		5'- ACCGTACCACCCAGAGATGAGA TTCAAGAGA TCTCATCTCTGGGTGGTACTT TTTC-3'
	Bottom		5'-TCGAGAAA AAGTACCACCCAGAGATGAGA TCTCTTGAA TCTCATCTCTGGGTGGTAC -3'
457	Top		5'- ACCGTGGAGGAAGCTGCATCGT TTCAAGAGA ACGATGCAGCTTCCTCCACTT TTTC-3'
	Bottom		5'-TCGAGAAA AAGTGGAGGAAGCTGCATCGT TCTCTTGAA ACGATGCAGCTTCCTCCAC -3'
534	Top		5'- ACCGGGATATGGCCACGTTCCT TTCAAGAGA AGGAACGTGGCCATATCCCTT TTTC-3'
	Bottom		5'-TCGAGAAA AAGGGATATGGCCACGTTCCT TCTCTTGAA AGGAACGTGGCCATATCCC -3'
568	Top		5'- ACCGGTTACCCTGACCATCTTC TTCAAGAGA GAAGATGGTCAGGGTAACCTT TTTC-3'
	Bottom		5'-TCGAGAAA AAGGTTACCCTGACCATCTTC TCTCTTGAA GAAGATGGTCAGGGTAACC -3'
718	Top		5'- ACCGTTCGTGTACAGCCAAAGA TTCAAGAGA TCTTTGGCTGTACACGAACTT TTTC-3'
	Bottom		5'-TCGAGAAA AAGTTCGTGTACAGCCAAAGA TCTCTTGAA TCTTTGGCTGTACACGAAC -3'

Figure 3.1 Anti-APOBEC3G shRNA Hairpin Sequences

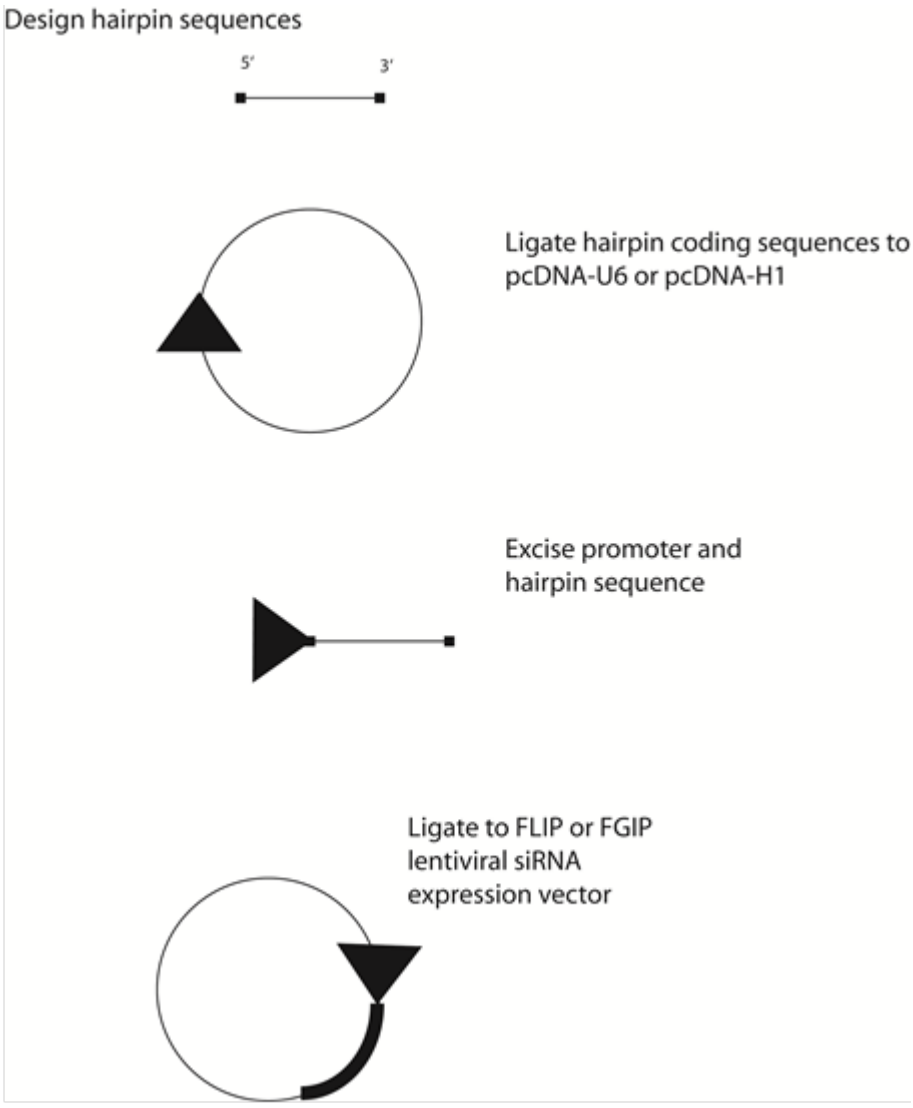

Figure 3.2 FG12 Cloning strategy

Engineering shRNA sequences in the FG12 vector requires a two-step cloning procedure. The shRNA sequence is first inserted into a pcDNA plasmid that contains either the H1 or U6 PolIII promoter. The promoter and the shRNA sequence are removed from the pcDNA plasmid, purified, then inserted into the FG12 shRNA expression vector that already includes marker and selection genes.

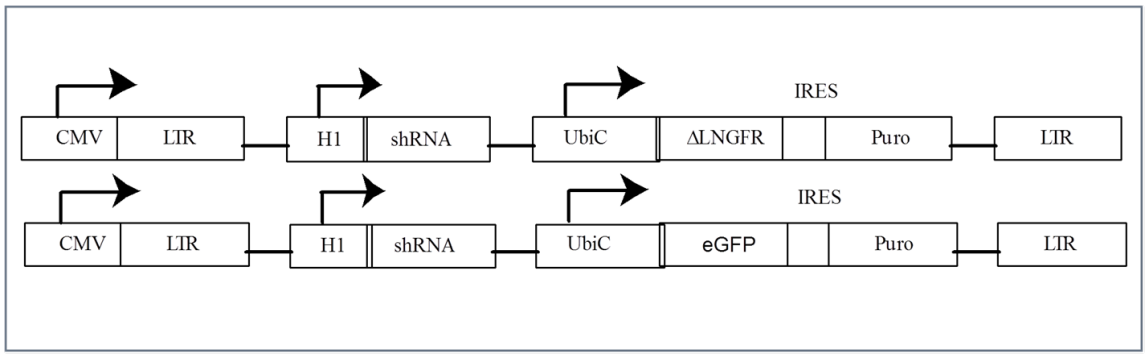

Figure 3.3 A3G Knockdown vectors

A3G knockdown vectors were designed based on the FG12 shRNA expression vector. Expression of the entire vector is driven by the CMV promoter. The HIV-1 LTR enhances downstream expression from two expression cassettes. First, shRNA expression is driven by either U6 or H1 PolIII promoters. Next, identification and selection markers are driven by the Ubiquitin C promoter. The top construct was designed to express a truncated version of the low affinity nerve growth factor receptor that can be used as a surface to mark transduced cells. The bottom construct was designed to express the fluorescent marker enhanced green fluorescent protein.

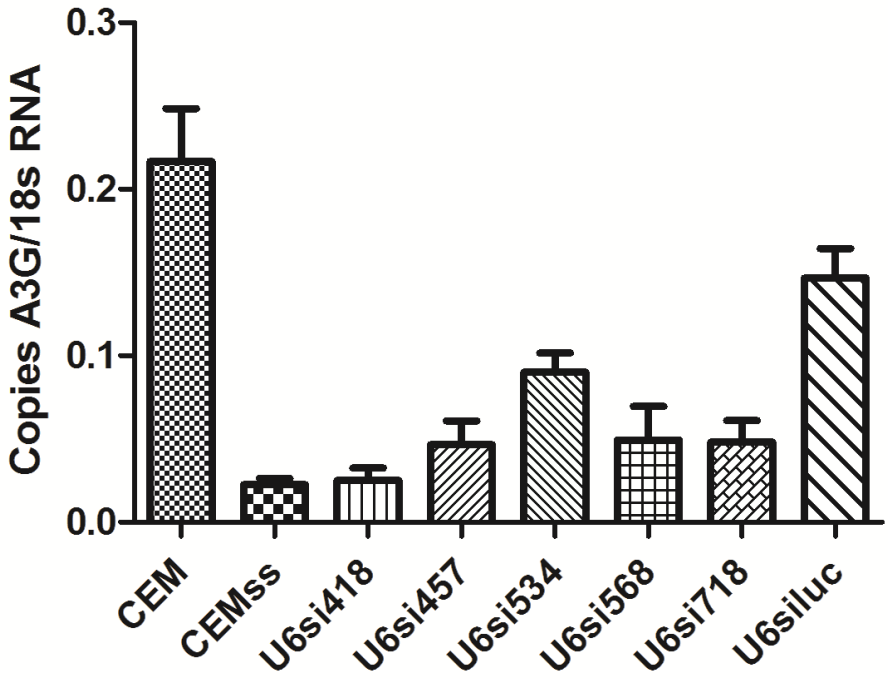

3.4 qRT-RTPCR for A3G Transcripts in Transduced CEM Cells

CEM cells were transduced with FLIP vectors containing each of the 5 A3G knockdown sequences. Forty-eight hours later they were MACS sorted for ΔLNGFR expression and assayed by quantitative reverse transcriptase-mediated real-time PCR for A3G mRNA relative to 18s rRNA. All sequences are effective in diminishing A3G expression and are different from both nontransduced CEMs and CEMs transduced with the siluc control.

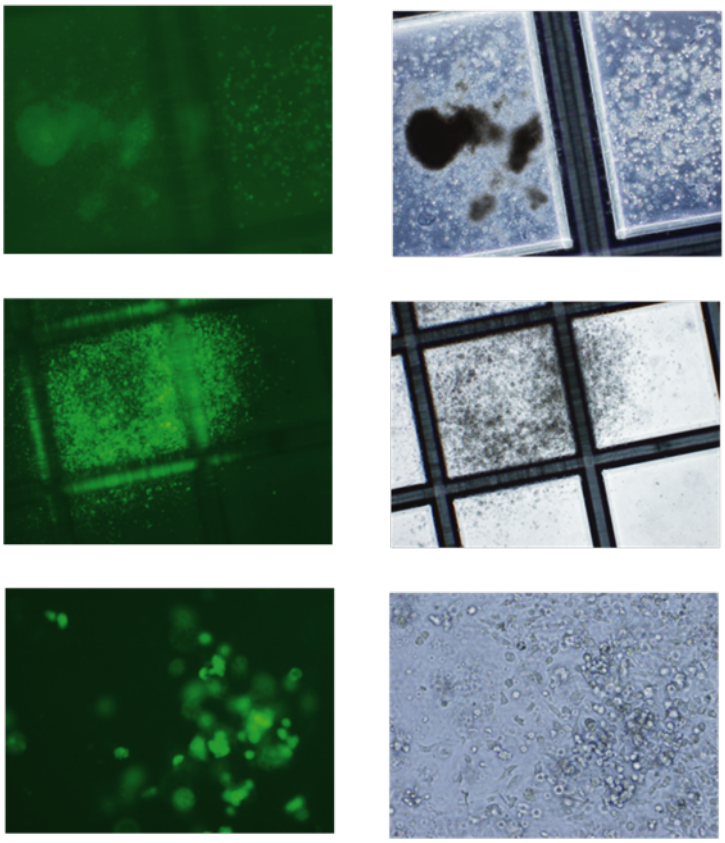

Figure 3.5 FGIP Vector Expression in Hematopoietic Colonies

Two weeks following plating, FGIP colonies appear morphologically normal and express eGFP. Erythroid and macrophage colonies, top, granulocyte colonies, middle, and mixed granulocyte-monocyte colonies, bottom, all appear to tolerate transduction by FGIP A3G knockdown vectors.

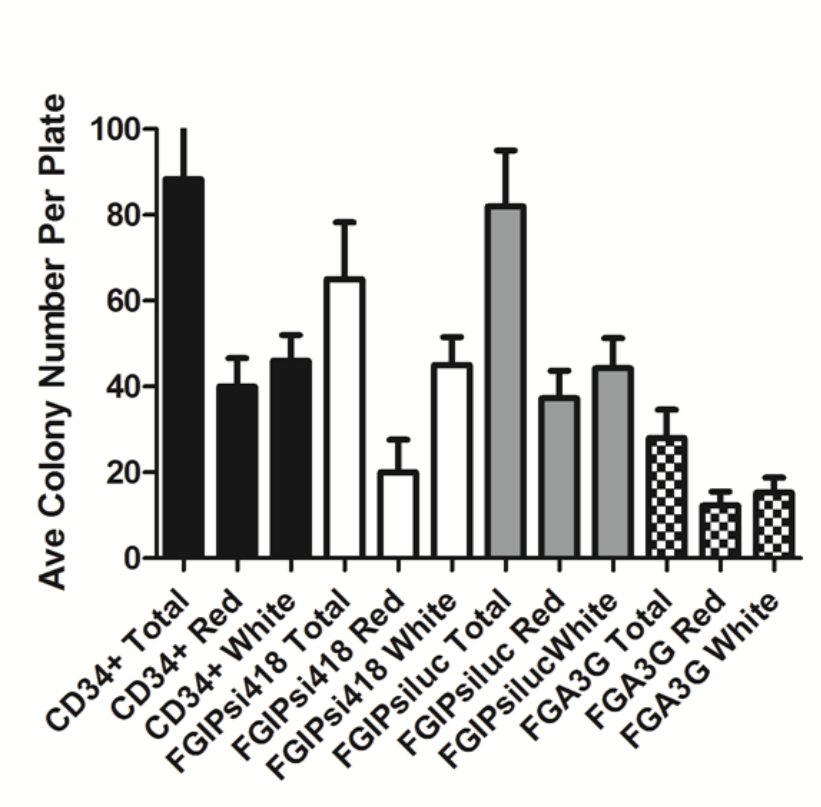

Figure 3.6 Colony Forming Assays from A3G Manipulated Progenitors

Fetal liver derived CD34+ HPC were transduced with A3G knockdown or overexpression vectors, then plated in complete methylcellulose. Control FGIPsiluc transduced cultures were similar to nontransduced while FGIPsi418 transduced cultures showed a significant defecit in erythroid colony formation (*$p<0.01$). The FGA3G overexpression vector diminished overall colony growth.

A. B.

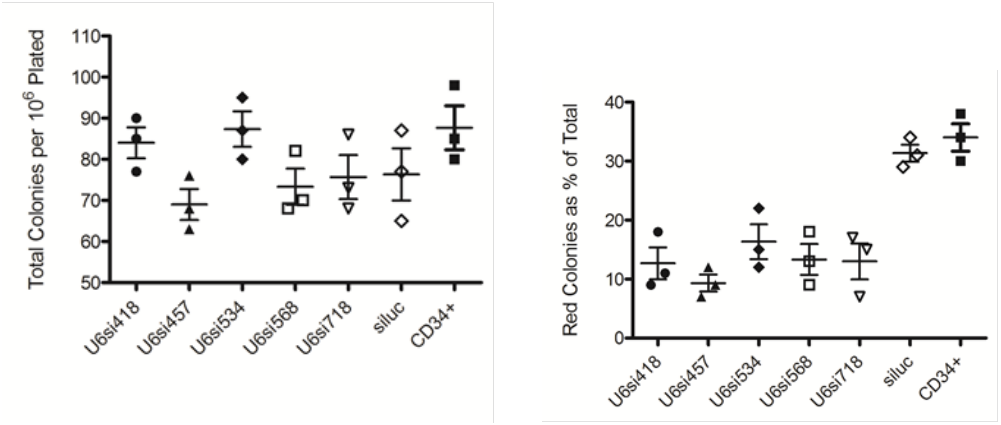

Figure 3.7 U6 A3G knockdown

A. Five different shRNA sequences were tested for their ability to knockdown A3G expression in fetal liver derived CD34+ hematopoietic progenitor cells from three different donors. As a control for exogenous RNA expression, shRNA targeting firefly luciferase was used. Each A3G knockdown sequence significantly diminished the growth of erythroid colonies compared to nontransduced HPCs ($p>0.001$) while the siluc control vector did not.

B. Total colony number was relatively consistent across cultures. There were no significant differences between the total number of colonies grown from each.

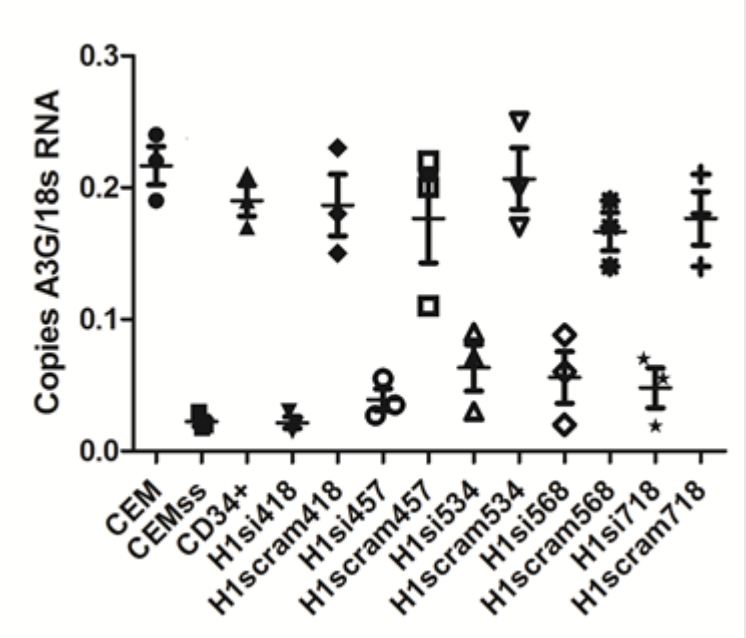

Figure3.8 qRTPCR Analysis of A3G Knockdown from the H1 Promoter with Scramble Controls

Consistent with previous results, the A3G knockdown shRNA sequences are also effective under the control of the H1 promoter. Each was tested in fetal liver derived CD34+ HPC from three different donors transduced with FLIP vectors. Cells were sorted for ΔLNGFR expression 48 hours post-transduction and analyzed by qRT-RTPCR for A3G expression. Corresponding scramble control sequences were also designed and tested. All shRNA sequences are significantly different from their scramble controls (*$p<0.001$). Scramble control vectors did not diminish A3G mRNA significantly when compared to nontransduced CD34+HPC.

A.

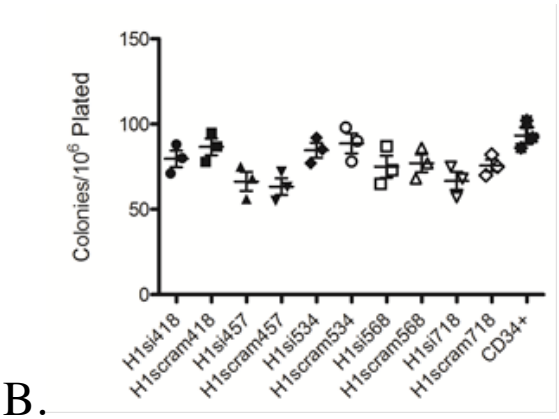

B.

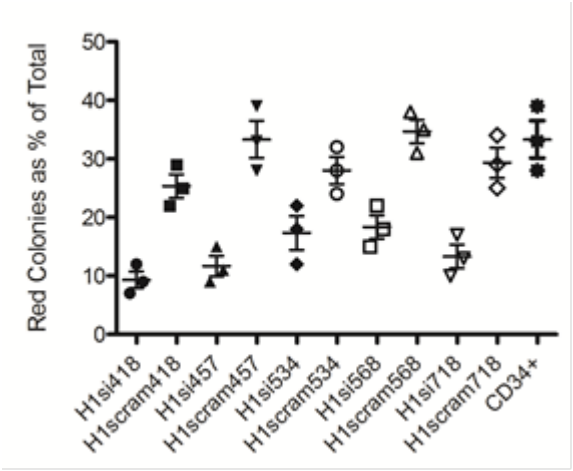

Figure 3.9 Colonies from A3G Knockdown Constructs Under the H1 Promoter

A. Total colonies from CD34+ HSC transduced with A3G knockdown and corresponding scramble control sequences are not significantly different from each other or from nontransduced cells.

B. The relative percentage of erythroid colonies is diminished in all cultures derived from CD34+HPC transduced with A3G knockdown vectors while those derived from control transduced sequences do not differ in erythroid potential from nontransduced cells

A.

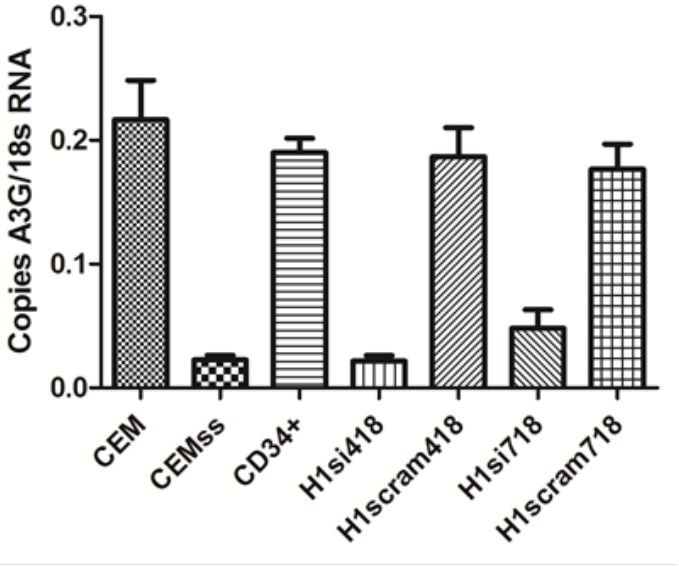

B.

CD34+ **si418** **scram418** **si718** **scram718**

Figure 3.10 APOBEC3G Protein Depletion

A. qRT-RTPCR analysis of A3G transcripts in fetal liver derived CD34+ HPC. Results represent three donors, each sample assayed in triplicate. Cells that were transduced withA3G knockdown constructs are depleted in A3G expression compared to scramble controls which do not appear to impact A3G expression significantly.

B. Western blot analysis of CD34+ HPC transduced with the same vectors confirms depletion of A3G protein as well. 50 μg whole cell extract from each sample was assayed.

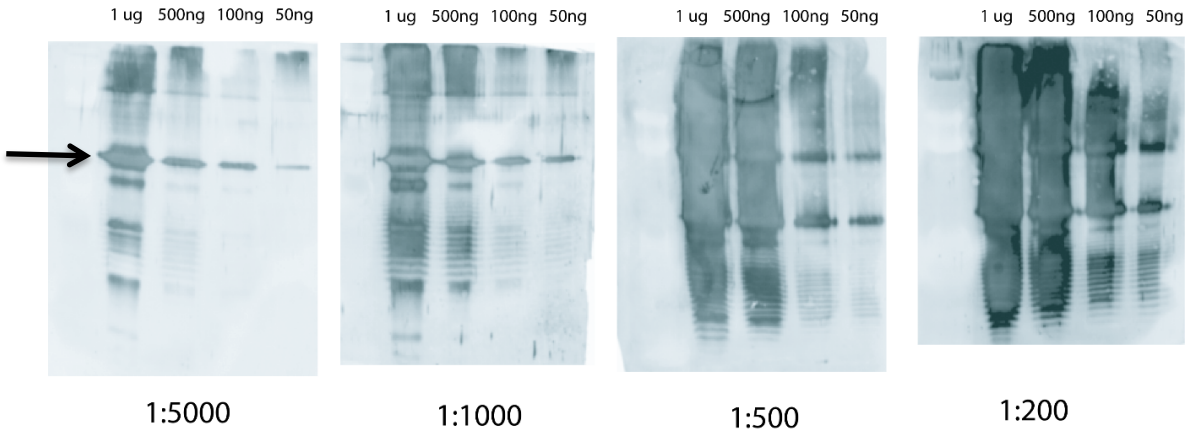

Figure 3.11 Titrations of αA3G antisera

Rabbit αA3G sera was raised against a synthetic A3G peptide. Various concentrations of bacterial lysate from E coli engineered to overexpress A3G were tested against various concentrations of A3G antisera. It was determined that 50ng of lysate was ideal for the standard when antisera is used at a concentration of 1:1000. Arrow indicates the band for A3G.

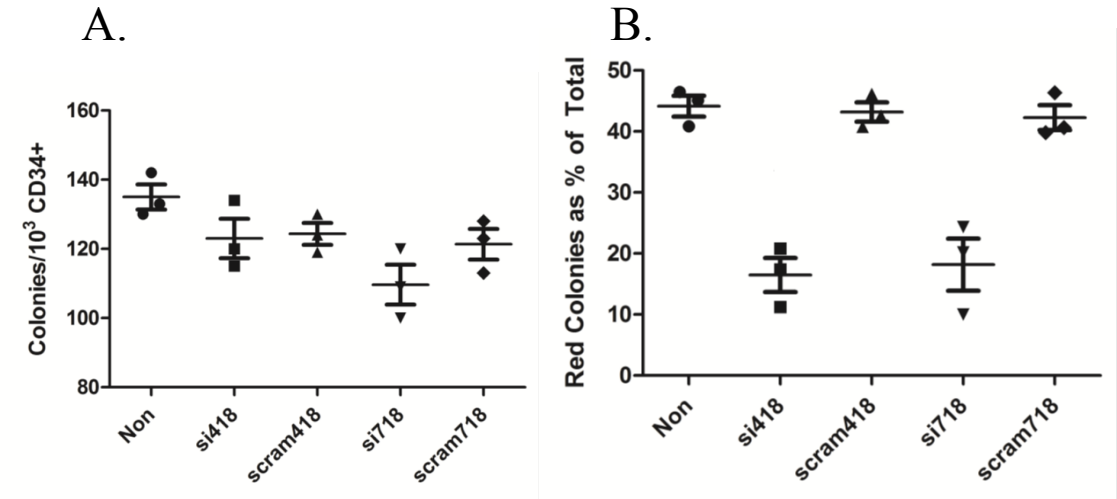

Figure 3.12 Colony Forming Assays: A3G Knockdown and Scramble Controls

A. Consistent with previous results, there are no significant differences in the total colony numbers in cultures derived from fetal liver CD34+ HPC from three donors transduced with FLIP vectors containing either A3G knockdown sequences or corresponding scramble control sequences.

B. Consistent with previous results, cultures derived from cells transduced with A3G knockdown vectors give rise to significantly fewer erythroid colonies than those derived from cells transduced with scramble control sequences or nontransduced CD34+ HPC.

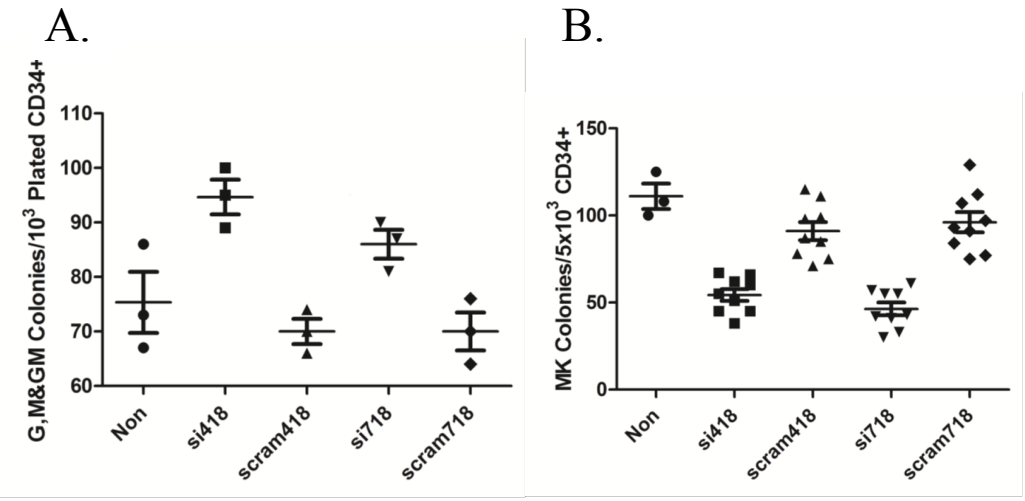

Figure 3.13 A3G Knockdown in Myelopoiesis and Megakaryopoiesis

A. While the erythroid colonies were diminished in the context of A3G knockdown, the opposite was true of myeloid colonies. There was an apparent shift away from erythropoiesis and towards myelopoiesis when A3G is depleted in HPCs.

B. Like erythropoiesis, megakaryopoiesis was impaired when A3G expression is diminished. HPC transduced with the si418 construct gave rise to 54+/-4 megakaryocyte colonies per 5,000 cells plated while HPC transduced with the corresponding scramble sequence gives rise to 91+/-5 per 5,000 cells plated ($p<0.0001$). HPC that were transduced with the si718 construct gave rise to 46+/-4 megakaryocyte colonies per 5,000 cells plated while HPC that were transduced with the corresponding control sequence gave rise to 96+/-6 colonies per 5,000 cells plated ($p<0.0001$).

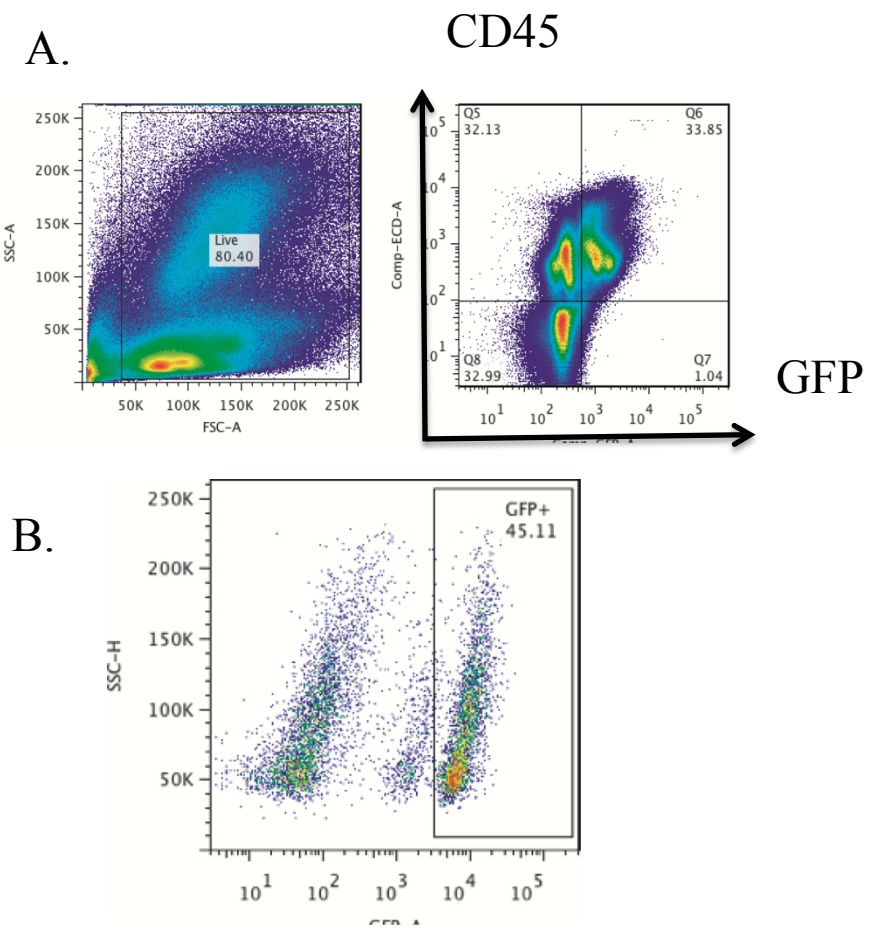

Figure 3.14 Reconstitution of BLT Marrow and Sort

A. The bone marrow of the BLT mouse showed significant reconstitution with human leukocytes as is evidenced by flow cytometry. More than 60% of cells in the marrow expressed the human CD45 leukocyte antigen and approximately half of them were positive for GFP indicating vector transduction.

B. CD34+ were MACS sorted to high purity and the FACS sorted to high purity for GFP expression to obtain vector transduced human hematopoietic progenitors.

A. B.

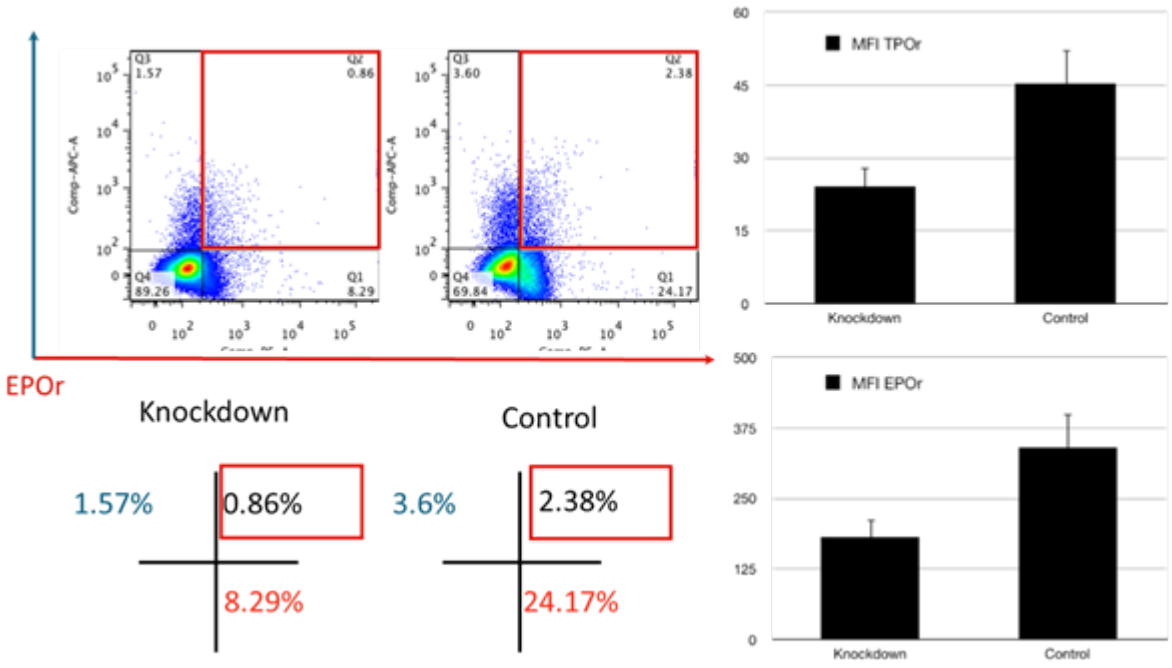

Figure 3.15 Flow Cytometric Analysis of BLT Marrow

A. Expression of both the erythropoietin receptor and the thrombopoietin receptor were significantly reduced in mice reconstituted with A3G knockdown cells. Crosses in lower figure represent the distribution of the quadrants in the flow cytometry panels above.

B. Mean Fluoresence Intensity (MFI) when measured across all mice is significantly reduced for the erythropoietin receptor and the thrombopoietin receptor in A3G knockdown animals.

A

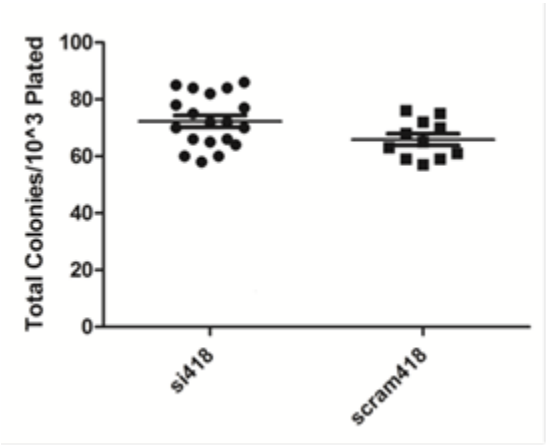

B

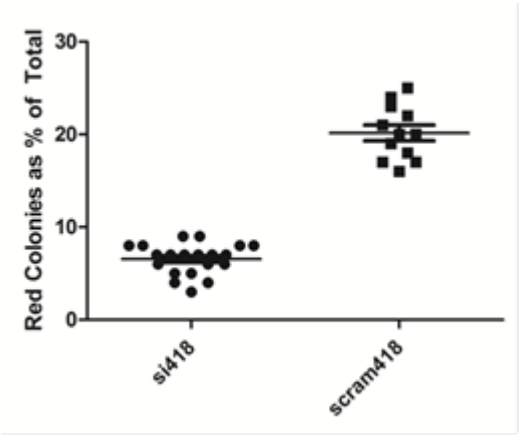

Figure 3.16 Colonies Derived from A3G Knockdown Mice are Deficient in Erythropoiesis

A. The total number of colonies derived from CD34+ HPC from the bone marrow of BLT mice is similar in A3G knockdown cultures compared to scramble control.

B. The percentage of red colonies in the A3G knockdown cultures is significantly lower than that in scramble controls.

Each mark represents one methylcellulose plate. Three plates were made for each mouse, n=5 in the knockdown group, n=3 in the scramble control group.

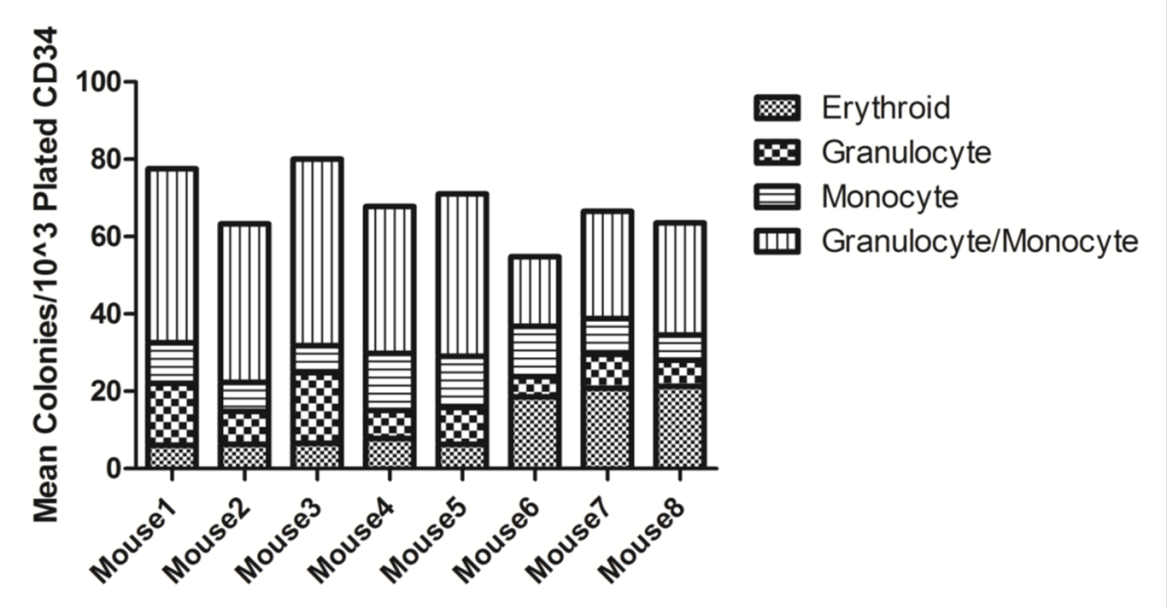

Figure 3.17 Colonies Derived from A3G Knockdown Mice are Deficient in Erythropoiesis

Mouse1-5 were reconstituted with A3G knockdown vector FGIPsi418 transduced hematopoietic progenitors while mouse 6-8 were reconstituted with scramble control vector FGIPscram418t transduced hematopoietic progenitors. While total colonies remain the same between groups there is an apparent skewing in lineage commitment in A3G knockdown mice compared to scramble controls.

A.

EIF3
HBB
HBD
HBG1
HGBA1
ERAF
A3G
CCR8
Platelet Factor 4
PGDS
Thrombin Receptor
Kell Blood Group
Ankyrin1, erythrocytic
Angiopoietin 1
Kell Blood Group Precursor
GATA-1

B.

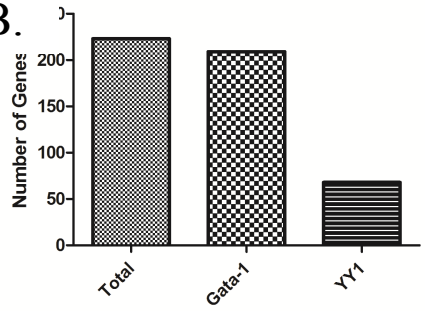

Figure 3.18 Microarray Analysis of CD34+ HPC Depleted of A3G

A. RNA was harvested from cells used in the experiment in Figure 3.12 and Figure 3.13 and hybridized to Gene 1.0 ST GeneChips™ and results analyzed with dChip comparing A3G knockdown to scramble controls from three donors 48 hours post transduction. A number of genes critical to human hematopoiesis and megakaryopoiesis were found to be downregulated when A3G is depleted. Some relevant genes are listed here.

B. TELiS analysis of dyregulated genes shows the vast majority to have a Gata-1 binding site within their respective promoters. The ubiquitious YY1 promoter is found in less than half of these.

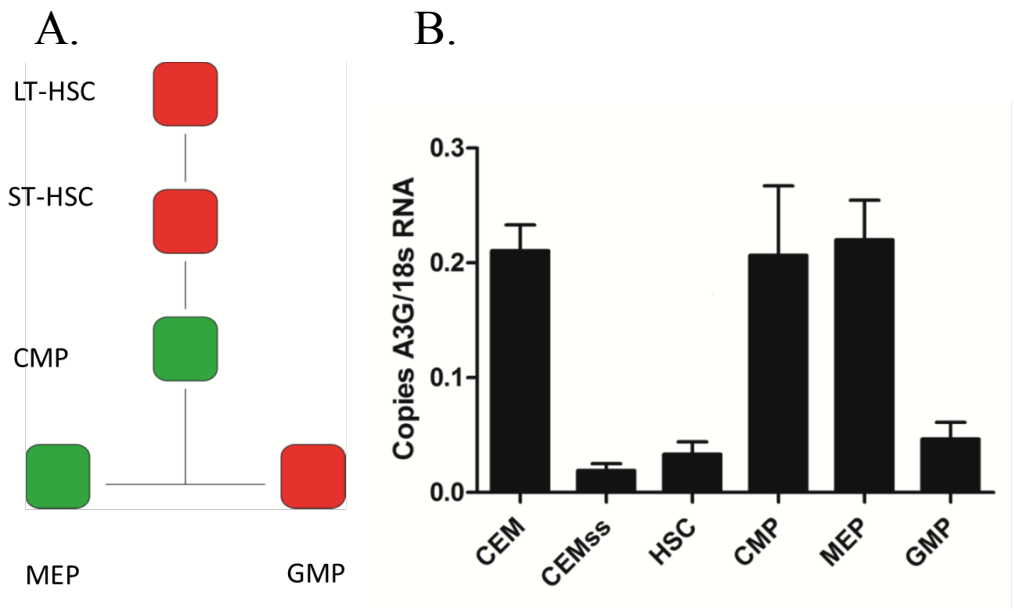

Figure 3.19 Levels of A3G mRNA Fluctuate in Early Hematopoiesis

A. Heat map representing levels of A3G in early hematopoiesis as catalogued by the dMap database of differential gene expression through hematopoiesis. Red indicates relatively low expression of A3G while green indicates high expression. According to microarray analysis for RNA, levels of A3G are very low in the earliest progenitors and rises in development to the CMP and MEP while it drops on differentiation to the GMP. B. qRT-RTPCR analysis of sorted hematopoietic progenitors confirms dMap showing high levels of A3G mRNA relative to 18s rRNA in the CMP and MEP but low in the HSC and GMP.

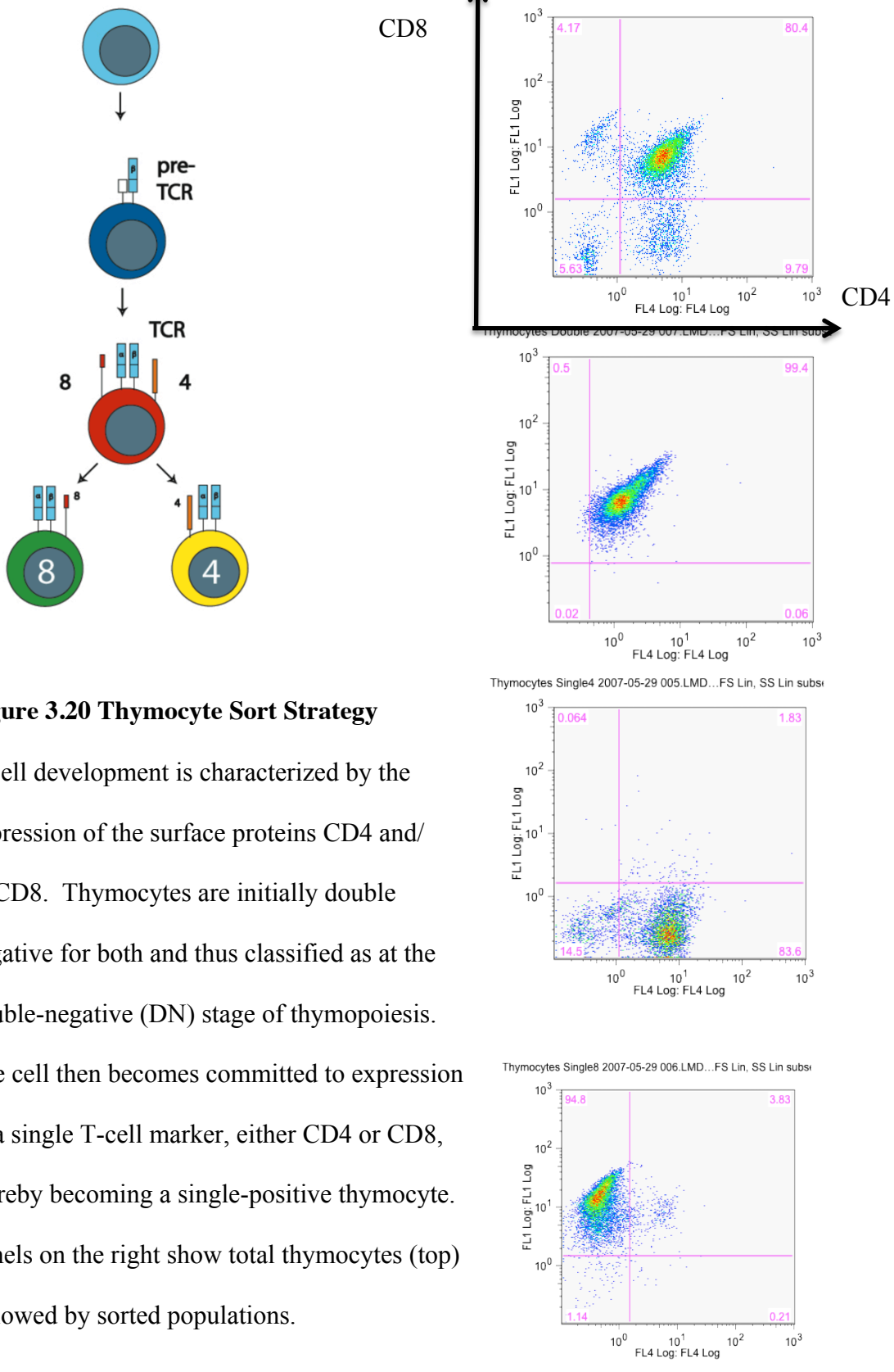

Figure 3.20 Thymocyte Sort Strategy

T-cell development is characterized by the expression of the surface proteins CD4 and/ or CD8. Thymocytes are initially double negative for both and thus classified as at the double-negative (DN) stage of thymopoiesis. The cell then becomes committed to expression of a single T-cell marker, either CD4 or CD8, thereby becoming a single-positive thymocyte. Panels on the right show total thymocytes (top) followed by sorted populations.

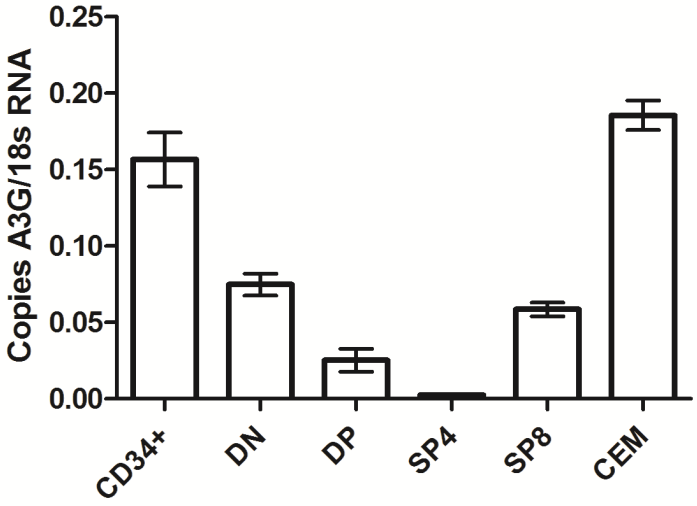

Figure 3.21 A3G in Thymocytes

qRT-RTPCR analysis of A3G expression in thymocytes reveals fluctuations in A3G expression that decline progressively through development from the CD34+ progenitor to each of the single-positive mature thymocytes, except for the apparent rebound in expression from the CD4CD8 double positive thymocyte to the CD8 single positive thymocyte.

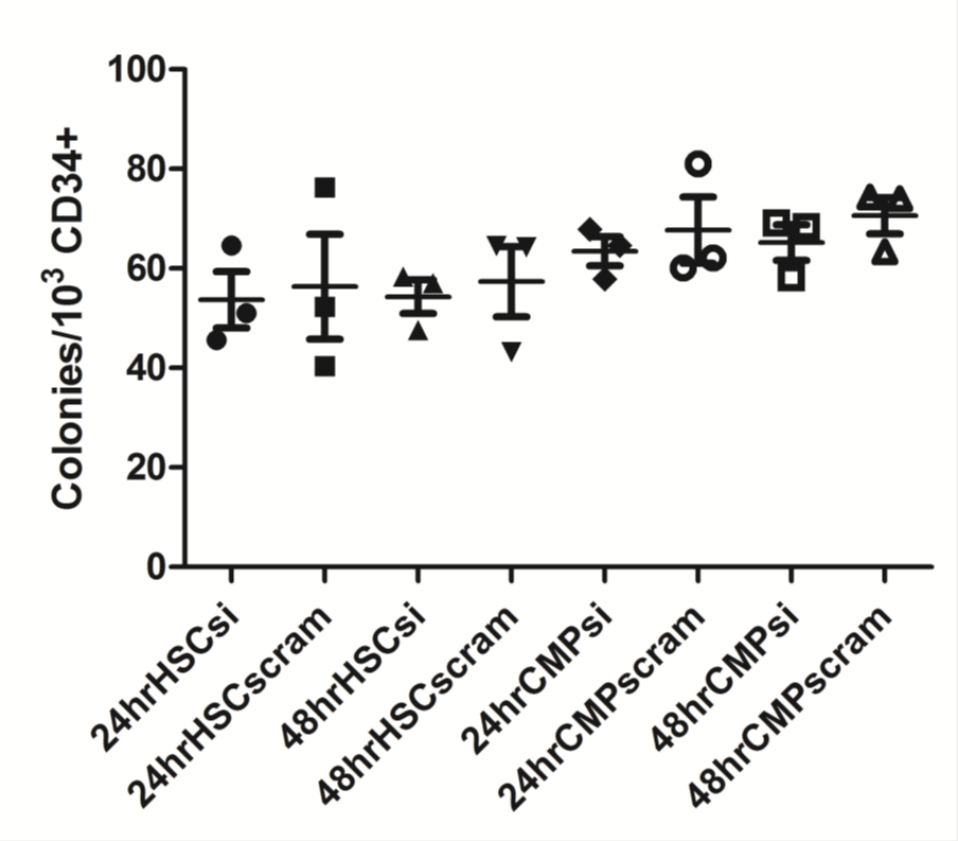

Figure 3.22 A3G Knockdown in sorted progenitors does not impair gross colony development

Either HSC or CMP were transduced with A3G knockdown or scramble control sequences and sorted either 24 or 48 hours post-transduction for ΔLNGFR expression before being plated in complete methylcellulose. Data represent three donors, each mark is the mean of three plates per donor. Error bars represent standard error of the mean. There are no significant differences between samples as determined by student's t test, two tailed.

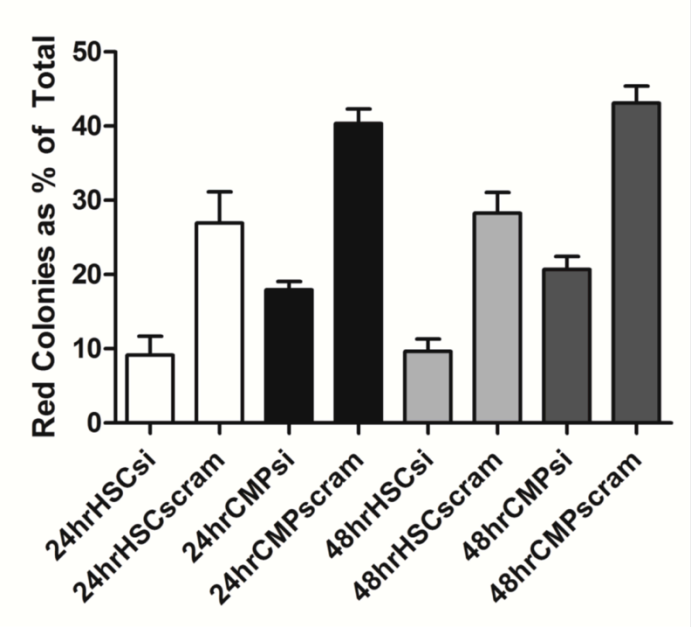

Figure 3.23 A3G Knockdown in Sorted HPC Skews Lineage Commitment

When A3G is knocked down in HSC or CMP, lineage commitment is skewed away from erythroid in methylcellulose cultures when transduced progenitors are sorted either 24 or 48 hours post transduction. 9+/-3% colonies derived from siRNA transduced HSC were erythroid while 27+/-4% of colonies were derived from control scramble418 transduced HSC (p=0.0028). 18+/-1% of colonies derived from siRNA transduced CMP are erythroid while 40+/2% of colonies from control cells are erythroid . At 48 hours, HSC transduced with siRNA against A3G give rise to 10+/-2% erythroid colonies while scramble transduced HSC give rise to 28+/-3% erythroid colonies (p=0.0045). At 48 hours the CMP depleted of A3G give rise to 20+/-2% erythroid colonies while control transduced CMP give rise to 43+/-2% erythroid colonies (p=0.0015)

Name	Fold+/-	
IL6 Signal Transducer	+3.7	
Dicer	+3.4	
Heterogenous nuclear ribonucleoprotein H1	+3.4	
IL6r	3.34	*
CD84	+3.3	
Splicing factor-proline glutamine rich	+3.2	
IL9r	+3.1	
Mediator Complex Subunit 25	+2.5	
IL8	+2.4	
Transcription elongation factor B3	2.4	
Mediator Complex subunit 18	+2.1	
Mediator complex 13	+2.05	
Mediator complex 26	+2.03	
mRNA-decapping enzyme 2	+2.	
Interferon response factor 4	-2.03	
Thrombospondin 1	-2.03	
Hemoglobin beta	-2.1	
Platelet glycoprotein 2b	-2.2	
IL12r	-2.2	*
Hemoglobin alpha	-2.3	
Thrombospondin 2	-2.4	
Epor	-2.44	*
Platelet glycoprotein 1b	-2.5	
Proplatelet Basic Protein	-2.52	
Trasferrin2r	-2.7	*
Nicastrin	-2.7	
CD55	-2.7	
Glycophorin-A	-2.8	*
CytokineR	-3.1	
Platelet factor 4	-3.2	
CD44	-3.7	
Thrombin receptor 2	-3.7	
Hemoglobin delta	-3.9	
Delta-like 1	-3.14	
C-terminal binding protein 1	-3.55	
nuclear factor (erythroid-derived 2)-like 2	-4.24	

Figure 3.24 Dysregulated Gene Expression in A3G Depleted CMP

* Indicates results that were confirmed by qRT-RTPCR

Chapter 4

Discussion

It is apparent that multilineage human hematopoiesis is disrupted in the context of HIV infection. When hematopoietic progenitors are infected with pseudotyped reporter virus, hematosuppression is evident in colony forming assays for myeloid/erythroid lineage development compared to uninfected cells from the same culture. These results suggest that this occurs at least in part by direct infection. Indeed, all lineages are impaired both in size and number of colonies that develop from progenitors exposed to virus (Fig2.2). Interestingly the rate of infection is too low to account for the severe phenotype. This indicates that indirect mechanisms of pathogenesis are also involved. A number of previous studies have implicated various viral gene products in this effect. The studies indicate that hematosuppression can occur without viral env or vpr gene products.

It is clear that receptors necessary for viral entry are present on early and intermediate hematopoietic progenitors (Fig2.5). All progenitor populations except for the MEP show some degree of coreceptor expression, that is CD4 with either CXCR4 or CCR5. All intermediate progenitors, the CMP, the GMP, and the MEP all show significant CXCR4 expression. It is interesting that CMP clearly shows coreceptor expression, certainly far beyond that of the MEP, yet shows the lowest levels of infection (Fig2.7).

When each separate population of intermediate progenitors is sorted to high purity and incubated with wild-type $HIV_{89.6}$, infection can be detected in each population of intermediate hematopoietic progenitors. Permissivity increases with development,

particularly towards the megakaryocyte and erythroid lineages. The HSC and CMP show very low levels of infection, while the ability to infect rises in the GMP and is highest in the MEP. Interestingly, permissivity does not seem to correlate with CD4 expression as the MEP was found to express neither CD4 or CCR5, though it expresses relatively high levels of CXCR4. While this suggests exclusive X4 mediated entry, all other populations express significant levels of X4 but seemingly remain resistant to infection. Still, the mechanism of virus entry remains to be tested.

The BLT mouse recapitulates bone-marrow based human hematopoiesis and in many ways models HIV-1 pathogenesis. Hematopoietic progenitors isolated from the bone marrow of HIV-1 infected BLT mice show a similar phenotype to those infected in vitro. All myeloid and erythroid lineages are severely impaired for growth (Fig2.10). When analyzed by PCR, a portion of these isolated progenitors are shown to harbor proviral DNA (Fig2.9). Moreover, a portion of the differentiated colonies derived from these cells also harbor proviral DNA. This indicates that an early or intermediate progenitor must have been infected in vivo. Furthermore, this suggests that infected progenitors can differentiate to terminal phenotypes that harbor proviral DNA. It remains unclear if any cells infected with replication competent or latent virus could survive and differentiate. The implications of infection of multipotent progenitors with viable virus is profound. Infection of a single CMP or GMP could potentially give rise to a tremendous number of progeny that harbor virus. While these progenitor populations are short-lived, there is tremendous expansion as they develop to terminal phenotypes. Importantly, we show relatively high infection rate of the MEP in vitro in contrast to receptor expression. At

best, the MEP only expresses CXCR4 yet this population shows the highest susceptibility to infection. Further, this is the population that appears to be most susceptible to the effects of infection and shows the greatest pathology in the face of infection.

While it is evident that hematopoiesis is severely impaired in the presence of untreated infection and there is a significant amount of cell death, it is clear that a fraction of terminally differentiated cells derived from isolated progenitors that survive harbor viral DNA. Whether or not these cells are capable of producing virus remains to be tested. These results may seem to conflict with recent findings from Carter et al (89) as to whether progenitors can become infected and survive to terminal differentiation. While Carter el al show infection and survival in multiple lineages, they did so with a vector lacking most of the HIV viral genome. Our claims further do not conflict with Durand et al (91) as his group was looking in patient samples with highly-active antiretroviral therapy (HAART) controlled viremia. *In vivo*, the intermediate hematopoietic populations are relatively short-lived, small in number, and their infection very well may be controlled by HAART.

There are a number of possible mechanisms by which HIV infection may impair hematopoiesis. HIV may directly infect HPCs, which may in itself be a pathogenic process. Alternatively HIV could infect the stromal elements of the bone marrow. Stromal elements of the marrow are responsible for maintaining the cytokine environment that supports the maintenance and development of hematopoietic progenitor populations.

This is the first exploration of HIV restriction factors in early and intermediate hematopoiesis. According to published databases of gene expression and then confirmed in sorted progenitors by PCR, A3G is the only one of the known HIV restriction factors that is expressed in early hematopoiesis. Further, it is the only one whose expression is modulated through the process of hematopoiesis. APOBEC3G is clearly a multifunctional protein. Other than its function as a retroviral restriction element, it has been suggested that A3G is involved in RNA editing due to its localization to p-bodies and direct association with the critical RNA editing proteins Ago2, GW182, and rck/p54 (148).

Here we have shown that APOBEC3G plays a role in human hematopoietic development. The major fluctuations in A3G expression throughout multilineage hematopoiesis is inconsistent with its already accepted roles in retroviral and retroelement restriction. When A3G expression is knocked down by siRNA in hematopoietic progenitors *in vitro*, there is a shift in lineage commitment. Interestingly, HPC transduced with A3G knockdown vectors give rise to the same number of colonies as those transduced with control vectors (fig3.10A). However, formation of erythroid and megakaryocyte colonies is decreased while granulocyte and monocyte colonies increase with no apparent defect in the colonies themselves. In addition, there are not any apparent differences in granulocyte, monocyte, and mixed granulocyte-monocyte colony distribution between groups (Fig3.10B).

Further, the phenotype is maintained in an animal model for three months. The colony forming potential of HSC derived from humanized mice engrafted with A3G knockdown

CD34+ HSC exhibit impaired erythroid colony formation in methylcellulose compared to HSC derived from mice engrafted with a control sequence (Fig3.18).

Initially, microarray analysis was performed on the bulk population of CD34+ cells when A3G was depleted to gain insight into the mechanism by which A3G may be acting. While the results were consistent with the observations of skewed lineage commitment in the absence of A3G, the degree of dysregulation of gene expression was too low to rule out the loss of cells that are committed to megakaryocyte and erythroid lineages. Indeed, there are significant fluctuations in A3G levels just within the early and intermediate hematopoietic progenitors, all of which express CD34+. When microarray analysis of the impact of A3G knockdown is performed instead on a highly purified population of common myeloid progenitors, results are again consistent with the phenotype seen in methylcellulose cultures (Fig3.25). However, there are significant differences in gene expression observed. A number of genes important to early hematopoiesis are dysregulated. More interesting is the ontology analysis. The most dysregulated genes are significantly associated with RNA editing. This is consistent with A3G being associated with p-bodies and microRNA activity (Fig3.26).

The process of human hematopoiesis is a complicated one involving multiple known and unknown factors. It is evident that blood cell development is certainly directed by tightly controlled expression of transcription factors and cytokines. More and more relevant factors are constantly being revealed. The APOBEC family member AID is required for the terminal differentiation of B cells to plasma cells. It has also been shown that AID

can participate in the demethylation process and thus engage in epigenetic programming (156).

The possibility that A3G may be exerting its effects on hematopoiesis through microRNA regulation is compelling and warrants further study. We now know that microRNAs clearly play a role in human hematopoiesis (157). Further, microRNAs are also thought to be responsible for maintenance of some terminal blood cell phenotypes. It is possible that A3G through its interactions with p-body proteins, is involved in the miRNA regulatory pathway and may be, at least in part, responsible for regulating miRNA mediated phenotypic maintenance. While epigenetic control via demethylation has been proposed as an ability of the APOBEC family of deaminases (158), nuclear localization of A3G has not been reported to date. Still, A3G could be working in concert with other APOBEC3 family members or other nuclear shuttle proteins to impart its activity. Regardless, it is becoming clear that the role for A3G in the human body extends beyond its ability to restrict productive retroviral infection or mobility or retrotransposable elements. While the mechanism remains to be elucidated, it is apparent that APOBEC3G is somehow involved in one of the steps leading to human megakaryo-erythroid lineage commitment.

Overall, these studies demonstrate both *in vitro* and *in vivo* that HIV infection of and disruption of the antiviral factor APOBEC3G in hematopoietic progenitor cells affects lineage development. As manipulation of A3G expression is being considered as a potential therapeutic target, it is critical to understand the role of the protein in hematopoiesis. Further studies are needed to determine the role of viral accessory

proteins, immune activation, and HAART on bone marrow dysregulation, as well as the exact molecular mechanisms underlying the activity of A3G in hematopoiesis. Given the strong drive to use stem cell based interventions against HIV infection involving innate restriction factors, elucidating the impact of HIV infection and APOBEC3G manipulation on the bone marrow is of utmost importance.

Chapter 5

Materials and Methods

Plasmid DNA Preparation

All plasmid DNA was prepared by transformation of Stbl3 chemically competent E. coli (Invitrogen/Life Technologies, Grand Island, NY). 10ng plasmid DNA was incubated with cells for thirty minutes on ice. Cells were then heat shocked at 42° C for thirty seconds and then returned to ice. Cells were then spread onto LB agar plates containing ampicillin (100mg/ml) and incubated for 18 hours at 37° C. Individual bacterial colonies were picked and grown in 3 mL liquid cultures in LB broth supplemented with 100mg/ml Ampicillin on a shaker (210rpm) for 12 hours. DNA was extracted using a miniprep kit (Qiagen, Valencia, CA) following the manufacturer's protocol. Large-scale preparation of plasmid DNA was carried out using a maxiprep kit (Qiagen, Valencia, CA) following the manufacturer's protocol.

Cell Lines

293T, 293FT, and HeLa cells were all maintained in DMEM (Gibco/Life Technologies, Grand Island, NY) supplemented with 10% fetal bovine serum (FBS)(Gibco/Life Technologies, Grand Island, NY) and penicillin(1U/ml) and streptomycin (1μg/ml). CEM and CEMss cell lines were maintained in RPMI (Gibco/Life Technologies, Grand Island, NY) supplemented with 10% FBS and penicillin and streptomycin. All cell lines were maintained in a 37°C 5% CO2 incubator.

Transfection and Virus Prep

Vesicular stomatitis virus glycoprotein (VSV-G) pseudotyped lentiviral vectors were produced in HEK 293FT cells by cotransfection of one plasmid encoding the VSV-G envelope, one encoding the Δ8.2 (Δvpr) packaging vector, and one of each respective lentiviral vector using liposome-mediated transfection (Lipofectamine 2000, Invitrogen) following manufacturer's protocol. Media was changed 12 hours post transfection to OMEM (Gibco, Life Sciences) supplemented with 2%FBS. Viral supernatants were harvested 48 hours later, passed through a 45 micron vacuum filter (Millipore, Billerica, MA), and stored at -80˚ C until use. Infections with the reporter virus used Retronectin (Takara) coated plates at a concentration of 100ug/ml to enhance infection.

Vector supernatants were harvested 48 hours later and concentrated on centrifugal filter columns (Amicon Ultracel, Millipore) by manufacturer's protocol. To maximize infection efficiency, non-tissue culture treated plates were coated with recombinant fibronectin (Retronectin, Takara) at a concentration of 1ug/ml and incubated at 4C for 12 hours, washed with PBS, then blocked for 30min at room temperature with PBS-2%FBS. Virus (moi=5) and CD34+ cells were added together to the coated plates, and incubated for 24 hours at 37C. Cells were then removed from plates, washed with sterile PBS, and added to fresh tissue culture plates with fresh media and incubated at 37C 5%CO2.

$HIV_{89.6}$ was constructed by liposome mediated transfection of 293FT as described above but with the the proviral plasmid p89.6 (AIDS reagent program). Clarified viral supernatants were harvested forty-eight hours post-transfections and maintained at -80 C until use.

Primary Cells

Human hematopoietic progenitors were maintained in StemSpan® serum-free media (Stem Cell Technologies, Vancouver, BC) supplemented with SCF,100ng/ml, (Invitrogen/Life Technologies, Grand Island, NY), TPO, 100ng/ml(Invitrogen/Life4 Technologies, Grand Island, NY), FLT3L, 100ng/ml (Invitrogen/Life Technologies, Grand Island, NY), and pen/strep in a 5% CO2 37˚ C incubator.

Isolation of Mononuclear Cells From Cord Blood and Fetal Liver

Human hematopoietic progenitor cells were obtained from either cord blood or fetal liver obtained with IRB approval. To obtain mononuclear cells from cord blood, it was first diluted 1:1 with sterile PBS and then subjected to Ficoll-Hypaque (Stem Cell Technologies, Vancouver, BC) density gradient centrifugation. Liver was first mechanically homogenized and then enzymatically digested hyaluronidase, collagenase, and dnase for 90 minutes at 37˚ C on a rocking platform. Twenty-five mL of each cell suspension was underlayed with twelve mL Ficoll-Hypaque (Stem Cell Technologies, Vancouver, BC) and centrifuged at 2400 rpm for twenty minutes without braking. The interface, or the buffy coat, contains the monocuclear cells, including hematopoietic progenitors. The interface from each tube was transferred to a fresh 50 mL conical tube and washed with sterile PBS.

Cell Sorting

Hematopoietic progenitor cells were isolated from buffy coats by magnetic associated cell sorting (MACS) using CD34+ direct isolation kit (Miltenyi Biotec, Auburn, CA) and MACS LS separation columns (Miltenyi Biotec, Auburn, CA). Up to $10x10^6$ cells were incubated in 100 μl MACS buffer (PBS, 0.5%ACD-A)+5% huAB serum and incubated

for 30 minutes at 4˚C protected from light. Cells were washed with 1mL PBS, pelleted, and resuspended in 3mL MACS buffer. The cell suspension was then applied to a LS column (Miltenyi Biotec, Auburn, CA) mounted on a magnet that had been prepared by washing with 3mL of MACS buffer. After the cell suspension was allowed to flow through the column , it was washed three times with 3mL MACS buffer. To increase purity, each sample was passed over two columns when MACS sorting. The eluted 5ml suspension from the first column sort was immediately applied to a second LS column mounted on a magnet. After the suspension was allowed to flow through the column, the column was washed three times with 3mL MACS buffer. The column was then removed from the magnet and the labeled cells were eluted by flushing the column with 5mL MACS buffer.

For experiments using replication competent HIV, the buffy coat was first depleted of CD3, CD14, and CD16 using purified murine antibodies conjugated to goat anti-mouse magnetic beads (Miltenyi Biotec, Auburn, CA) and then each sample passed over two LS columns (Miltenyi Biotec, Auburn, CA) on magnets. The flow through was enriched for CD34 using C34 magnetic beads (Miltenyi Biotec, Auburn, CA) and then each sample was passed over two LS columns.

When trying to obtain the CD34+CD38+ intermediate hematopoietic progenitors , a CD34+ multisort kit (Miltenyi Biotec, Auburn, CA) was used that allows release of the initial antiCD34-magnetic bead complex. Up to $10x10^6$ cells isolated from the buffy coat of either umbilical cord blood or fetal liver tissue. Cells were washed with sterile PBS, pelleted, and resuspended in 400μL MACS buffer+huAB and mixed with 100μl of anti-

CD34 multisort beads (Miltenyi Biotec, Auburn, CA). This mixture was incubated for 30 min at 4˚C and then washed with 10mL MACS buffer and resuspended in 3mL MACS buffer.

Released cells were then washed and incubated with antiCD38 microbeads to obtain an enriched CD34CD38 double positive population. Released cells were stained with CD38 PE, CD45RA FITC, and CD110 APC for FACS performed at the Broad Stem Cell Institute Flow Cytometry Core. FACS was also used to separate GFP+/- cells. FACS was performed on a FACS ARIA (Becton Dickson, Franklin Lakes, NJ).

For FACS sorting, multipotent progenitors (MPP) were defined as CD34+ CD38-, the common myeloid progenitor (CMP) as CD34+ CD38+ CD45RA- CD110-, the granulocyte monocyte progenitor (GMP) as CD34+ CD38+ CD45RA+ CD110-, and the megakaryocyte erythroid progenitor (MEP) as CD34+ CD38+ CD45RA- CD110+. All flow cytometry data was analyzed with FlowJo software (TreeStar, Inc. Ashland, OR).

Thymocyte subsets were sorted from fetal thymus using the CD4+ multisort and CD8+ direct sort kits (Miltenyi Biotec, Auburn, CA) for MACS following manufacturer's protocol. Each sort step was repeated on an autoMACS (Miltenyi Biotec, Auburn, CA) to increase purity. CD34+ cells were isolated from homogenized fetal liver by MACS using a direct CD34+ isolation kit (Miltenyi Biotec, Auburn, CA) following manufacturers protocol. Each sample was passed over two LS columns (Miltenyi Biotec, Auburn, CA) to achieve a high purity. ΔLNGFR+ cells that were used for plating in methylcellulose were sorted via MACS over two MS columns (Miltenyi Biotec, Auburn, CA) to achieve high purity using a CD271-APC sort kit (Miltenyi Biotec, Auburn, CA)

following manufacture's protocol. Cells were stained with CD34-PE (BD Biosciences, San Jose, CA) and assayed for purity by flow cytometry.

CD34+ were isolated from processed murine bone marrow as above. Cells were further sorted for GFP expression on a FACS Aria at the UCLA-Broad Stem Cell Research core facility.

Methylcellulose Colony Forming Assays

To determine the developmental potential of hematopoietic progenitor populations, cells were seeded in Methocult-H4435 complete methylcellulose (Stem Cell Technologies, Vancouver, BC) at a concentration of 1,000 cells/ml and plated in 3 cm gridded plates, 1ml/plate, 3 plates per mouse. When examining megakaryopoiesis, hematopoietic progenitors were plated at a density of 5,000/ml in Megacult-C semi-solid methylcellulose media specifically formulated to support megakaryopoiesis megakaryocytes (Stem Cell Technologies, Vancouver, BC). When assaying colony forming potential of cells exposed to HIV, AZT (10uM) and Indinovir (100nM) were added to the media prior to plating. Colonies were counted two weeks later in a blinded fashion using a Nikon microscope at a magnification of 400x.

When colonies were picked for PCR assays, only discrete, individual colonies were picked with a with a pipette tip, washed three times in 500ul sterile PBS and stored at -80˚ C until DNA extraction.

Lentiviral Vector Construction and Knockdown of A3G

Nucleotide sequences intended to knockdown the expression of A3G were designed with the assistance of the Ambion online siRNA design tools. Five different sequences were

initially designed and tested. When designing stable expression of siRNA, a hairpin sequence must be engineered. This hairpin will be processed by cellular machinery to produce active siRNAs in the cytoplasm.

As the FG12 vector has very few unique restriction sites, a subcloning strategy is used to insert the siRNA sequences into FG12. First, oligonucleotide sequences that encode the hairpin are annealed and cloned into a pBluescript vector that contains the appropriate promoter, either U6 or H1. To facilitate this, the sequences for unique restriction sites that allow this insertion were engineered into the oligonucluotides. For sequences intended for insertion under the U6 promoter, the 5' terminus of the oligo was engineered as the NheI restriction site while the 3' terminus of the oligo was engineered to be the XhoI restriction site. For sequences intended to be inserted under the H1 promoter, the 5' terminus was designed as the XbaI restriction site and the 3' terminus was the XhoI restriction site. Top and bottom strand oligos were annealed in annealing buffer (10mM Tris, pH7.5, 50mM NaCl, 1mM EDTA) in a beaker of boiling water that was allowed to cool to room temperature. The oligos were then subjected to standard ethanol precipitation and resuspended in water. One μg of the pBluescript-U6 vector was prepared by simultaneous digestion with NheI and XhoI in NEB2 restriction digest buffer and incubated for one hour in a 37˚C water bath. The linear DNA fragment of interest was purified by agarose gel electrophoresis. The products of the digestion reaction were electrophoresed in a 1% agarose gel made with modified TAE for one hour at 80 volts. The gel was then visualized on a UV light box and the large bands were excised with a razor blade. DNA was extracted from the gel slices using the QIAEXII gel extraction kit

(Qiagen, Carlsbad, CA) following manufacturer's protocols. To anneal the shRNA oligos to the plasmid, they were mixed in a 3:1 oligo:vector molar ratio in the presence of 1μl T4 ligase buffer (New England Biolabs, Ipswich, MA) and incubated overnight at 4° C. The products of this ligation reaction were used to transform Stbl3 bacteria as previously described. Transformed cells were plated on amp selection LB plates and twenty four hours later, individual colonies were picked and expanded by miniprep procedure. DNA was extracted from miniprep cultures as described and then sequenced to confirm correct oligo insertion (Laragen, Culver City, CA).

Once the correct oligo insertion was confirmed, the oligo encoding the shRNA against A3G and its promoter were excised with the restriction enzymes BLAH and BLAH in a simultaneous digestion as described. The smaller of the two DNA fragments was isolated and purified by agarose gel electrophoresis as described. A ladder was also run in the gel to confirm the correct size of the oligo.

The FG-12 vector was prepared by digestion with corresponding enzymes to allow insertion of the shRNA expression cassette. The vector was also purified by agarose gel extraction following electrophoresis as previously described.

Vector was ligated with insert at a 1:1 molar ratio. The ligation was performed as described above as was the transformation of chemically competent bacteria with the products of each of the ligation reactions. Again, bacteria were plated and individual colonies were harvested eighteen hours later. Miniprep DNA cultures were grown from 5 colonies of each transformation. DNA was extracted from each as described and

sequenced. Once the insertion was confirmed by sequencing, large scale preparations of each plasmid were performed.

A3G knockdown sequences were first cloned into the pBluscript cloning vector and then subcloned with the U6 or H1 polII promoter into FG12/LNGFR-IRES-Puro or the FG12/eGFP-IRES-Puro vector. Each was initially assayed for its ability to deplete A3G expression in the CEM cell line, known to express high levels of A3G transcript and protein. Successful knockdown was confirmed by qRT-PCR. However, western blots were unsuccessful in this cell line due to excessive cross-reactivity with the antibody. Further attempts were made in cell lines engineered to overexpress A3G obtained from the NIH AIDS Reagent Repository including modified HeLa and 293 lines. Unfortunately, there again was excessive cross-reactivity in these lines with the antibody. Knockdown was confirmed by RTPCR but western blots were excessively difficult to interpret.

A marker cassette was inserted under the control of the UbiC Pol3 promoter that contains a truncated, low-affinity nerve growth factor receptor as a marker(ΔLNGFR), followed by an IRES, then finally the puromycin resistance gene. ΔLNGFR has been shown to be effective and non-toxic in clinical trials(30) For some experiments, eGFP was used in place of dLNGFR.

Antibodies and Flow Cytometry

anti-CD4 ECD (Beckman Coulter, Brea, CA, clone GK1.5), anti-CCR5 PerCP-Cy5.5 (BD Pharmingen, clone 3A9), anti-CXCR4 Pc7 (BD Pharmingen, San Jose, CA clone 12G5), anti-CD34 APC (Beckman Coulter, clone 8G12), anti-CD38 PE (Beckman

Coulter, clone LS198-4-3), anti-CD45RA FITC (BD Pharmingen, clone HI100), anti-CD123 e450 (eBiosciences, San Diego, CA, clone 6H6), anti-CD110 APC (R&D Systems, Minneaopolis, MN, clone 167639). anti-CD34 PE (Beckman Coulter), pure CD3 (BD Pharmingen, clone HIT3a), pure CD14 (BD Pharmingen, clone M5E2), pure CD16 (BD Pharmingen, clone , goat anti-mouse beads (Miltenyi Biotech, Auburn, CA) Antibodies used in this study: CD4:Pc7 CD8:PE CD34:APC BD Pharmingen, CD45: BD Pharmingen, CD271-AF647 BD Pharmingen.

Prior to staining for flow cyt ometry, cells were counted to determine concentration. Up to $1x10^6$ cells were resuspended in 100 μL PBS with 5% human AB serum and ACD-A (Sigma, and antibodies added at a concentration of 1 μg/$1x10^6$, mixed and incubated for 30 min at 4C. Cells were then washed with 1mL MACS buffer and resuspended in 500 μL MACS buffer if being analyzed by flow cytometry immediately. If being stored for later analysis, following staining, samples were washed and fixed in 1% paraformaldehyde. Samples were run on a BD LSRII and analyzed with FloJo software.

Quantitative Reverse Transcriptase Mediated Real Time Polymerase Chain Reaction

RNA was isolated using the miRNeasy Kit (Qiagen, Valencia, CA) following manufacturer's protocol. RNA was eluted in nuclease free water and either assayed immediately or stored at -70C until use. All qRT-RTPCR reactions to assay A3G transcripts were done with the Qiagen 1-step RT-PCR kit (Qiagen,Valencia,CA). 5μl of sample RNA was added to 15μl reaction mix in a 96-well plate. The reaction mix consisted of 5 μl of A3G oligo mixture. This consists of o.5μl APOF primer, 0.25 APOR

primer, 0.025 APOR probe, and 4.225 μl water. The mix additionally contains 5 μl Qiagen OneStep RT-PCR buffer, 1μl of 0.4 mM dNTP, 0.5 μl of the Qiagen OneStep RT-PCR enzyme mix, 0.25 μl RNaisin, and 3.25μl nuclease-free water. A3G copy number was normalized to copy number of 18s ribosomal RNA. Standards for A3G RNA and 18s rRNA were created by RT-PCR amplification of A3G under an SP6 promoter and serial dilutions made based on spectrophotometric quantification. Quantitative reverse transcriptase mediated polymerase chain reactions were performed using the Qiagen One Step RT-PCR kit on a BioRad IQcycler. Primers for A3G : (APOF: CGCAGCCTGTGTCAGAAAAG , APOR: CCAACAGTGCTGAAATTCGTCATA, APOProbe: 6-FAM-CCGGTGCCACCATGAAGATCA-BHQ). The cycling conditions for the reaction are: 1 cycle for 30 minutes at 50˚ C, followed by 1 cycle for 10 min at 55˚ C, followed by 1 cycle for 15 minutes at 95˚ C, followed by 40 cyclesof: 15 seconds at 95˚ C, 30 seconds at 55˚ C, and 1min at 60˚ C]

qRT-RTPCR with ABI Validated Primers

All subsequent qRT-RTPCR reactions to detect mRNA were carried out in two steps using validated primers and reagents from Applied Biosystems, Inc (Life Technologies, Carlsbad, CA). and following manufacturer's protocol. These include the assays for GATA-1, Glycophorin-A, IL-6r, and Epor. First cDNA is synthesized in 20μl reactions containing 2μl Taqman® RT buffer, 4.4μl of 25mM $MgCl_2$, 4 μl of 2.5mM dNTPs, 1 μl of 50μM random hexamers, 0.4μl of RNase inhibitor at 20U/L, o.5 μl of Multiscribe™ RT at 50U/μl, 5 μl of RNA template. The reverse transcription reaction was carried out

in three thermocyler steps: 10 minutes at 25˚C, followed by 30 minutes at 48˚C, concluding with 5 minutes at 95˚C. The qRTPCR reactions were carried out in 50μl: 25 μl 2x SYBER® Green master mix, 5 μl primer/probe mix, and 20 μl nuclease-free water. The thermal cycler conditions were as follows: 1 cycle at 50˚C for 2 minutes, 1 cycle at 95˚C for 10 minutes, 40 cycles of: 95˚C for 15 seconds followed by 60˚C for 1 minute. Results were normalized to expression of 18s ribosomal RNA as described above.

qRT-RTPCR Analysis of microRNA Expression in A3G Depleted Progenitors

Levels of transcripts of miRNA known to be relevant to hematopoiesis were tested with assays prepared by Exiqon (Woburn, MA) following manufacturer's protocols. Briefly, cDNA synthesis and real-time PCR were carried out in separate, sequential reactions. Reverse transcription reactions were assembled in 20μl: 5μl template RNA, 4μl 5x reaction buffer, 2μl enzyme mix, and 10μl nuclease-free water. Reactions were incubated for 60 minutes at 42˚C. Next, cDNA was diluted 1:80 with nuclease-free water for use in qRT-PCR experiments. 10μl qRT-PCR reactions were assembled using 4μl diluted cDNA, 1μl primer mix, 5μl SYBR® Green master mix. The real-time PCR cycle conditions were one cycle of 95˚C for 10 minutes, followed by 40 cycles of 95˚ C for 10 seconds and then 60˚C for 1 minute.

qRTPCR to Detect Viral DNA

Detection of viral DNA was accomplished through the use of quantitative real-time PCR. DNA from cells was first isolated by standard phenol-chloroform extraction followed by

ethanol precipitation. qPCR was carried out in 25 μL reactions with 10 μL TaqMan® Core Reagents Kit mix (ABI Biosystems/Life Technologies, Carlsbad, CA), 5 μL nuclease free water, 5 μL template DNA and 5 μL of a primer/probe set. Primers BGF1 (5'-CAACCTCAAACAGACACCATG-3') (300 nM) and BGR1 (5'-TCCACGTTCACCTTGCCC-3') (150 nM) as well as probe BGX1 (6FAM-5'-CTCCTGAGGAGAAGTCTGCCGTTACTGCC-3') (200 nM) were used to amplify cellular β-globin which we used as an internal standard. Primers SR1 (5'-CAAGTAGTGTGTGCCCGTCTGT-3') (300 nM) and 661 (5'-CCTGCGTCGAGAGATCTCCTCTGG-3') (150 nM) along with probe ZXF 6FAM 5' -/56FAM/TGTGACTCT/ZEN/GGTAGCTAGAGATCCCTCAGACCA/3IABkFQ/-3' (200 nM) were used to amplify the Gag/LTR junction, which indicates full length viral DNA. Known quantities of standards were run in parallel, creating a standard curve for both HIV and β-globin and sample DNA was quantified by extrapolation from the standard curve. Standards with levels of 1-10x10^5 copies of cloned HIV DNA were used and DNA derived from 1-10x10^5 normal human blood peripheral lymphocytes was used for the β-globin standards. Samples were amplified using an IQCycler (BioRad) system and analysis was done with iQ5 software (Bio-Rad). Thermocycling conditions were as follows: 50ºC for 2 minutes, 95ºC for 10 minutes, and 40 cycles of 95ºC for 15 seconds followed by 60ºC for 1 minute. All qPCR reactions were run in triplicate.

Western Blots

Cell pellets of $1x10^6$ cells were lysed in 100 μl of 2x SDS lysis buffer (20mM dithiothreitol, 6% SDS, 0.25 M Tris, pH 6.8, 10% glycerol) on ice for 30 minutes. Lysates were clarified by centrifugation to remove any cellular debris. Protein concentration was determined by a standard Bradford assay (Biorad, Hercules, CA). For each sample, 50ug whole cell extract was mixed with running buffer. Samples were loaded on a 8% polyacrylamide loading gel and run on 10% polyacrylamide resolving gel next to the 10 μl Benchmark™ protein ladder (Invitrogen/Life Technologies, Carlsbad, CA) on a BioRad (Hercules, CA) electrophoresis box for one hour at 100 volts. Electrophoresed proteins were then transferred to HyBond™ ECL™ nitrocellulose membranes (Amersham, GE Healthcare Biosciences, Pittsburg, PA) with a semi-dry transfer apparatus (BioRad Transblot EC) for 15 minutes at 25 volts. Membranes were blocked with PBS-5% milk for six hours at 4˚C, incubated with pRab anti-A3G overnight at 4˚C at a 1:1000 dilution in blocking buffer, washed, and incubated one hour with goat anti-rabbit hoseradish peroxidase at a 1:1000 dilution at room temperature. Membranes were developed with ECL™ plus (Amersham, GE Healthcare Biosciences, Pittsburg, PA) and scanned on a Typhoon phosphorimager (Amersham, GE Healthcare Biosciences, Pittsburg, PA). Anti-A3G serum was raised in rabbits against the synthetic A3G peptide NH2--QDLSGRLRAILQNQENC-- -OH by Antibody Solutions, Mountainview, CA.

NSG-BLT Mice

All work involving mice was carried out under the approval of the UCLA Animal Research Committee. Bone marrow-liver-thymus mice were constructed as previously

described. Following sublethal irradiation (300rad using a cobalt 60 source) to remove murine hematopoietic cells, non-obese severe combined immunodeficient common gamma chain knockout (NSG) mice were implanted with pieces of human fetal liver and thymus beneath the kidney capsule and injected with allogeneic CD34+ cells to seed the bone marrow. Four weeks later, mice were analyzed for engraftment of human cells and immune reconstitution by flow cytometric analysis of peripheral blood. Cells were stained with CD45, CD3, CD4, and CD 8. Once engraftment of human cells was confirmed, 150ng p24 $HIV_{89.6}$ was delivered by retro-orbital injection. Infection was assayed every four weeks by flow cytometry an NOD-SCID-common Gamma chain knockout (NSG) mice were housed and maintained under UCLA IRB protocol.
Mice were sub-lethally irradiated and implanted with pieces of fetal liver and thymus underneath the kidney capsule, and transduced CD34+ cells in matrigel™ (BD Bioscien ces, San Jose, CA), then injected by tail vein with transduced fetal liver CD34+ cells. Three months following transduction, animals were sacrificed and bone marrow harvested.

Statistics

Data were analyzed with paired or unpaired Student's t test as indicated. All statistical analyses were performed with GraphPad Prism v5.0 (GraphPad Software). Values with $P < 0.05$ were considered significant.

Microarray Analysis with dCHIP

Gene lists were generated using three criteria. The variation across sam ples was determined by standard deviation/mean and the range was set to be 0.6 to 1000. The

presence call was set at 20% and the expression level to be greater than 50 in greater than 50% of samples. The knockdown group as a whole was compared to the scramble control sequence group as a whole. Three criteria were used for the comparison. The experimental/ baseline and the baseline/experimental was set at greater than 2 fold. The absolute difference between groups, experimental-baseline and baseline-experimental, was set at greater than 50 and the p value for testing experimental=baseline <0.05. Further, samples were permuted to obtain a false discovery rate of n! where n is the number of samples. Gene lists were analyzed on the Database for Annotation, Visualization, and Integrated Discovery (DAVID) website maintained by the NIAID at the NIH (www.abcc.ncifcrf.org). Both functional annotation and gene functional classification analysis were performed with these online tools.

References

1. Hoang,T., *The origin of hematopoietic cell type diversity*. Oncogene, 2004. 23(43):7188-98.
2. Laiosa, C.V., et al., *Determinants of lymphoid-myeloid lineage diversification*. Annu Rev Immunol, 2006. 24: 705-38.
3. Mercer, E.M., et al., *Factors and networks that underpin early hematopoiesis*. Sem Immunol, 2011.
4. Zlotoff, D.A.,et al., *The long road to the thymus: the generation, mobilization, and circulation of T-cell progenitors in mouse and man*. Semin Immunopathol, 2008. 30(4):371-82. Epub 2008 Oct 17. Review.
5. Boehm, T., *Thymus development and function*. Curr Opin Immunol, 2008. 20(2):178-84. Epub 2008 Apr 9. Review.
6. Rothenberg, E.V*., T cell lineage commitment: identity and renunciation*. J Immunol, 2o11. 186: 6649-55.
7. Pontikoglou, C., et al., *Bone marrow mesenchymal stem cells: biological properties and their role in hematopoiesis and hematopoietic stem cell transplantation*. Stem Cell Rev. 2011. 7(3):569-89. Review.
8. Anjos-Afonso F, Bonnet D. *Flexible and dynamic organization of bone marrow stromal compartment*. Br J Haematol. 2007. 139(3):373-84. Review.
9. Karcher, D.S., A.R. Frost. *The bone marrow in human immunodeficiency virus (HIV)-related disease*. Morphology and clinical correlation. Am J Clin Pathol, 1991. 95:63-71.
10 de Graaf CA, Metcalf D. *Thrombopoietin and hematopoietic stem cells*. Cell Cycle. 2011. 10(10):1582-. Review.
11 Tarasova, A., et al., *Principal signalling complexes in haematopoiesis: structural aspects and mimetic discovery*. Cytokine Growth Factor Rev, 2011. 22(4):231-53. Review.
12 Yu M, Cantor AB., *Megakaryopoiesis and thrombopoiesis: an update on cytokines and lineage surface markers*. Methods Mol Biol, 2012. 788:291-303. Review.
13 de Walle, I.V., et al., *Jagged2 acts as a Delta-like Notch ligand during early hematopoietic cell fate decisions*. Blood, 2011. 117: 4449-59.
14 Huang, Y.H., et al., *Distinct transcriptional programs in thymoctes responding to T cell receptor, Notch, and positive selection signals*. PNAS, 2004. 101(14): 4936-41.
15 Martinez, J. and M. Busslinger*, Life beyond cleavage: the case of Ago2 and hematopoiesis*. Genes Dev, 2007. 21: 1983-8.
16 Bissels, U., et al*., Combined characterization of microRNA and mRNA profiles delineates early differentiation pathways of CD133+ and CD34+ hematopoietic stem and progenitor cells.* Stem Cells, 2011. 29(5): 847-57.
17 Li, H., et al., *microRNA regulation in megakaryocytopoiesis*. Brit J Haematology, 2011. 155: 298-307.

18 Pillai, R.S., *MicroRNA function: Multiple mechanisms for a tiny RNA?* RNA, 2005. 11(12):1753-61.
19 Martinez J, Busslinger M. *Life beyond cleavage: the case of Ago2 and hematopoiesis*. Genes Dev, 2007. 21(16):1983-8. Review
20 Wilson, N.K., et al., *Combinatorial transcriptional control in blood stem/progenitor cells: genome-wide analysis of ten major transcriptional regulators*. Cell Stem Cell 2010 vol. 7 (4) pp. 532-44
20 Li, H., et al., *microRNA regulation in megakaryocytopoiesis*. Brit J Haematology, 2011. 155: 298-307.
21 Iwasaki, H., et al., *The order of expression of transcription factors directs hierarchical specification of hematopoietic lineages*. Genes Dev. 2006 vol. 20 (21) pp. 3010-21
22 Xiao-Ling L., et al., *Differential gene expression in human hematopoietic stem cells specified toward erythroid, megakaryocytic, and granulocytic lineage*. J Leukoc Biol, 2007. 82 (4): 986-100
23 Rosenfeld, S.J., N.S. Young, *Viruses and bone marrow failure*. Bood Rev, 1991. 5: 71-77.
24 Karcher, D.S., et al., *The bone marrow in human immunodeficiency virus (HIV)-related disease. Morphology and clinical correlation*. Am J Clin Pathol, 1991. 95(1): 63-71..
25 Stutte, H.J., et al., *Pathophysiological mechanisms of HIV-induced defects in haematopoiesis: pathology of the bone marrow*. Res Viol, 1990. 141(2): 195-200.
26 Sloand, E., *Hematologic complications of HIV infection*. AIDS Rev, 2005. 7:187-196.
27 Garzia,M. et al., *Morphological diagnosis by bone marrow aspirate of toxoplasmosis infection in an HIV-positive patient*. Lab Hematol, 2007. 13:27-29.
28 Kulkosky, J., et al., *Pathogenesis of HIV-1 infection within bone marrow cells*. Leuk Lymphoma, 2000. 37: 497-515
29 Murugan, P., et al*., Gleatinous transformation of bane marrow in acquired immunodeficiency syndrome*. Pathology, 2007. 39:287-8.
30 Kurtin, P.J., et al., *Histoplasmosis in patients with acquired immunodeficiency syndrome. Hematologic and bone marrow manifestations*. Am J Clin Pathol, 1990. 93: 367-72
31 Janka, G.E., *Hemophagocytic syndromes*. Blood Rev, 2007. 21:245-53.
32 World Health Organizatiom
33 Kogan M, Rappaport J., *HIV-1 accessory protein Vpr: relevance in the pathogenesis of HIV and potential for therapeutic intervention*. Retrovirology, 2011. 8:25. Review.
34 Ott M., et al., *The control of HIV transcription: keeping RNA polymerase II on track*. Cell Host Microbe. 2011. 10(5):426-35. Review.
35 Checkley MA , et al. *HIV-1 envelope glycoprotein biosynthesis, trafficking, and incorporation.* J Mol Biol, 2011. 410(4):582-608. Review.

36 Grewe B, Uberla K. *The human immunodeficiency virus type 1 Rev protein: ménage à trois during the early phase of the lentiviral replication cycle*. J Gen Virol, 2010. 1(Pt 8):1893-7. Review.
37 Navarro F., Landau N.R. *Recent insights into HIV-1 Vif*. Curr Opin Immunol, 2004. 16(4):477-82. Review.
38 Laguette N., et al, *Human immunodeficiency virus (HIV) type-1, HIV-2 and simian immunodeficiency virus Nef proteins*. Mol Aspects Med, 2010. 31(5):418-33. Review.
39 Greenbaum, N.L., *How Tat targets TAR: structure of the BIV peptide-RNA complex*. Structure, 1996. 4(1):5-9. Review.
40 Doranz, B.J., et al., *Chemokine receptors as fusion cofactors for human immunodeficiency virus type 1 (HIV-1)*. Immunol Res, 1997. 16(1):15-28. Review.
41 Freed EO, Martin MA. *The role of human immunodeficiency virus type 1 envelope glycoproteins in virus infection*. J Biol Chem, 1995. 13;270(41):23883-6. Review
42 Piller, S.C., et al., *Nuclear import of the pre-integration complex (PIC): the Achilles heel of HIV?* Curr Drug Targets, 2003. 4(5):409-29. Review.
43 Marchand, C., et al., *Mechanisms and inhibition of HIV integration*. Drug Discov Today Dis Mech, 2006. 1;3(2):253-260.
44 Arhel, N., *Revisiting HIV-1 uncoating*. Retrovirology. 2010. 7:96. Review.
45 Checkley, M.A., *HIV-1 envelope glycoprotein biosynthesis, trafficking, and incorporation.* J Mol Biol, 2011. 22;410(4):582-608. Review.
46 Weiss, E.R., H. Göttlinger, *The role of cellular factors in promoting HIV budding*. J Mol Biol, 2011. 410(4):525-33. Review.
47 Hammer, S.M., Clinical practive. *Management of newly diagnosesed HIV infection*. N Engl J Med, 2005. 353:1702-10.
48 Palella, F.J., et al., *Declining morbidity and mortality among patients with advanced human immunodefieciency virus infection*. HIV Outpatient Study Investigators. N Eng J Med, 1998. 338:853-60.
49 Maltêz, F., et al., *Recent advances in antiretroviral treatment and prevention in HIV-infected patients*. Curr Opin HIV AIDS, 2011. Suppl 1:S21-30. Review.
50 Deeks, S.G., J.M. McCune, *Can HIV be cured with stem cell therapy?* Nature Biotech, 2010. 28(8):807-10
51 Kambal, A.G., et al., *Generation of HIV-1 resistant and functional macrophages from hematopoietic stem cell-derived induced pluripotent stem cells*. Mol Ther, 2011. 19(3): 584-93.
52 Kitchen, S.G., et al., *In vivo suppression of HIV by antigen specific T cells derived from engineered hematopoietic stem cells*. PLoS Path, 2012. 8(4): e1002649
53 Kitchen, S.G., et al., *Stem cell-based anti-HIV gene therapy*. Virology, 2011. 411(2): 260-72
54 Kitchen, S.G., J.A. Zack, *Stem cell-based approaches to treating HIV infection*. Curr Opin HIV AIDS, 2011. 6(1): 68-73.

55 Marche, C., et al., *Bone marrow findings in HIV infection: a pathological study*. Prog AIDS Pathology, 1990. 2: 51-60.
56 Jaresko, G.S*., Etiology of neutropenia in HIV- infected patients*. Am J Health Sys Pharm, 1999. 56(5):5-8
57 Harbol, A.W., et al., *Mechanisms of cytopenia in human immunodeficiency virus infection*. Blood Rev, 1994. 8: 241-51.
58 Treacy, M.L., et al., *Peripheral blood and bone marrow abnormalities in patients with HIV related disease*. Brit J Haematol, 1987. 55(3): 289-94.
59 Oksendhendler, E. and M. Seligmann, *HIV-related thrombocytopenia*. Immunodefic Rev, 1990. 2(3): 221-31.
60 Donahue, R.E., et al., *Suppression of in vitro haematopoiesis following human immunodeficiency virus infection*. Nature, 1987. 326(6109): 200-3.
61 Scadden, D.T., et al., *Humman immunodeficiency virus infection of human bone marrow stromal fibroblasts*. Blood, 1990. 76(2): 86-88.
62 Schwartz, G.N., et al., *Inhibitory effects of HIV-1 infected stromal cell layers on the production of myeloid progenitor cells in human long-term bone marrow cultures*. Exp Hematol, 1994. 22(13): 1288-96.
63 Zucker-Franklin, D.S., et al*., Internalization of human immunodeficiency virus type I and other retroviruses by megakaryocytes and platelets*. Blood, 1990. 75(10): 1920-3.
64 Freedman, A.R., et al., *Human immunodeficiency virus infection of eosinophils in humn bone marrow cultures*. J Exp Med, 1991. 174(6): 1661-4.
65 Zauli, G.L., et al*., Impaired survival of bone marrow GPIIb/IIa+ megakaryocytic cells as an additional pathogenetic mechanism of HIV-1-related thrombocytopenia*. Br J Haematol, 1996. 92(3): 711-17.
66 Chelucci, C.M., et al., *Productive human immunodeficiency virus-1 infection of purified megakaryocytic progenitors/precursors and maturing megakaryocytes*. Blood, 1998. 91(4): 1225-34.
67 Zauli, G.M., et al., *Impaired in vitro growth of purified CD34+ hematopoietic progenitors in human immunodeficiency virus-1 seropositive thrombocytopenic individuals*. Blood, 1992. 79(10): 2680-7.
68 Golard, R., J. Khoury, *Images in HIV/AIDS HIV and myelodysplasia*. AIDS Read, 2009. 19: 156-7
69 Scadden, D.T., et al., *Pathophysiology and management of HIV-associated hematologic disorders*. Blood, 1989. 74(5): 1455-63.
70 Schwartz, G.N., et al*., Negative regulators may mediate some of the inhibitory effects of HIV-1 infected stromal cell layers on erythropoiesis and myelopoiesis in human bone marrow long term cultures*. J Leuk Biol, 1995, 57(6):948-55.
72 Banda, N.K., et al., *HIV-gp120 induced cell death in hematopoietic progenitor CD34+ cells*. Apoptosis, 1997. 2(1): 61-8.
73 Zhang, M., et al., *HIV-1 determinants of thrombocytopenia at the stage of CD34+ progenitor cell differentiation in vivo lie in the viral envelope gp120 V3 loop region*. Virology, 2010. 401(2): 131-6.

74 Zauli, G.M., et al*., Inhibitory effect of HIV-1 envelope glycoproteins gp120 and gp160 on the in vitro growth of enriched CD34+ hematopoietic progenitor cells*. Arch Virol, 1992. 122(3-4): 271-80.
75 Koka, P.S., et al., *Human immunodeficiency virus type-1 induced hematopoietic inhibition is independent of productive infection of progenitor cells in vivo*. J Virol, 1999. 73(11): 9089-97.
76 Sundell, I.B. and P.S. Koka, *Chimeric SCID-hu model as a human hematopoietic stem cell host that recapitulates the effects of HIV-1 on bone marrow progenitors in infected patients*. J Stem Cells, 20006. 1(4): 283-300.
77 Kirchoff, F. and G. Silvestri, *Is Nef the elusive cause of HIV-associated hematopoietic dysfunction?* J Clin Invest, 2008. 118(5): 1622-1625.
78 Calenda, V.P., et al., *Involvement of HIV nef protein in abnormal hematopoiesis in AIDS: in vitro study on bone marrow progenitor cells*. Eur J Haematol, 1994. 52(2): 103-7.
79 Isgro, A.W., et al., *Altered clonogenic capability and stromal cell function characterize bone marrow of HIV-infected subjects with low CD4+ T cell counts despite viral suppression during HAART*. Clin Infect Dis, 2008. 46(12): 1902-10.
80 Bahner, I., et al*., Infection of human marrow stroma by human immunodeficiency virus-1 (HIV-1) is both required and sufficient for HIV-1-induced hematopoietic suppression in vitro: demonstration by gene modification of primary human stroma*. Blood, 1997. 90:1787-98.
81 Koka, P.S., et al*., Human immunodeficiency virus inhibits multilineage hematopoiesis in vivo*. J Virol, 1998. 72(6): 5121-7.
82 Geissler, R.G., et al, *Decreased haematopoietic colony growth in long-term bone marrow cultures of HIV-positive patients*. Res Virol, 1993. 144(1): 69-73.
83 Alexaki, A., B. Wigdahl, *HIV-1 infection of bone marrow hematopoietic progenitor cells and their role in trafficking and viral dissemination*. PLOS Pathog, 2008. 4(12): e10000215
84 Isgrò, A., et al., *Immunodysregulation of HIV disease at bone marrow level*. Autoimmun Rev, 2005. 4(8):486-90. Review.
85 Levine, A.M., et al. *Hematologic Aspects of HIV/AIDS*. Hematology Am Soc Hematol Educ Program, 2001. 463-78. Review
86 Kaczmarski, R.S., et al., *Detection of HIV in haemopoietic progenitors*. Br J Haematol, 1992. 82(4): 764-9.
87 Potts, B.J., et al*., CD34+ bone marrow cells are infected with HIV in a subset of seropositive individuals*. J immunol, 1992. 149(2): 689-97.
88 Molina, J.M., et al., *Lack of evidence for infection of or effect of growth of hematopoietic progenitor cells after in vivo or in vitro exposure to human immunodeficiency virus*. Blood, 1990. 76(12): 2476-82.
89 Carter, C.C., et al., *HIV-1 infects multipotent progenitor cells causing cell death and establishing latent cellular reservoirs*. Nat Med, 2010. 16(4): 446-51.
90 Carter, C.C., et al., *HIV-1 utilizes the CXCR4 chemokine receptor to infect multipotent hematopoietic stem and progenitor cells*. Cell Host Microbe, 2011. 9(3): 223-234.

91 Durand, C.M., et al., *HIV-1 DNA is detected in bone marrow populations containing CD4+ T cells but is not found in purified CD34+ hematopoietic progenitor cells in most patients on antiretroviral therapy*. J Infect Dis, 2012. 205(6): 1014-8.
92 Weiss, R.A., *HIV receptors and cellular tropism*. IUBMB Life, 2002. 53(4-5):201-5. Review.
93 Baribaud F., Doms R.W.,*The impact of chemokine receptor conformational heterogeneity on HIV infection*. Cell Mol Biol, 2001 Jun;47(4):653-60. Review.
94 Wilen C.B., et al., *Molecular mechanisms of HIV entry*. Adv Exp Med Biol, 2012. 726:223-42. Review.
95 Deichmann, M., et al., *Expression of the Human Immunodeficiency Virus Type-1 coreceptors CXCR-4 (fusin, LESTR) and CKR-5 in CD34+ hematopoietic progenitor cells*. Blood, 1997. 89:3522-8.
96 Ruiz, M.E., et al., *Peripheral blood-derived CD34+ progenitor cells: CXC chemokine receptor 4 and CC chemokine receptor 5 expression and infection by HIV*. J Immunol, 1998. 161:4169-76.
97 Shen, H.T., et al., *Intrinsic human immunodeficiency virus type 1 resistance of hematopoietic stem cells despite coreceptor expression*. J Virol, 1999. 73(1): 728-37.
98 Denton, P.W., and J.V. Garcia, *Novel humanized murine models for HIV research*. Curr HIV/AIDS Rep, 2009. 6(1): 13-9
99 Melkus, M.W., et al., *Humanized mice mount specific adaptive and innate immune responses to EBV and TSST-1*. Nat Med, 2006. 12(11):1316-22.
100 Denton, P.W., et al., *Systemic administration of antiretrovirals prior to exposure prevents rectal and intravenous HIV-1 transmission in humanized BLT mice.* PLoS One, 2010. 5(1):e8829.
101 Long, B.R. and C.A, Stoddart. *Alpha interferon and HIV infection cause activation of human T-cells in NSG-BLT mice*. J Virol, 2012. 86(6): 3327-36.
102 Denton PW, Olesen R, Choudhary SK, Archin NM, Wahl A, Swanson MD, Chateau M, Nochi T, Krisko JF, Spagnuolo RA, Margolis DM, Garcia JV.
103 Denton PW, Garcia JV. *Mucosal HIV-1 transmission and prevention strategies in BLT humanized mice.*Trends Microbiol, 2012. 20(6):268-74
104 Denton, P.W., et al., *Antiretroviral pre-exposure prophylaxis prevents vaginal transmission of HIV-1 in humanized BLT mice*. PLoS Med, 2008. 5(1):e16
105 Lahouassa, H., et al., *SAMHD1 restricts the replication of human immunodeficiency virus type 1 by depleting the intracellular pool of deoxynucleoside triphosphates*. Nat Immunol, 2012.
106 Laguette, N., et al., *SAMHD1 is the dendritic- and myeloid-cell-specific HIV-1 restriction factor counteracted by Vpx*. Nature, 2011.
107 Tokarev, A., et al., *Antiviral activity of the interferon-induced cellular protein BST-2/tetherin*. AIDS Res Hum Retroviruses, 2009. 25(12):1197-210. Review.
108 Emerman, M*., How TRIM5alpha defends agains retroviral invasions*. PNAS, 2006. 103(14):5249-50.

109 Andrew A, Strebel K. *HIV-1 Vpu targets cell surface markers CD4 and BST-2 through distinct mechanisms*. Mol Aspects Med, 2010. 31(5):407-17. Epub 2010 Sep 19. Review.
110 Novershtern, N., et al., *Densely interconnected transcriptional circuits control cell states in human hematopoiesis*. Cell, 2011. 144:296-309.
111 Zhang, J., D.M. Webb, *Rapid evolution of primate antiviral enzyme APOBEC3G*. Hum Mol Genet, 2004. 13(66):1785-91.
112 Sawyer, S.L., et al., *Ancient adaptive evolution of the primate antiviral DNA-editing enzyme APOBEC3G*. PLos Biol, 2004, 2(9):e275.
113 Low, A., et al., Enhanced replication and pathogenesis of Moloney murine leukemia virus in mice defective in the murine APOBEC3 gene. Virology, 2009. 385(2):455-63.
114 Okeoma, C.M., et al., APOBEC3 inhibits mouse mammary tumour virus replication in vivo. Nature, 2007, 445(7130):927-30.
115 Gooch, B.D., B.R.Cullen, *Functional domain organization of human APOBEC3G*. . Virology. 2008 vol. 379 (1):118-24
116 Simon, J.H., et al., *Evidence for a newly discovered cellular anti-HIV-1 phenotype*. Nat Med, 1998. 4(12):1397-400.
117 Stopak, K., et al., *HIV-1 vif blocks the antiviral activity of APOBEC3G by impairing both its translation and intracellular stability*. Mol Cell, 2003. 12:591-601
118 Bishop, K.N., et al., *APOBEC3G inhibits elongation of HIV-1 reverse transcripts*. PLoS Pathog, 2008. 4(12) :e1000231
119 Bishop, K.N., et al., *APOBEC3G inhibits elongation of HIV-1 reverse transcripts*. PLoS Path, 2008. 4(12):e1000231.
120 Harris, R.S., et al., *DNA deamination mediates innate immunity to retroviral infection*. Cell, 2003. 113:803–9.
121 Bishop, K.N., et al., *Antiviral potency of APOBEC proteins does not correlate with cytidine deamination*. J Virol, 2006. 80(17): 8450-8.
122 Iwatani, Y., et al., *Deaminase-independent inhibition of HIV-1 reverser transcription by APOBEC3G*. Nuc Acid Res, 20007. 35(21):7096-108.
123 Sheehy, A.M., et al., *The antiretroviral enzyme APOBEC3G is degraded by the proteasome in response to HIV-1 Vif*. Nat Med, 2003. 9(11) :1404-7
124 Marin, M., et al., *HIV-1 vif protein binds the editing enzyme APOBEC3G and induces its degradation*. Nat Med, 2003. 9(11):1398-1403.
125 Yu, X., et al., *Induction of APBEC3G ubiquitination and degradation by an HIV-1 vif-cul5-scf complex*. Science, 2003. 302:1056-60.
126 Wichroski, M.J., et al., *Analysis of HIV-1 viral infectivity factor-mediated proteasome-dependent depletion of APOBEC3G*. J Biol Chem, 2005. 280(9):8387-96.
127 Marin, M., Rose, K.M., Kozak, S.L., Kabat, D., 2003. *HIV-1 Vif protein binds the editing enzyme APOBEC3G and induces its degradation*. Nat. Med. 9, 1398–1403.

128 Niewiadomska, A.M., et al., *Differential inhibition of long interspersed element 1 by APOBEC3 does not correlate with high-molecular-mass-complex formation of p-body association*. J Virol, 2007. 81(17):9577-83.
129 Muckenfuss, H., et al., *APOBEC3 proteins inhibit human LINE-1 retrotransposition*. J. Biol. Chem, 2006. 281: 22161–72.
130 Schumacher, A.J., et al., *The DNA deaminase activity of human APOBEC3G is required for Ty1, MusD and HIV-1 restriction*. J. Virol, 2008. 82:2652–60.
131 Bogerd, H.P., et al., *Cellular inhibitors of long interspersed element 1 and Alu retrotransposition*. Proc. Natl. Acad. Sci., 2006. 103, 8780– 5.
132 Khatua, A.K., et al., *Inhibition of LINE-1 and Alu retrotransposition by exosomes encapsidating APOBEC3G and APOBEC3F*. Virology, 2010. 400: 68-75.
133 Wissing, S., et al., *Endogenous APOBEC3B restricts LINE-1 retrotransposition in transformed cells and human embryonic stem cells*. J Biol Chem, 2011.
134 Stenglein, M.D., et al., *Two regions within the amino-terminal half of APOBEC3G cooperate to determine cytoplasmic localization* . J Virol, 2008. 82(19):9591-9
135 Shirakawa, K., et al., *Phosphorylation of APOBEC3G by protein kinase A regulates its interaction with HIV-1 vif*. Nat Struc Mol Biol, 2008. 15(11):1184-91
136 Demorest, Z.L., et al*., Phosphorylation directly regulates the intrinsic DNA cytidine deaminase activity of activation-induced deaminase and APOBEC3G protein*. J Biol Chem, 2011. 286(30):26568-75.
137 Farrow, M.A., et al., *NFAT and IRF proteins regulate transcription of the anti-HIV gene, APOBEC3G*. J Biol Chem. 2011 Jan 28;286(4):2567-77.
138 Wang, F., et al., *APOBEC3G upregulation by alpha interferon restricts human immunodeficiency virus type 1 infection in human peripheral plasmacytoid dendritic cells*. J Gen Virol, 2008. 89:722-30.
139 Cheney, K.M., Á. McKnight, *Interferon-alpha mediates restriction of human immunodeficiency virus type-1 replication in primary human macrophages at an early stage of replication*. PLoS One. 2010 Oct 20;5(10):e13521.
140 Zhou, Y., et al., *A critical function of toll-like receptor-3 in the induction of anti-human immunodeficiency virus activities in macrophages*. Immunology. 2010 Sep;131(1):40-9.
141 Koning, F.A., et al., *Defining APOBEC3 expression patterns in human tissues and hematopoietic cell subsets*. J Virol, 2009. 83(18):9474-85.
142 Peng, G., et al., *Myeloid differentiation and susceptibility are linked to APOBEC3 expression*. Blood, 2007. 110:393-400.
143 Stopak, K.S., et al., *Distinct patterns of cytokine regulation of APOBEC3G expression and activity in primary lymphocytes, macrophages, and dendritic cells*. J Biol Chem, 2007. 282(6):3539-46.
144 Pion, M., et al., *APOBEC3/F mediates intrinsic resistance of monocyte-derived dendritic cells to HIV-1 infection*. J Ex Med, 2006. 203(13):2887-93.
145 Kuraoka, M., et al., *AID expression during B-cell development: searching for answers*. Immunol Res, 2011. 49(1-3):3-13.

146 Powell, C., et al., *Injury-dependent Müller glia and ganglion cell reprogramming during tissue regeneration requires Apobec2a and Apobec2b*. J Neurosci, 2012. 32(3):1096-109.
147 Bennett, R.P., et al., *Nuclear Exclusion of the HIV-1 host defense factor APOBEC3G requires a novel cytoplasmic retention signal and is not dependent on RNA binding*. J Biol Chem, 2008. 28 (12):7320-7
148 Gallois-Montbrun, S., et al., *Antiviral Protein APOBEC3G Localizes to Ribonucleoprotein Complexes Found in P Bodies and Stress Granules*. Journal of Virology 2007
149 Wichroski, M.J., et al., *Human retroviral host restriction factors APOBEC3G and APOBEC3F localize to mRNA processing bodies*. PLoS Pathog, 2006. 2(5):e41
150 Gallois-Montbrun, S., et al*., Comparison of Cellular Ribonucleoprotein Complexes Associated with the APOBEC3F and APOBEC3G Antiviral*. JVirol, 2008. 82(11):5636-42
151 Kozak, S.L, et al., *The anti-HIV-1 editing enzyme APOBEC3G binds HIV-1 RNA and messenger RNAs that shuttle between polysomes and stress granules*. J Biol Chem, 2006. 281(39):29105-119.
152 Huang, J., et al*., Derepression of microRNA-mediated protein translation inhibition by apolipoprotein B mRNA-editing enzyme catalytic polypeptide-like 3G (APOBEC3G) and its family members*. J Biol Chem, 2007. 282(46):33632-40.
153. Murray, L., et al., *Optimization of retroviral gene transduction of mobilized primitive hematopoietic progenitors by using thrombopoietin, Flt3, and Kit ligands and RetroNectin culture*. Hum Gene Ther, 1999. 10(11):1743-52.
154 Rurrrieri, L., et al., *Cell-surface marking of CD34+ restricted phenotypes of human hematopoietic progenitor cells by retrovirus-mediated gene transfer*. Hum Gene Therapy, 1997. 8(13): 1611-23.
155 Lauer, U.M., et al*., A prototype transduction tag system (delta LNGFR/NGF) for noninvasive clinical therapy monitoring*. Cancer Gene Therapy, 2000.
156 Bhutani, N., et al., *Reprogramming towards pluripotency requires AID-dependent DNA demethylation*. Nature, 2010.
157 Chen, C.Z., H.F. Lodish. *MicroRNAs as regulators of mammalian hematopoiesis*. Sem Immunol, 2005. 17: 155-65.
158 Morgan, H.D., et al., *Activation-induced cytidine deaminase deaminates 5-methylcytosine in DNA and is expressed in pluripotent tissues*. J Biol Chem, 2004. 279(50):52353-60.